Alma Mater Studiorum – Università di Bologna

DOTTORATO DI RICERCA IN

Scienze Chimiche

Ciclo XXVI

Settore Concorsuale di afferenza: 03/C1

Settore Scientifico disciplinare: CHIM/06

Synthesis and surface modification of silver and gold nanoparticles. Nanomedicine applications against Glioblastoma Multiforme.

Presentata da: **Locatelli Erica**

Coordinatore Dottorato	**Relatore**
Chiar.mo Prof. Aldo Roda	**Prof. Mauro Comes Franchini**

Esame finale anno 2014

Medaglione

Dottorando: Locatelli Erica

Curriculum: Nanoscienze e Nanotecnologie

Tutor: Prof. Mauro Comes Franchini

Titolo della Tesi: Synthesis and surface modification of silver and gold nanoparticles. Nanomedicine applications against Glioblastoma Multiforme.

Relazione:

La Dott.ssa Locatelli Erica durante il triennio del suo dottorato di ricerca si è occupata della sintesi di nanoparticelle metalliche di oro e argento, e del loro successivo intrappolamento in micelle costituite da co-polimeri biocompatibili per applicazioni nel campo del drug delivery ed in particolare alla lotta contro il glioblastoma multiforme, tumore dalla prognosi particolarmente infausta. Nello specifico è stata messa a punto la sintesi di nanosfere di argento e di nanonocilindri di oro in soluzione acquosa e successivamente le due nanostrutture sono state funzionalizzate con leganti organici appositamente sintetizzati per renderle lipofiliche piuttosto che idrofiliche. Infine sono stati sintetizzati copolimeri biocompatibili e biodegradabili a base di acido poli-lattico-co-glicolico (PLGA) e di glicole polyetilenico (PEG). A questo punto si è proceduto allo sviluppo di vari sistemi nanostrutturati complessi costituiti da micelle polimeriche, contenenti al loro interno le nanostrutture di oro e argento, singolarmente o legate tra loro tramite reazione di Click chemistry, oppure le nanostrutture ed eventuali farmaci antitumorali; tali micelle sono inoltre state funzionalizzate in superficie con opportuni agenti di *targeting* per drug delivery attivo o di *imaging*. Dopo aver caratterizzato i vari prodotti ottenuti con svariate tecniche analitiche (NMR, AAS, DLS, IR, HPLC, TGA, UV-Vis, etc…) essi sono stati testati da gruppi collaboratori sia tramite tests *in vitro* ed *in vivo*. I risultati sono stati assai incoraggianti in quanto i nanosistemi mostrano una buona biodistribuzione, capacità di raggiungere il sito tumorale con buoni up-take, possibilità di essere usati quali agenti di *imaging* diagnostico per una diagnosi precoce del tumore, ed infine una ottima citotossicità contro il glioblastoma multiforme, con in un caso particolare l'ottenimento della riduzione della massa tumorale *in vivo* in topi del 22% dopo singola somministrazione.

Durante il triennio del dottorato di ricerca la dott.ssa Locatelli Erica è stata coautrice di 11 lavori con peer-review. Ha partecipato a 5 conferenze nell'ambito del progetto europeo Save-

Me (CP-IP 263307-2) con 3 presentazioni orali in lingua inglese, ad una scuola di dottorato nazionale (XXXVI Corso Estivo "A. Corbella", Gargnano, Brescia, 2011) e ad una internazionale (NN13 & ISSON13, Salonicco, Grecia, 2013) con presentazione di posters. Ha inoltre svolto un periodo di ricerca di 4 mesi presso l'istituto di biofarmaceutica di Francoforte (Germania) sotto la supervisione del Professor Jorg Kreuter, durante i quali si è occupata di sintesi di nanoparticelle proteiche a base di siero albumina umana, acquisendo nuove conoscenze nell'ambito della preparazione e caratterizzazione di sistemi biocompatibili per drug delivery.

Index

Abstract

List of abbreviations

List of publications

Abstract

In the last decades noble metal nanoparticles (NPs) arose as one of the most powerful tools for applications in nanomedicine field and cancer treatment. Glioblastoma multiforme (GBM), in particular, is one of the most aggressive malignant brain tumors that nowadays still presents a dramatic scenario concerning median survival. Gold nanorods (GNRs) and silver nanoparticles (AgNPs) could find applications such as diagnostic imaging, hyperthermia and glioblastoma therapy. During these three years, both GNRs and AgNPs were synthesized with the "salt reduction" method and, through a novel double phase transfer process, using specifically designed thiol-based ligands, lipophilic GNRs and AgNPs were obtained and separately entrapped into biocompatible and biodegradable PEG-based polymeric nanoparticles (PNPs) suitable for drug delivery within the body. Moreover, a synergistic effect of AgNPs with the Alisertib drug, were investigated thanks to the simultaneous entrapment of these two moieties into PNPs. In addition, Chlorotoxin (Cltx), a peptide that specifically recognize brain cancer cells, was conjugated onto the external surface of PNPs. The so-obtained novel nanosystems were evaluated for *in vitro* and *in vivo* applications against glioblastoma multiforme. In particular, for GNRs-PNPs, their safety, their suitability as optoacoustic contrast agents, their selective laser-induced cells death and finally, a high tumor retention were all demonstrated. Concerning AgNPs-PNPs, promising tumor toxicity and a strong synergistic effect with Alisertib was observed (IC50 10 nM), as well as good *in vivo* biodistribution, high tumor uptake and significative tumor reduction in tumor bearing mice. Finally, the two nanostructures were linked together, through an organic framework, exploiting the click chemistry azido-alkyne Huisgen cycloaddition, between two ligands previously attached to the NPs surface; this multifunctional complex nanosystem was successfully entrapped into PNPs with nanoparticles' properties maintenance, obtaining in this way a powerful and promising tool for cancer fight and defeat.

List of abbreviations

AAS: atomic absorption spectroscopy

AgNPs: silver nanoparticles

BBB: blood brain barrier

Cy5: cyanine 5

Cltx: chlorotoxin

CTAB: hexadecyltrimethylammonium bromide

CuAAC: Copper-catalyzed azide alkyne cycloaddition

DLS: Dynamic light scattering

EDC: 1-ethyl-3-(3-dimethylaminopropyl) carbodiimide

EPR: Enhanced Permeability and Retention

FDA: Food and Drug Administration

GBM: glioblastoma multiforme

GNRs: gold nanorods

HPLC: high performance liquid chromatography

ICP-AES: inductively coupled plasma atomic emission spectroscopy

IR: infrared

LSPR: localized surface plasmon resonance

NMR: nuclear magnetic resonance

NPs: nanoparticles

PDI: polidispersity index

PEG: poly(ethylene glycol)

PLGA: poly(lactic-co-glycolic) acid

PNPs: polymeric nanoparticles

PVP: polyvinylpyrrolidone

RES: Reticuloendothelial System

RuAAC: Ruthenium-catalyzed azide alkyne cycloaddition

sulfo-NHS: *N*-hydroxysulfosuccinimide

TEM: transmission electron microscopy

UV-Vis: ultraviolet-visible

List of publications

Papers included and discussed in the present thesis.

1. M. Comes Franchini, J. Ponti, R. Lemor, M. Fournelle, F. Broggi, E. Locatelli: "Polymeric entrapped thiol-coated gold nanorods: cytotoxicity and suitability as molecular optoacoustic contrast agent". *J. Mater. Chem.*, **2010**, *20*, 10908–10914.

Abstract: The behaviour of polymeric entrapped thiol-coated GNRs in culture medium under biological conditions was analysed. The in vitro cytotoxicity was studied by a Colony Forming Efficiency assay on immortalized mouse fibroblasts (Balb/3T3) obtaining a dose–effect relationship in which a half inhibitory concentration (IC50) was 20.3mM. The suitability of the new nanomaterial as an optoacoustic contrast agent was investigated in phantom studies using a hardware platform suitable for retrieving clinically relevant data. Spherical alginate phantoms containing GNR-2-PNPs at different concentrations were synthesized and the optoacoustic signal amplitudes were measured as a function of concentration. Signals could be obtained with satisfying signal-to-noise ratio (SNR) down to concentrations of 11 mM corresponding to subtoxic concentration in our in vitro model. The nanomaterial proved to be a suitable and promising contrast agent for different optoacoustic imaging modalities including multispectral approaches.

2. E. Locatelli, G. Ori, M. Fournelle, R. Lemor, M. Montorsi, M. Comes Franchini: "Click Chemistry for the Assembly of Gold Nanorods and Silver Nanoparticles". *Chem. Eur. J.* **2011**, *17*, 9052 – 9056.

Abstract: Click chemistry based on a 1,3-dipolar cycloaddition between lipophilic gold nanorods (GNRs) containing an acetylene group with spherical silver nanoparticles containing an azide has been accomplished (see scheme). Phantom experiments show that this organic transformation did not affect the suitability of the gold nanorods as contrast agents for optoacoustic imaging.

3. E. Locatelli, F. Broggi, J. Ponti, P. Marmorato, F. Franchini, S. Lena, M. Comes Franchini: "Lipophilic Silver Nanoparticles and Their Polymeric Entrapment into

Targeted-PEG-Based Micelles for the Treatment of Glioblastoma". *Adv. Healthcare Mater.* **2012**, *1*, 342–347.

Abstract: A simple method for the synthesis of lipophilic Ag NPs has been developed. The coated Ag NPs have been entrapped into a FDA-approved and targetable PEG-based polymeric nanoparticles, and this nanocarrier has been conjugated with the peptide chlorotoxin. Uptake experiments have shown a cell-specific recognition of the Ag-1-PNPs-Cltx on U87MG cell lines in comparison to Balb/3T3. The uptake of Ag into the cells was quantified and an interesting cytotoxic effect (IC50 = 45 μM) has been found on glioblastoma cell lines.

4. E. Locatelli, M. Comes Franchini: "Biodegradable PLGA-b-PEG polymeric nanoparticles: synthesis, properties, and nanomedical applications as drug delivery system". *J Nanopart Res,* **2012**, *14*, 1316-1333.

Abstract: During the past decades many synthetic polymers have been studied for nanomedicine applications and in particular as drug delivery systems. For this purpose, polymers must be non-toxic, biodegradable, and biocompatible. Polylactic-co-glycolic acid (PLGA) is one of the most studied polymers due to its complete biodegradability and ability to self-assemble into nanometric micelles that are able to entrap small molecules like drugs and to release them into body in a time dependent manner. Despite fine qualities, using PLGA polymeric nanoparticles for in vivo applications still remains an open challenge due to many factors such as poor stability in water, big diameter (150–200 nm), and the removal of these nanocarriers from the blood stream by the liver and spleen thus reducing the concentration of drugs drastically in tumor tissue. Polyethylene glycol (PEG) is the most used polymers for drug delivery applications and the first PEGylated product is already on the market for over 20 years. This is due to its stealth behavior that inhibits the fast recognition by the immune system (opsonization) and generally leads to a reduced blood clearance of nanocarriers increasing blood circulation time. Furthermore, PEG is hydrophilic and able to stabilize nanoparticles by steric and not ionic effects especially in water. PLGA–PEG block copolymer is an emergent system because it can be easily synthesized and it possesses all good qualities of PLGA and also PEG capability so in the last decade it arose as one of the most promising systems for nanoparticles formation, drug loading, and in vivo drug delivery applications. This review will discuss briefly on PLGA-b-PEG synthesis and physicochemical properties, together with its improved qualities with respect to the single PLGA and PEG polymers. Moreover, we will

focus on but in particular will treat nanoparticles formation and uses as new drug delivery system for nanomedical applications.

5. E. Locatelli, W. Bost, M. Fournelle, J. Llop, L. Gil, F. Arena, V. Lorusso, M. Comes Franchini: " Targeted polymeric nanoparticles containing gold nanorods: a therapeutic approach against glioblastoma". *J Nanopart Res*, **2014**, 16, 2304-2013.

Abstract: Chlorotoxin-targeted polymeric nanoparticles containing entrapped gold nanorods as potential therapeutic agent for glioblastoma multiforme have been developed and evaluated. In first proof of concept experiments, in vitro specific uptake in cancer cells and selective laser-induced cell death have been shown. In vivo studies with optical imaging showed increased retention of targeted NPs in the tumor.

6. E. Locatelli, M. Naddaka, C. Uboldi, G. Loudos, E. Fragogeorgi, V. Molinari, A. Pucci, T. Tsotakos, D. Psimadas, J. Ponti, M. Comes Franchini: "Targeted delivery of silver nanoparticles and alisertib: in vitro and in vivo synergistic effect against glioblastoma". *Nanomedicine*, **2014**, In press.

Abstract: Targeted biocompatible nanoplatforms presenting multiple therapeutic functions have great potential for the treatment of cancer. Materials & methods: Multifunctional nanocomposites formed by polymeric nanoparticles (PNPs) containing two cytotoxic agents – the drug alisertib and silver nanoparticles – were synthesized. These PNPs have been conjugated with a chlorotoxin, an active targeting 36-amino acid-long peptide that specifically binds to MMP-2, a receptor overexpressed by brain cancer cells. Results: The individual and synergistic activity of these two cytotoxic agents against glioblastoma multiforme was tested both *in vitro* and *in vivo*. The induced cytotoxicity in a human glioblastoma–astrocytoma epithelial-like cell line (U87MG) was studied *in vitro* through a trypan blue exclusion test after 48 and 72 h of exposure. Subsequently, the PNPs' biodistribution in healthy animals and their effect on tumor reduction in tumor-bearing mice were studied using PNPs radiolabeled with ^{99m}Tc. Conclusion: Tumor reduction was achieved *in vivo* when using silver/alisertib@PNPs–chlorotoxin.

Papers concerning other research fields

1. E. Locatelli, L. Gil, L. L. Israel, L. Passoni, M. Naddaka, A. Pucci, T. Reese, V. Gomez-Vallejo, P. Milani, M. Matteoli, J. Llop, J. P. Lellouche, M. Comes Franchini: "Biocompatible nanocomposite for PET/MRI hybrid imaging". *Int. J. Nanomed*., **2012**, *7*, 6021–6033.

Abstract: A novel nanocarrier system was designed and developed with key components uniquely structured at the nanoscale for early cancer diagnosis and treatment. In order to perform magnetic resonance imaging, hydrophilic superparamagnetic maghemite nanoparticles (NPs) were synthesized and coated with a lipophilic organic ligand. Next, they were entrapped into polymeric NPs made of biodegradable poly(lactic-co-glycolic acid) linked to polyethylene glycol. In addition, resulting NPs have been conjugated on their surface with a 2,2′-(7-(4-((2-aminoethyl)amino)-1-carboxy-4-oxobutyl)-1,4,7-triazonane-1,4-diyl)diacetic acid ligand for subsequent ^{68}Ga incorporation. A cell-based cytotoxicity assay has been employed to verify the in vitro cell viability of human pancreatic cancer cells exposed to this nanosystem. Finally, in vivo positron emission tomography-computerized tomography biodistribution studies in healthy animals were performed.

2. V. Rebuttini, A. Pucci, P. Arosio, X. Bai, E. Locatelli, N. Pinna, A. Lascialfari, M. Comes Franchini: "Zirconia-doped nanoparticles: organic coating, polymeric entrapment and application as dual-imaging agents". *J. Mater. Chem. B*, **2013**, *1*, 919-923.

Abstract: Zirconia nanoparticles doped with Eu^{3+}, Tb^{3+} and Gd^{3+} ions have been synthesized following the benzyl alcohol route. The nanoparticles were coated with N-hydroxydodecanamide and encapsulated in PLGA-b-PEG-COOH nanomicelles. The magnetic and fluorescent properties of these hybrid nanocarriers were investigated, proving them to be potential dual-imaging contrast agents.

3. A. Pucci, E. Locatelli, J. Ponti, C. Uboldi, V. Molinari, M. Comes Franchini: "Click chemistry on the surface of PLGA-b-PEG polymeric nanoparticles: a novel targetable fluorescent imaging nanocarrier".

Abstract: In the quest for biocompatible nanocarriers for biomedical applications, a great deal of effort is put on engineering the nanocomposites surface in order to render them specific to the particular purpose. We developed biocompatible PLGA-b-PEG-based

nanoparticles carrying a double functionality (i.e., carboxylic and acetylenic) able to serve as flexible highly selective grafting centers for cancer diagnosis and treatment. As a proof of concept, the nanocarrier was successfully functionalized with a tailored fluorescent molecule by means of click chemistry and with a targeting agent specific for glioblastoma multiforme via amidic bond formation.

4. J. Vandooren, N. Berghmans, C. Dillen, I. Van Aelst, I. Ronsse, L. L. Israel, I. Rosenberger, J. Kreuter, J. P. Lellouche, S. Michaeli, E. Locatelli, M. Comes Franchini, M. K. Aiertza, L. Sánchez-Abella, I. Loinaz, D. R. Edwards, L. Shenkman, G. Opdenakker: "Intradermal air pouch leukocytosis as an in vivo test for nanoparticles". *Int. J. Nanomed.* **2013**, *8*, 4745–4756.</br>

Abstract: The need for test systems for nanoparticle biocompatibility, toxicity, and inflammatory or adaptive immunological responses is paramount. Nanoparticles should be free of microbiological and chemical contaminants, and devoid of toxicity. Nevertheless, in the absence of contamination, these particles may still induce undesired immunological effects in vivo, such as enhanced autoimmunity, hypersensitivity reactions, and fibrosis. Here we show that artificial particles of specific sizes affect immune cell recruitment as tested in a dermal air pouch model in mice. In addition, we demonstrate that the composition of nanoparticles may influence immune cell recruitment in vivo. Aside from biophysical characterizations in terms of hydrodynamic diameter, zeta potential, concentration, and atomic concentration of metals, we show that – after first-line in vitro assays – characterization of cellular and molecular effects by dermal air pouch analysis is straightforward and should be included in the quality control of nanoparticles. We demonstrate this for innate immunological effects such as neutrophil recruitment and the production of immune-modulating matrix metalloproteases such as MMP-9; we propose the use of air pouch leukocytosis analysis as a future standard assay.

5. D. Psimadas, G. Baldi, C. Ravagli, M. Comes Franchini, E. Locatelli, C. Innocenti, C. Sangregorio, G. Loudos: "Comparison of the magnetic, radiolabeling, hyperthermic and biodistribution properties of hybrid nanoparticles bearing $CoFe_2O_4$ and Fe_3O_4 metal cores". *Nanotechnology*, **2014**, *25***, 25101-25110.

Abstract: Metal oxide nanoparticles, hybridized with various polymeric chemicals, represent a novel and breakthrough application in drug delivery, hyperthermia treatment and imaging techniques. Radiolabeling of these nanoformulations can result in new and

attractive dual-imaging agents as well as provide accurate in vivo information on their biodistribution profile. In this paper a comparison study has been made between two of the most promising hybrid core–shell nanosystems, bearing either magnetite .Fe_3O_4/ or cobalt ferrite .$CoFe_2O_4$/ cores, regarding their magnetic, radiolabeling, hyperthermic and biodistribution properties. While hyperthermic properties were found to be affected by the metal-core type, the radiolabeling ability and the in vivo fate of the nanoformulations seem to depend critically on the size and the shell composition.

1. Introduction

1.1 Nanomedicine, Nanotechnology and Drug Delivery: an overview.

Nanotechnology is a cutting-edge branch of applied science and technology, which deals with the control of matter at dimensions between one and one hundred nanometers and the subsequent realization of devices in such a scale. These dimensions allow matter to have a high ratio of surface area to volume, not present neither in bulk material nor in molecular scale, enabling materials to acquire unique properties (optical, electronic, magnetic, chemical and biologic), which consent nanotechnology to work in a multidisciplinary area of investigation, involving many fields of research, including chemistry, biology, physics, and even medicine.[1]

Nanomedicine represents the medical application of the opportunities arising from nanotechnology: indeed by engineering nanomaterials that have specific size, structure, shape, chemical composition and surface chemical characteristic it is possible to obtain new drug delivery systems, diagnostic tools, contrast agents, scaffolds for tissue engineering and a variety of medical devices for the treatment, prevention and diagnosis of numerous diseases.[2] Some nanomaterials gained approval by Food and Drug Administration (FDA) and are nowadays commonly used in medicine (**Figure 1.1.1**).

Table 1. Examples of Nanomaterials in Clinical Use.*

Nanomaterial	Trade Name	Application	Target	Adverse Effects	Manufacturer	Current Status
Metallic						
Iron oxide	Feridex	MRI contrast	Liver	Back pain, vaso-dilatation	Bayer Schering	FDA approved
	Resovist	MRI contrast	Liver	None	Bayer Schering	FDA approved
	Combidex	MRI contrast	Lymph nodes	None	Advanced Magnetics	In phase 3 clinical trials
	NanoTherm	Cancer therapy	Various forms	Acute urinary retention	MagForce	In phase 3 clinical trials
Gold	Verigene	In vitro diagnostics	Genetic	Not applicable	Nanosphere	FDA approved
	Aurimmune	Cancer therapy	Various forms	Fever	CytImmune Sciences	In phase 2 clinical trials
Nanoshells	Auroshell	Cancer therapy	Head and neck	Under investigation	Nanospectra Biosciences	In phase 1 clinical trials
Semiconductor						
Quantum dot	Qdots, EviTags, semiconductor nanocrystals	Fluorescent contrast, in vitro diagnostics	Tumors, cells, tissues, and molecular sensing structures	Not applicable	Life Technologies, eBioscience, Nanoco, CrystalPlex, Cytodiagnostics	Research use only
Organic						
Protein	Abraxane	Cancer therapy	Breast	Cytopenia	Abraxis Bioscience	FDA approved
Liposome	Doxil/Caelyx	Cancer therapy	Various forms	Hand–foot syndrome, stomatitis	Ortho Biotech	FDA approved
Polymer	Oncaspar	Cancer therapy	Acute lymphoblastic leukemia	Urticaria, rash	Rhône-Poulenc Rorer	FDA approved
	CALAA-01	Cancer therapy	Various forms	Mild renal toxicity	Calando	In phase 2 clinical trials
Dendrimer	VivaGel	Microbicide	Cervicovaginal	Abdominal pain, dysuria	Starpharma	In phase 2 clinical trials
Micelle	Genexol-PM	Cancer therapy	Various forms	Peripheral sensory neuropathy, neutropenia	Samyang	For phase 4 clinical trials

* MRI denotes magnetic resonance imaging.

Figure 1.1.1: some of the nanomaterials undergoing clinical trials or FDA approved. *B.Y.S. Kim, N. Engl. J. Med., 2010, 2434-2443.*

One of nanomedicine's major efforts is in the development of new and more efficient cancer treatments: to improve the efficiency of currently available chemo-therapeutic agents as well as to enable new early pre-symptomatic cancer diagnosis, have assumed dramatic importance in the last few decades since still in 2012 one in 4 deaths in Europe and United States is due to cancer.[3]

Compared with traditional contrast agents and chemotherapeutic drugs, nanomedicine offers the possibility to incorporate multiple functions in a single system holding great promises of simultaneous monitoring, treatment and targeting of cancer: the term "theranostic" was specifically coined to describe the combination of diagnostic capability and therapeutic efficacy held in a single system (**Figure 1.1.2**).[4]
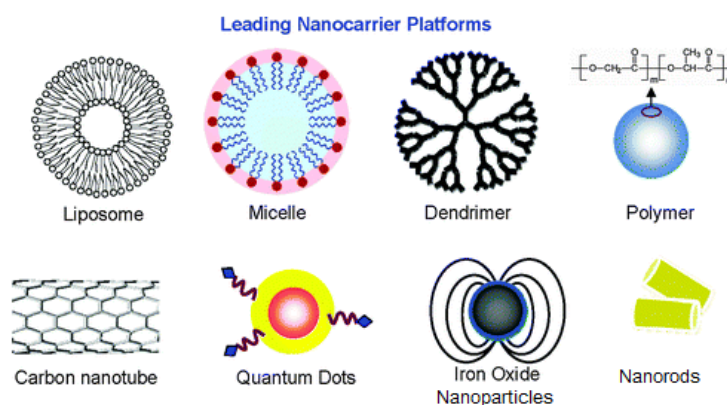

Figure 1.1.2: examples of nanocomposites nowadays developed. Adapted from *W. X. Mai.Integr. Biol., 2013, 5, 19-28.*

Moreover, nanomedicine enables the delivery of a drug in a nanosystem within the biological systems and through the biological barriers, which provide advantages due to the high degree of transport and drug protection from immune system so that efficacy can be greatly improved and new therapies became possible. With the term "drug delivery" is generally described the aim of a controlled delivery of drugs to their site of action, without affecting healthy organs, and the release of the same in a time-dependent manner. Drug delivery simultaneously solves common problems ascribed to poor drugs solubility in water and consequently low absorption by the body, short in vivo lifetime due to elevated clearance, leading to various advantages such as an improvement of the therapeutic index, a reduction of the dose of drug to be administered and consequently minimization of the unwanted side effects.[5]

To specifically target drugs to the desired site of action, especially anti-cancer drugs to tumors, is becoming a challenge that is currently addressed: most of the nowadays-developed

nanosystems for drug delivery take advantages of the particular characteristics of the disease microenvironment and angiogenesis. It is known that tumor or inflamed tissues present an hyper vascularization and leaky connected endothelial cells respect to healthy tissues that allow easy penetration of nanosystems with suitable dimensions; meanwhile they also present a decreased or damaged lymphatic drainage that reduce execration of the nanosystems once entered into the tissues: this set of conditions takes name of Enhanced Permeability and Retention (EPR) effect and the delivery of a drug taking advantages only of that phenomenon is generally recognised as "passive targeting" (**Figure 1.1.3**). A more efficient drug delivery can be achieved with the so-called "active targeting" that consists in the grafting to the surface of nanosystems of specific ligands able to bond the receptors overexpressed by cancer cells or desired endothelial tissues cells.[6]
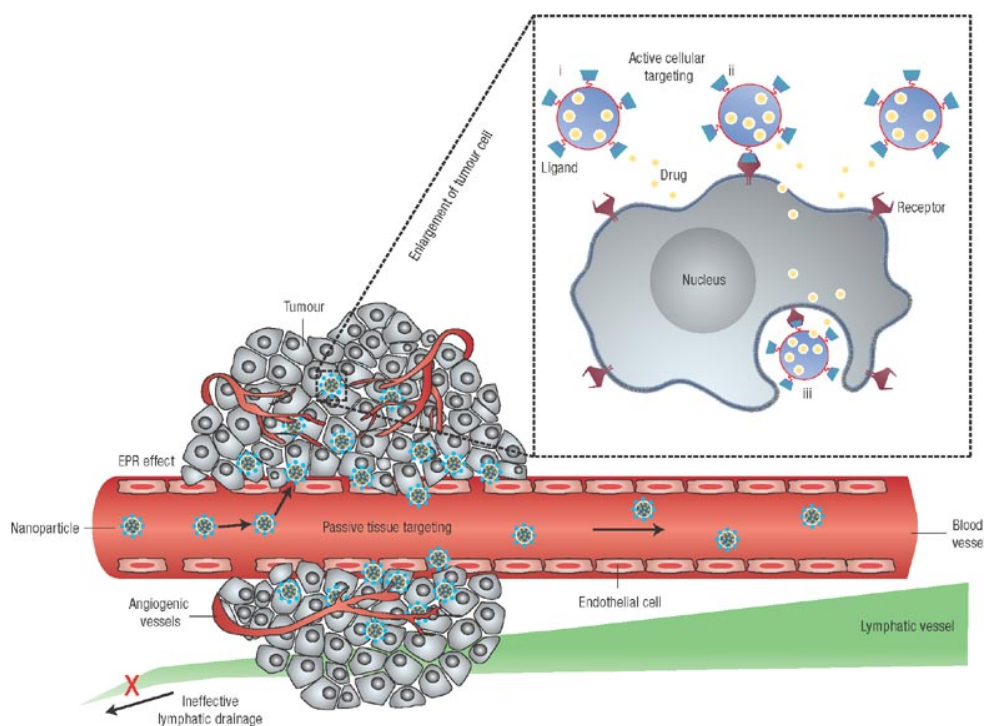

Figure 1.1.3: passive and active targeting of nanosystems. From *D. Peer, Nature Nanotechnology 2007, 2, 751-760.*

Proteins, peptides, monoclonal antibodies or small molecules, able to recognize selectively membrane cellular sites, have been widely used in order to enable an efficient active targeting and to obtain a drug release with higher concentration only in the desired site of action. These kinds of ligands must be on the outer shell of a nanosystem since they have to be free for receptors recognition and not hidden into the nanosystem matrix. For surface modification and anchoring of the ligands, covalent bonding of agents is generally preferred to physical

adsorption or ionic interaction: its stronger nature prevents leaching from the nanoparticles surface under physiologic conditions avoiding random dispersion within the body.[7] Targeting and surface modification of a nanosystem may help not only to reach the desired site of action but also to prolong circulation time and residence time of a drug within the body. This is true especially for injectable particles because, in order to achieve the desired benefits, a drug delivery nanosystem must be present in the bloodstream long enough to reach and recognize its therapeutic site of action. Unfortunately small molecules are rapidly eliminated from the body through the excretory system, especially kidneys, but most of all every foreign object, be it a small molecule or a larger nanosystem, once entered the bloodstream undergo the phenomenon of opsonisation and consequently attack of the immune system and of the Reticuloendothelial System (RES) organs (for instance liver and spleen).

Once entered the bloodstream a foreign organism is immediately surrounded by opsonin proteins so that it becomes subjected to the attack of phagocytic cells.

The phagocytosis brings to the disruption and removal of the undesired materials from the body: in case of nanoparticles, especially polymeric nanoparticles, which cannot be completely destroyed during this process, sequestration from the RES organs frequently occurs. Nanomedicine has long dealt whit this liming factor and even if a completely resolution and prevention of opsonisation is not still achieved, many methods and correlations have been found in order to slow this process. It has been demonstrated that particles' surface charge and nature is generally related to opsonozation, where hydrophilic as well as neutrally charged particles are less subject to opsonisation than hydrophobic and strongly charged ones. For this reason, one of the most adopted techniques to reduce body clearance is the coating of the nanosystem's surface with shielding moieties such as long chain hydrophilic polymers, which can help to avoid opsonisation and early elimination.[8]

A drug delivery system should not only to have a long blood circulation time to effectively reach the desired site of action but it would also need to permeate through the biological barriers normally protecting tissues and organs. These barriers are numerous and of different nature but the most challenging one to cross remains the Blood Brain Barrier (BBB). The BBB is present all along capillaries in the central nervous system and consists of tight junctions made of adjacent endothelial cells that generally are not found in other body capillaries. Its role consists in the maintaining of an extremely regulated brain microenvironment acting like a physical barrier letting enter into the brain the required nutrients and protecting from virus and bacteria but also from harmful hydrophilic molecules

(**Figure 1.1.4**). The only exchange allowed through the BBB is the one of small hydrophobic molecules such as oxygen, carbon dioxide and hormones.[9]
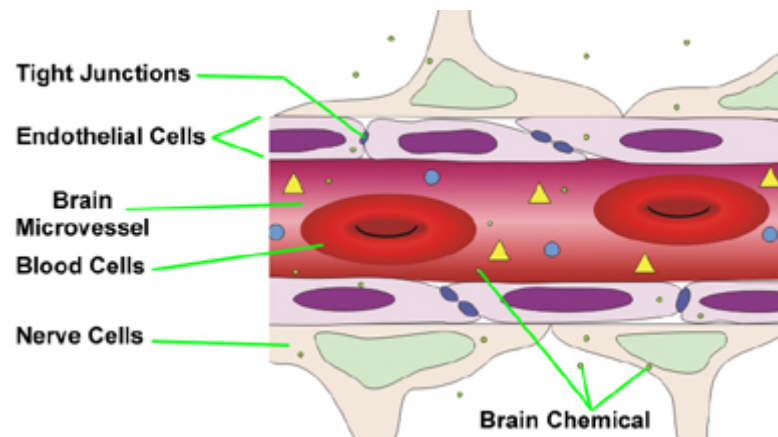

Figure 1.1.4: schematic representation of the Blood Brain Barrier. *J. Whitebread, The Blood-Brain Barrier and OCD, Section 23 PSY1001 Fall 2011*

Since capillaries in all the body compartments have numerous channels, which allow permeation of molecules up to the size of proteins, capillary permeability is not considered a limiting factor in drug delivery. On the contrary for drug delivery to the brain this factor became of crucial importance and all the predictions for drugs or nanosystems engineering has to be made taking into account BBB low permeability. Nonetheless a number of molecules, such as important nutrient, sugars and amino acids can cross the BBB: this is possible thanks to intramembrane transport proteins that allow a "facilitated diffusion" through the barrier; a specific designed active targeting exploiting these proteins may solve, almost in part, the challenging drug delivery to the brain.[10]

1.2 Glioblastoma multiforme

Cancer remains today one of the leading causes of death in United States and Europe for people from one to 65 years old.[11] Medicine has made many strides in cancer treatment and prevention as well as in improvement of quality life for patients with untreatable cancers, but only few sub-types of cancers can be treated in a satisfactory way presenting a good survival rate. Still today, cancer prevention and early detection, instead of therapy, remain the best possibilities for an increment in the survival rate. Cancers that became easily detectable with common and non-expensive techniques (like ultrasound or sample taking) along with cancers that undergo an intensive prevention screening program are today the ones in which the best results were obtained in terms of death reduction and life prolongation. Besides, other types of cancer which present serious difficulties in detection, due to their nature or location in body, remain practically untreatable, and few or nothing at all was possible in order to improve survival rate or patients' quality life.[12]

Among these untreatable tumors, brain cancers represent a large portion: they are in fact particularly hard to detect and treat because of their location, clearly not accessible by common diagnostic techniques and surgery. One of the most common and aggressive primary brain tumours is Glioblastoma multiforme (GBM). It is a tumor of the central nervous system, also known as glioma of grade IV, which exhibits one of the lower overall survival rates among all the other cancers. It was estimated that only the 20% of patients survive two years after diagnosis and this number drastically decrease after five years, with less of 5% of patients still alive.[13] GBM often affects one of the cerebral hemispheres, but in some cases it can be also found in the cerebellum or sometimes in the spinal cord; furthermore GBM rarely generates metastasis to other parts of the body. GBM tumors can be divided in two macro-categories based on the mode of genesis of the same: these are primary and secondary GBM. The so-called primary GBM is the most frequent case, which prevalently affects elderly patients (more than 60 years old) with a very fast progression, without requiring the presence of a pre-existing lesion. The so-called secondary GBM has a frequency of less than 10% among all the diagnosed tumors, but it affects younger patients (average age at diagnosis of 45 years old); it develops more slowly than the primary one, following the typical progression of a diffuse astrocytoma or anaplastic astrocytoma. In the first case, the median survival is three months after diagnosis while in the second it could increase from six months to one year.[14]

The dramatic scenario of GBM has not improved despite many efforts of traditional medicine and surgery: glioblastoma multiforme shows a large resistance to conventional treatment techniques such as radio- and chemotherapy.[15] Nowadays standard therapies consist in surgical removal of the tumor mass when possible, followed by radiation in association with chemotherapy, even though this treatment usually leads only to a small extension of patient's life, with a median survival of less than one year after diagnosis. Indeed, even in case of successful intervention, with complete removal of tumor mass and no damage at the central nervous system after surgery, glioblastoma multiforme usually recurs in almost all cases in a few months: the average time to recurrence after standard therapy is 7 months. This is why chemotherapy and radiotherapy are always applied after surgery. Recent studies suggest that combination of radio- and chemotherapy, rather than single therapy, is associated to a longer survival time. The aim of radiotherapy is to damage and destroy cancer cells remained in loco after surgery, before their possibility to resume proliferation. Thanks to this technique is possible to attack diseased cells focusing mainly on ionizing radiation in the area of interest, leaving healthy cells almost untouched or exhibited only to a few rays. Dose response relationships demonstrate that median survival rate of 13 weeks is obtained with a total radiation dose of less than 4500 cGy, while with a dose of 6000 cGy is possible to reach a median survival of 42 weeks: of course this dose is usually administered 5 days per week in doses of 1.8-2.0 Gy. Unfortunately, the responsiveness of glioblastoma multiforme to radiotherapy may vary considerably from one patient to another: in most of the cases, a phase of remission is induced by radiotherapy, which can endure for months, with recover of neurological deficits and of patient's health, but after that, tumor reoccurs with an enhancement in clinical deterioration and in expanded region.[16]

The use of chemotherapy has increased patients' possibilities and hope especially in association with the above-described techniques. The chemotherapeutic approach is very common in the treatment of cancer, though due to the poor selectivity of the drugs generally involved, it is impossible to discern diseased tissues from healthy cells, thus causing serious damage to the body and a pool of unwanted side effects, which may sometimes be so debilitating for patients to require the suspension of the therapy.

A novel and promising approach that is arising in these recent years is based on the development of specific therapies, deriving from the studies on the growth mechanism, the genesis of the tumor, the cells proliferation and communication, both at a macroscopic level and a microscopic one. This approach may allow focused therapies, different and specific for every cases, thus increasing the possibility of success by several times.

GBM is composed by a heterogeneous mixture of poorly differentiated cancer cells sometimes closely associated to stem cells. The mechanisms that lead to the genesis of GBM were largely investigated and nowadays several possible pathways were recognized as progenitors of the tumor. The most common ones involve the wrong regulation in the receptors of growth factors (EGFR and PTEN protein) or alteration of the reparative p53 protein.[17] Generally, in healthy cells a complex mechanism of regulation of cascade-signals takes place: these signals leads to several cells behaviors, such as differentiation, growth, reproduction etc...When one of those regulatory enzymes fails, a series of uncontrolled effects happens, such as an unwanted, extremely fast cells proliferation. For instance, PTEN is a protein encoded by the PTEN gene, which acts as a tumor suppressor by inhibiting the protein kinase and all the following cascade-signals thanks to its dephosphorylation ability; the direct result of this inhibition is a reduced and well-controlled cell proliferation.[18] Thus, any alteration of the PTEN protein or of its gene regulation can cause an imbalance in this cascade and produce a fast cell proliferation thus leading to the development of the tumor mass. For this reason PTEN protein, such as several other enzymes or complexes, became the target for the most innovative chemotherapy.

There are many different molecules tested and approved as chemotherapists able to attack one of the metabolic pathways of the tumor growth process or directly their cells DNA, causing cells irreproducibility or cells death, making chemotherapy the most important weapon to defeat cancer. Cancer cells, however, may sometimes develop mechanisms of resistance to the most used drugs, requiring an increase in dosage or administration of different molecules. In the case of glioblastoma chemotherapy has the main purpose of damaging the cells remained in the nervous system after surgery. Unfortunately, the only benefit of this treatment is nowadays the extension of the life of the patient to a few months, since there is still not a definitive cure. Among the drugs used on patients with glioblastoma are doxorubicin and paclitaxel, but recently temozolomide has proved to be particularly efficient when used in combination with radiotherapy, increasing life expectancy of the patient of several months (**Figure 1.2.1**).[19]
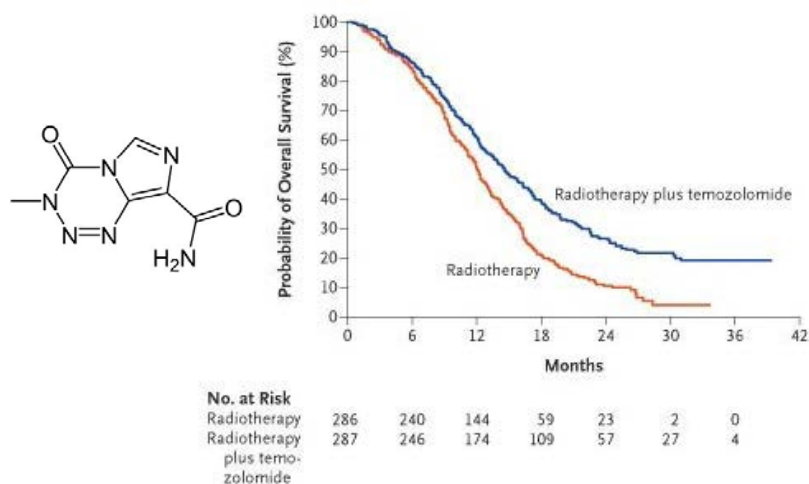
Figure 1.2.1: Temozolomide (left) and its effect on the overall survival when used in combination with radiotherapy (right). From *N. Eng. J. Med.*, **2005**, *352*, 987-996.

As it is possible to see, a more effective therapy is urgently required in order to really increase patients' hope and possibilities. Due to this in the last years, new drugs arose to increase the effectiveness of GBM treatment. These new drugs are based on the studies of the mechanism of tumor growth and progression and they are generally high specific against one selected pathways. Among all the other Alisertib (also known as MLN8237) is a small molecule able to inhibit the serine/threonine protein Aurora A kinase (AAK) that are finding application against several types of cancers (**Figure 1.2.2**). Indeed, AAK localizes itself to the spindle poles and microtubules during cells mitosis, and it is thought to regulate spindle assembly. Its deviant form is expressed in a wide variety of cancers, such as colon cancer, breast cancer and gliomas. The Alisertib activity may result in disruption of the assembly of the mitotic spindle apparatus, with the following disruption of chromosome segregation, and lead to the final inhibition of cell proliferation.
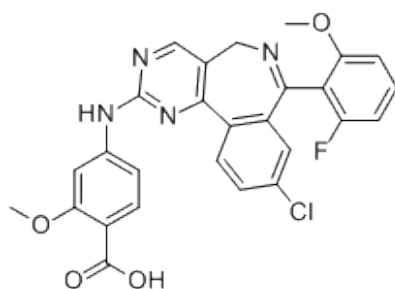

Figure 1.2.2: Alisertib (MNL8237).

Recent studies[20] suggest that Alisertib binds and inhibits Aurora A kinase over Aurora B kinase (ABK) with a selectivity of more than 200 times in cells culture, producing a dose-

dependent inhibition of proliferation of human tumor cell lines *in vitro*. This selectivity could also lead to a strong reduction of side effect on healthy cells generally caused by damage in the AKB pathways. On account of this promising activity Alisertib is now in phase II of preclinical trial as novel antineoplastic drugs for gynecological cancers, such as ovarian and fallopian tube tumors.[21]

In case of gliomas however, the reduced effectiveness of chemotherapy is usually determined by the poor ability of the drug to diffuse into the tumor area. The presence of the blood brain barrier makes difficult or impossible the effective dissemination of the drug into the diseased area. Several drugs including common doxorubicine, have shown good activity against GBM in studies *in vitro*, but once *in vivo* they failed because of their low lipophilicity and their high molecular weight, factors that limit the cross of the BBB in an effectual manner, making impossible to reach the tumor site with a sufficient concentration. Unfortunately, traditional techniques used to increase the accumulation of drug in the tumor area, as the disruption of the BBB with drugs, radiation, physical method or direct intracranial injection are highly invasive and cannot be exploited for prolonged treatments.

The use of nanomedicine drug delivery systems could leads to a sensible overcoming of these problems, especially by exploiting a drug delivery targeted towards the crossing of the BBB. Several studies have been carried out with the purpose of identifying possible receptors or enzymes that may help both in BBB crossing and/or in the tumor uptake thanks to various mechanisms of internalization.

One of the most promising agents is the Chlorotoxin, a 36 amino acids protein that was originally isolated from the venom of the Giant Israeli scorpion *Leiurusquinquestriatus*. Its amino acids sequence is MCMPCFTTDHQMARKCDDCCGGKGRGKCYGPQCLCR and nowadays it could be easily purchased by several companies on the market. Chlorotoxin presents two distinct binding domains designated α and β, each capable of binding tumor cells. As a matter of fact, this protein became known and was found particularly interesting thanks to its ability to bind selectively the trans-membrane matrix metalloproteinase two (MMP-2).[22] The MMP-2 is an enzyme presents in the membrane of several cells but it results particularly overexpressed in many cancer cell lines and it seems to act as promoter for tumor invasion, metastasis and angiogenesis. More specifically, even if MMP-2 can be overexpressed in several solid tumors (such as lung, prostate and melanoma cancer) as well as non-solid tumors (leukemia, myeloma, lymphoma etc…)[23] it is particularly found on glioma and astrocytoma cancer, including glioblastoma multiforme. Therefore, chlorotoxin interacts predominantly with isoforms of MMP-2, present in organelles involved in signal transduction,

cell invasion, adhesion, and motility, which are particularly up-regulated in cancer cells of neuroectodermal origin, but they are not present, or are only present at low level, in normal and healthy neurons or glia cells. This is the reason why chlorotoxin has become the favored targeting agent for glioma tumours and other primary human brain tumours.[24] The proposed interaction mechanism of chlorotoxin with the MMP-2 enzyme seems to involve also the chloride trans-membrane transport channel, with a reduction in the permeability of the membrane for the Cl^- ions and a consequent higher permeability to foreign agents: this is justified by the driving force to preserve unchanged the volume of cells. In conclusion the chlorotoxin could be internalized by glioma cells and, if conjugated to the surface of a nanosystem, it may enhance the natural, but low, tumor uptake provided by the EPR effect, increasing in this way also the cross of the BBB and providing in the end an optimal platform for the development of focused drug delivery systems.

1.3. Noble metal nanoparticles and their application in nanomedicine

1.3.1 Properties and advantages of nanoparticles.

At the present moment, there is not an overall internationally accepted definition of a nanoparticle. Some scientists generally considered a nanoparticle or a cluster as the aggregation of atoms in a number ranging between 3 and 10^7, while other defined nanoparticles as "objects with at list one of the three external dimensions in the nanoscale".[25] Surely in nanoparticles, due to the reduced dimensions, novel properties that are neither those of molecules nor those of bulk material arise and allow filling the gap between molecular chemistry and material science. These properties could be optical, electrical, electronic, magnetic, and biological so that they can be exploited in all the compartments of science.

Among all, in the last decades, metal nanoparticles have been the subject of increasing interest attributable to their unique optical properties, especially the great capacity for absorption and scattering of light. This ability is due to the resonant collective oscillation of the free electrons on the metal surface of the nanostructure in the presence of luminous radiation, a phenomenon called localized surface plasmon resonance (LSPR), which is common to all the nanoparticles but is particularly pronounced in those of transition metals.[26] For metal nanoparticles the surface plasmon band is observed like a strong absorption of light radiation and is particularly noticeable for noble metal Ag and Au.

Both for gold and silver nanoparticles, the frequency of LSPR is located in the visible range, which is the reason why colloidal solutions of these elements are strongly coloured (**Figure 1.3.1.1**) and have attracted interests since historical times as pigments for glass.

Figure 1.3.1.1: Colloidal solutions of silver (left) and gold (right) nanoparticles.

The phenomenon of the LSPR can be described in details thank to the theory of Gustav Mie (1908), who solved the Maxwell equations giving a quantitative explanation of the resonance. Generally, simplified equations deriving from Mie theory are used to explain the importance of many parameters that strongly affects LSPR intensity and wavelength.[27] By way of illustration, for many metals in the bulk state free electron behaviour is predominant and the wavelength of the plasmon absorption peak depends on the equation:

$$\lambda^2 = \lambda_p^{\,2} (\varepsilon^{\infty} + 2\varepsilon_m)$$

where

$$\lambda_p^{\,2} = (2\pi c)^2/\omega_p^{\,2}$$

is the metal's bulk plasma wavelength, ε^{∞} is the high frequency dielectric constant due to interband and core electrons' transitions, ε_m is the dielectric constant of the surrounding medium and the resonance frequency (ω_p) is given by:[28]

$$\omega_p = (N*e^2/\varepsilon_0*m_e)^{1/2}$$

where *N* is the concentration of free electrons in the metal, *e* is the charge of the electron, *m* is the mass of the electron and ε_0 is the vacuum permittivity.

Looking at the equations it becomes clear that the LSPR is strongly affected by several factors such as size and shape of the nanoparticles and most of all by the nature of the surrounding environment due to a direct dependence on the dielectric constant of the medium (ε_m) in which the nanoparticles are dispersed; every modification in the interface with the surrounding environment of these particles leads to significant shifts to the LSPR wavelength and intensity.

The tunability of LSPR by changing size, shape or medium refractive index of nanoparticles has been exploited for several applications in order to develop optical, nanomedicine and biosensor devices.

Moreover, owing to the plasmon resonance, metal nanoparticles could either radiate light through scattering phenomena (Mie scattering), or absorb light and rapidly convert it to heat: the first process has found great applications in optical and imaging field, while the second dissipation has enabled possibilities in several new areas, such as hyperthermia and cancer ablation.[29]

1.3.2 Gold nanostructures

Unlike other metal nanostructures, gold nanospheres have been known for centuries for their intense red-pink coloration and have been used in the creation of artefacts and for glass painting. The most famous artefact containing gold nanoparticles is the Lycurgus Cup (**Figure 1.3.2.1**), a Roman glass cage cup dating from the 4th century showing a red colour when lit from behind and a green one when lit from the front: it contains gold and silver nanoparticles of 70 nm diameter, probably formed during the glass manufacturing and deriving from waste of the previous works. The nature of the phenomenon was not known, but gold nanoparticles continued to be used during the following centuries as pigment and they were known as "Purple of Cassius", who used tin(II) chloride to reduced gold salts. It was only with the work of Michael Faraday in 1857 that the genesis of the colour becomes clear and was attributed to the small dimensions of gold nanoparticles.[30] After that several preparation's methods arose, the easier one remains the Turkevich method (1951).[31]

Figure 1.3.2.1: Lycurgus Cup

The typical red-pink colouration that made gold nanoparticles famous is attributable to the LSPR maximum absorption band of about 520 nm. This happens for gold nanospheres of around 10-20 nm diameters while an increase of size brings to a redshift of the absorption band's maximum: the colour could so varies from red to blue.

Apart from colour and painting purpose, more recently gold nanoparticles were firstly used as novel catalyst in organic and inorganic reactions, for instance the hydrogenation of ethylene or decomposition of hydrogen peroxide. Effects of size or combination of various other metals with gold nanoparticles were investigated and they still nowadays are under examination for the development of always-new efficient catalysts. In recent decades, they have also found applications in several other fields, from optical to nanomedicine.[32]

The extraordinary success that gold nanoparticles obtain for medical purpose is almost in part related to the fact that gold has always been considered a highly biocompatible material: it presents a very low toxicity even at high concentrations, no damage to organs occurs after prolonged exposition to gold nanoparticles, it is generally taken up by various organs especially by liver and spleen and could be excreted via the hepatobiliary system.[33] Even if additional studies have to be conducted prior to claim the non-toxicity of gold nanoparticles, this fact together with its unique properties has attracted great interest. As already said, the possibility to get more and different properties arises not only from changing size but also by varying shape; this is why during the last decades controllable synthesis of gold nanospheres as well as anisotropic structures have been developed and investigated especially for medical purpose (**Figure 1.3.2.2**).[34]
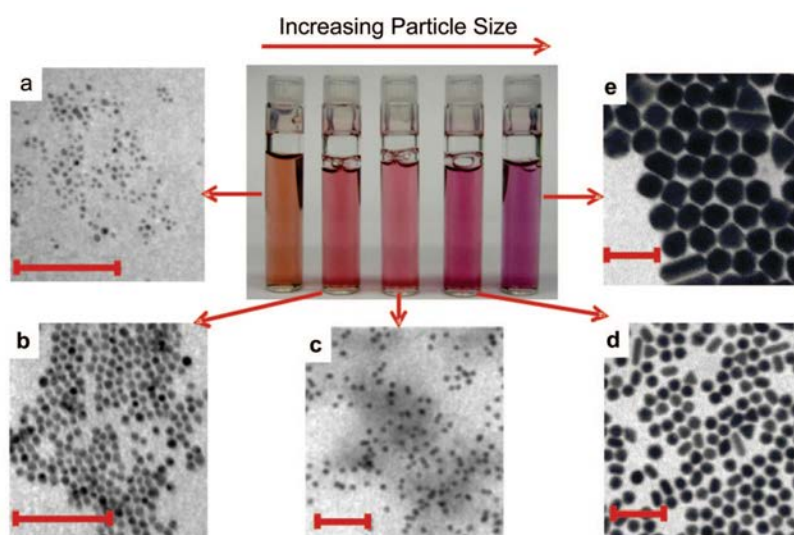

Figure 1.3.2.2: effect of varying size of gold nanoparticles. TEM images (scale bars 100 nm) and picture of different solutions of gold nanoparticles whit increasing size (from a to e). From *C.J. Murphy, Acc. Chem. Res., 2008, 41, 1721-1730.*

Particularly the nanostructures of gold in the form of rods, called gold nanorods (GNRs), have appeared fascinating. Indeed, they show two distinct plasmon resonance bands: the first, which falls around 520 nm as well as the nanospheres' one, is due to oscillations of electrons on the transversal (short) axis of the rod, and it is called transversal plasmon resonance (TPR), while the second, which falls instead to longer wavelengths, around 700 nm, is caused by oscillations of electrons along the longitudinal (long) axis and it is called longitudinal plasmon resonance (LPR). This second band is particularly interesting for nanomedicine applications owing to the fact that is much more intense than the other and can be finely

"moved" toward higher wavelengths (smaller frequencies) up to 1200 nm by increasing the aspect ratio (ratio between length and width) (**Figure 1.3.2.3**).
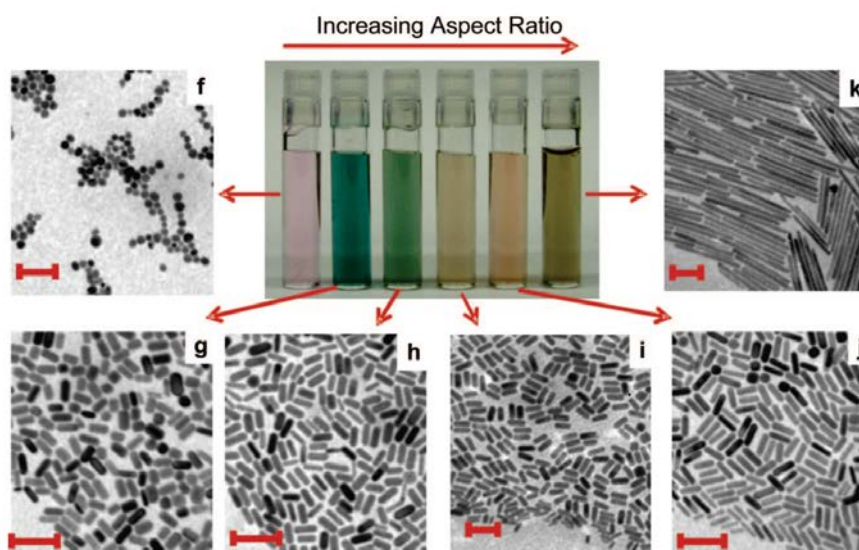

Figure 1.3.2.3: effect of varying the aspect ratio of gold nanorods. TEM images (scale bars 100 nm) and picture of different solutions of GNRs whit increasing aspect ratio (from f to j). From *C.J. Murphy, Acc. Chem. Res., 2008, 41, 1721-1730.*

It is known that in the range 800-1200 nm is placed the so-called Near Infrared Window (NIR): this represents for physicians a particularly attractive range of wavelengths due to the high transmittance (low absorbance) of water, deoxygenated haemoglobin and oxygenated haemoglobin in this, which allows the use of laser without interfering with or burning healthy tissues and organs (**Figure 1.3.2.4**).[35]
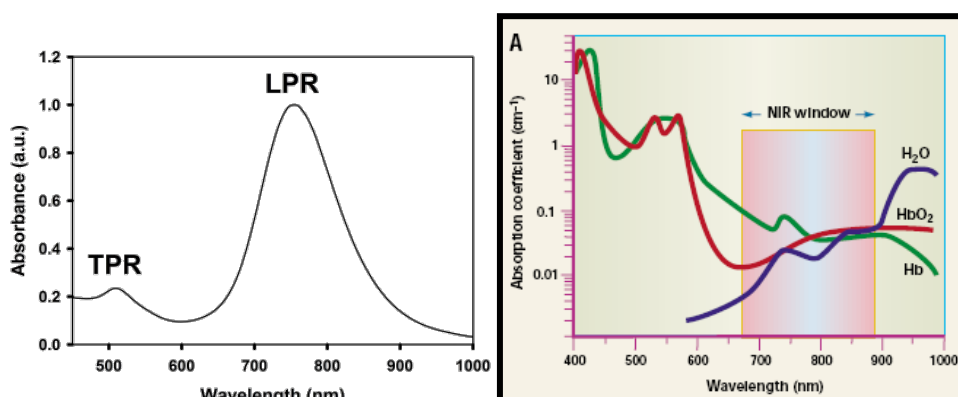

Figure 1.3.2.4: absorption spectra of GNRs (left) and absorbance of water, deoxygenated haemoglobin (Hb) and oxygenated haemoglobin (HbO$_2$) (right).

Due to these characteristics GNRs are finding applications in nanomedicine as real theranostic agents. Undeniably, they represent an innovative tool for diagnostic techniques that require the presence of a contrast agent. Several imaging modes can exploit GNRs, such as dark-field microscopy, optoacoustic and photo-optoacoustic imaging, two-photon enhanced luminescence, X-ray tomography, etc. GNRs present considerable advantages in comparison to other common contrast agents as molecular dyes, fluorophores or quantum dots in terms of prolonged stability, reduced photo bleaching under common imaging conditions, drastically reduced toxicity, enhanced absorption cross section and high scattering signal.[36] Moreover GNRs can be used as therapeutic tool due to the high capacity in absorbing radiation and convert it into heat. In GNRs more than 96% of the absorbed radiation is converted into heat by non radiative processes: this high optothermal conversion efficiency occurs as a consequence of the higher absorption cross section of GNRs than other nanostructures. GNRs rapidly absorb light but the relaxation process is slower and the result is energy release in form of heat. The generated local hyperthermia originates an increase in the temperature of the surrounding media of several degrees.[37] A so strong localized increment in temperature can be exploited to selectively destruction of cancer cells or diseased tissues as a powerful alternative to medical surgery or invasive therapies, making GNRs a real and appealing theranostic agent.

1.3.3 Silver nanoparticles

The history of silver's use has probably been long as well as the gold one. The people of the ancient Greeks, and Romans after them, already knew the bactericidal properties of silver and they exploited them for food and water disinfection, putting silver coins inside the amphorae to keep beverage and supplies fresh.

In centuries, products containing silver particles in the nanoscale dimensions have been developed and commercialized as pigments (see the Lycurgus cup, **Figure 1.2.2.1**), wound treatments and biocides. More recently, and especially in the last 100 years, silver nanoparticles (AgNPs) have also found applications in photographs, as conductive composites, new catalysts and from 1980 as enhancer of organic molecules' signals in Raman spectroscopy. In 1920 FDA approved the first silver solution for antibacterial purpose. Despite the fact that an extraordinary amount of researches has been conducted for the development of silver composites it was only in the last century that became clear that silver

nanoparticles and not simply silver ions were present in most of those products. In 1889, M. C. Lea[38] firstly reported the synthesis of a silver colloid stabilized with citrate and having a diameter between 7 and 9 nm, while in 1902 the stabilization of AgNPs by using proteins was reported and the so-obtained composite was firstly used in application for medical purpose.[39] Together with gold, also AgNPs possess unique optical properties due to the strong LSPR. For particles of around 10-20 nm the band falls in the visible range at 410 nm, giving the typical yellowish colour to the solutions (**Figure 1.3.3.1**).
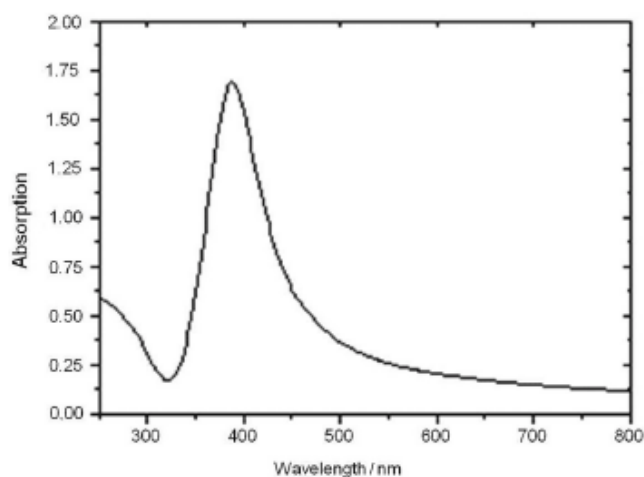

Figure 1.3.3.1: UV-Vis spectrum of silver nanoparticles in aqueous medium.

These special properties made AgNPs suitable for the development of sensors, optical and electronic devices so in the last decades a wide variety of papers and patents regarding their optimal synthesis were spread in the scientific community, making silver colloidal chemistry the most studied one. Silver is much more reactive than gold and the preparation of stabilized nanoparticles is more challenging than the previous one. Indeed AgNPs, as gold nanoparticles, are usually synthesised by reduction of silver salts with or in the presence of stabilizing agents such as citrate or polymers (polyvinyl alcohol or polyvinylpyrrolidone), which avoid a fast re-oxidation of the particles' surface and consequent aggregation in solution.[40]

Knowing the potential bactericidal activity of silver ions, AgNPs have attracted great interest for manufacturing of medical and highly specialized devices: textile industry inserts AgNPs into clothes and shoes to prevent sweat odour generation, toothbrushes with AgNPs on their surface were placed on the market to ensure high health and prevent colonies formation, etc. Silver ions are known for they ability to kill bacteria through different pathways: thiol groups present in amino acids and many other thiolated compounds represent an important target for

silver attributable the strong interaction between these two atoms. This leads to an increase of concentration of cations in the bacteria cells compartment with the consequence of a strong release of K^+ ions, which irreversibly alter the electrolyte transport. Moreover Ag^+ ions could enter in the active site of enzymes where sulphate or thiol groups are present blocking some essential metabolic process and leading to cell death. Silver ions also interact with metabolism with the result of an increased reactive oxygen species (ROS) production: this leads to the creation of imperfection in the double layers of membrane cells and brings to the collapse or the release of cytoplasm.

The activity of AgNPs as antibacterial agent is still under investigation, but the release of silver ions from the surface imperfections of the nanoparticles seems to be the driving force of the phenomenon. Certainly silver ions concentration is much lower in cells exposed to AgNPs than silver salts, because nanoparticles ions' release is slower and time dependent, while silver ions deriving from salts are immediately available (**Figure 1.3.3.2**).[41]
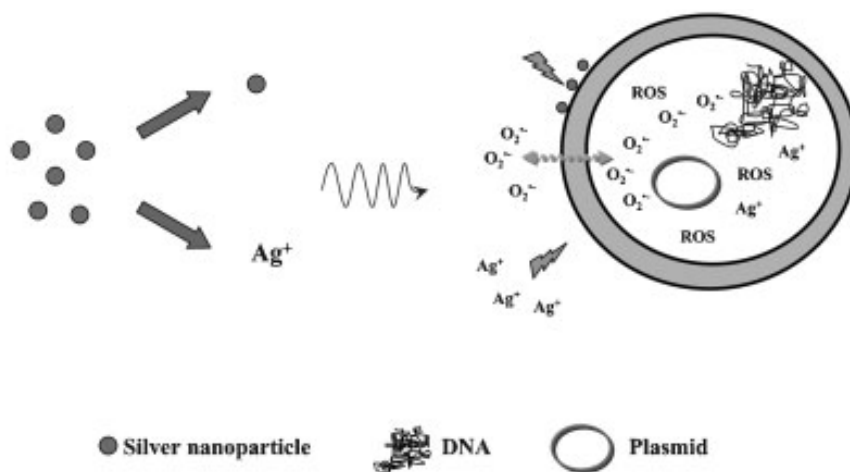

Figure 1.3.3.2: induced cell apoptosis by silver nanoparticles and silver ions.
E. T. Hwang, Small, 2008, 4, 746-750.

1.3.4 Surface modification of metal nanoparticles.

As already seen, the synthesis of metal nanoparticles generally occurs in water medium with the assistance of various kinds of surfactants, which stabilized the growing nanoparticles against aggregation phenomena.[42] These surfactants remain adsorbed or deposited onto the

nanoparticles surface once the process is finished, avoiding post-synthesis collapse of the created nanoparticles.

However, the possibility of transferring the nanoparticles already formed from the aqueous phase to an organic one offers several advantages: in fact, to be able to convey a therapeutic agent and/or a diagnostic tool within a cell it is necessary to entrap them in polymeric micelles that will perform the real drug delivery. This is actually quite complex, since it requires several conditions to be successful, for instance the obtainment of nanoparticles soluble in organic solvent.

The transfer of nanoparticles into an organic phase requires the development of specific ligands: these must replace the surfactants and simultaneously continue to prevent the aggregation phenomena, but at the same time, they must also ensure the solubility in common solvents.

A suitable method to coat nanostructures is the so-called self-assembled monolayer (SAM): it consists of an ordered monolayer, generally with an inclination of 30° respect to the surface, which is formed spontaneously by immersing a solid substrate in a solution containing particular molecules, with "amphifunctional" characteristics. Such molecules must present a "head" with a strong affinity to the metal surface, a central body usually constituted by a long chain and finally a "tail", or a functional group, which will determine the properties both of the monolayer formed and of the entire system (**Figure 1.3.4.1**).
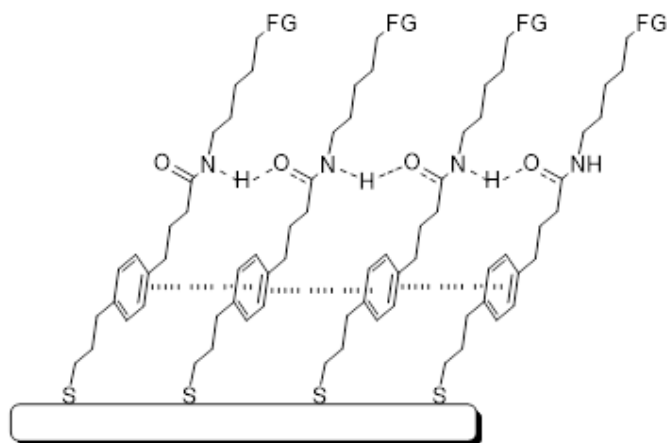

Figure 1.3.4.1: general representation of a SAM onto a metal structure.

For what concerns the functional group that must bind to the metal surface, several studies have been performed in order to evaluate their affinity with different kinds of metal. It is known as various organic molecules or functional groups are able of chemo-adsorb on

surfaces of inorganic solids. Typical examples of these molecules are amides, siloxanes, ethers, acetylacetonates, carboxylic acids, phosphonic acids, and hydroxamic acids:[43] all these molecules are able to provide excellent interactions with metal surfaces; in the specific case of gold, however, none of these presents an affinity as high as thiols due to the particularly strength of the interaction sulfur-gold;[44] for this reason in recent years researchers have indeed followed this trend and gold nanostructures have been coated with various organic ligands containing thiols but also disulfides functional groups. On the contrary, in the literature there are still a few examples regarding the functionalization of silver nanostructures using thiols groups, and in the majority of the studies conducted on these nanoparticles a coating with other functional groups, such as amines, has been preferred, although even this noble metal presents strong affinity with ligands containing sulfur.[45]

As regards the chain which constitutes the "body" of the ligand, previous research has demonstrated the importance of the presence of amide junctions and aromatic components, the first capable of forming hydrogen bridges between the various chains, the second able to give π-stacking interactions that ensure greater stability to the structure.[46]

Finally, the terminal functional group of the ligand must confer the desired properties to the entire system. By introducing appropriate functional groups at the end of the ligands it is possible to obtain stability in different solvents or for instance make them react with common reactions of organic chemistry once they are already firmly anchored to the nanoparticles' surface.

By exploiting these potentialities, many opportunities, still poorly investigated, become accessible, such as the possibility to attach biomolecules directly onto the nanoparticles surface, thus creating hybrid systems applicable in nanomedicine, or in addition, the assembly of two different nanostructured systems by surface chemical reaction, in order to obtain a single complex system where the properties of the nanostructures remain intact thanks to the link of separation formed by the ligands themselves. Indeed, in the literature there are several examples of the creation of complex nanostructured systems obtained by growing a nanoparticle on the surface of another already existing, but at the same time examples of conjunction of two of them by simply organic reactions are still few or missing.[47]

Among these simple organic reactions, the famous click chemistry must be mentioned. The click chemistry's concept was firstly introduced by Barry Sharpless in 2001 as an innovative synthetic strategy for the preparation of substances in a quickly and reliably manner.[48] The reactions that meet the cardinal principles of click chemistry are those that occur under mild reaction conditions, that do not involve harmful solvents, or that are solvent-free and produce

high yield, harmless by-products, high stereospecificity, high atom economy, easily isolable products. The reaction should possess a large thermodynamic driving force (greater than 84 KJ/mol) in order to obtain a single reaction product, condition made possible thanks to reagents strongly activated known as spring-loaded reagents. It is clear that it is nearly impossible for a reaction to meet all the above criteria, but some of them are very close to the goal such as nucleophilic substitutions of epoxides and aziridines, additions to activated carbon-carbon double bonds, the Diels-Alder cycloaddition and 1,3-dipolar cycloadditions.[49]

The 1,3-dipolar cycloaddition reactions are an important class of reactions for the synthesis of polyfunctionalised heterocycles in a regio- and stereoselective manner.

The most famous example is the Huisgen's cycloaddition, whose copper catalyzed version is often simply known as the click reaction.[50] It provides for the coupling between an azide and an acetylene functional group forming a triazole, which can be variously substituted; however both azides and alkynes are kinetically stable and for that reason the reaction requires high temperatures and long times to be completed, or specific catalysts.

Copper (I) is the most used catalyst, insomuch that the reaction in this case takes the name of Copper-catalyzedazide alkyne cycloaddition (CuAAC); more specifically, copper catalyst not only greatly accelerates the reaction bringing it to completeness in a few hours, but at the same time leads to the regioselective generation of only the 1,4-regioisomer and not both the 1,4- and 1,5- as is the case of the non-catalyzed reaction. In recent years further possible catalysts have been investigated: among these ruthenium gave excellent results, in the so called "Ruthenium-catalyzed azide alkyne cycloaddition" (RuAAC),[51] which is capable, as copper is, to accelerate the reaction and to make it regiospecific, but generating only the opposite regioisomer, namely the 1,5 -substituted triazole. (**Figure 1.3.4.2**)
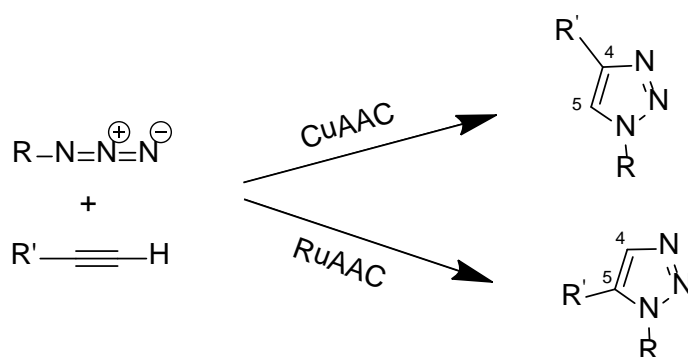

Figure 1.3.4.2: schematic representation of the Huisgen copper- and ruthenium-catalized azide alkyne cycloaddition.

Moreover, this reaction presents other substantial advantages since it can be conducted in common solvents such as tetrahydrofuran (THF), *N,N*-dimethylformamide (DMF), dimethylsulfoxide (DMSO), but also in water; it also occurs at ambient temperature, does not fear the presence of air and essentially generates no by-products, therefore it can be considered ideal for the reaction of complex and labile systems, such the nanostructured ones.

1.4. Polymeric nanoparticles

1.4.1 Advantages, properties and materials

As discussed in chapter one, the transport and delivery processes of nanoparticles through the body are of critical importance to obtain satisfactory results in nanomedicine. These processes are strongly affected by the physic-chemical characteristics of the nanoparticles, such as size, shape, surface charge, as well as their chemical properties. For instance, it has been demonstrated that nanoparticles with a mean diameter smaller than 60–70 nm are excreted fast via urinary system, while larger nanoparticles, with diameter larger than 250 nm can be easily sequestrated by liver or spleen: this shows how important the control of nanoparticles size is for successful applications *in vivo*.[52] In light of these considerations, it is clear how much importance plays the choice of materials for the creation of nanoparticles and nanocarriers especially. Nanoparticles for drug delivery applications are generally prepared from a wide variety of materials,[53] including metals, lipids and polymers.[54]

Metal nanoparticles, as previously shown in chapter two, surely offer the most promising opportunities in terms of special properties, therapeutic efficacy, imaging possibilities etc., but they also present several limitations for medical application when used alone, especially due to their fast elimination from body and/or degradation in physiological conditions.

In addition to this, polymeric nanoparticles (PNPs) have spread for applications in drug delivery and nanomedicine because they proved to be easily synthesizable with tunable characteristics and able to entrap and transport common poor water-soluble drugs greatly improving their solubility, bioavailability, retention time and release profile.[55] By using polymeric nanoparticles, several disadvantages belonging to traditional therapies can be overcome. These generally concern a not efficient drug absorption in body, a too fast elimination through kidneys or liver and the spread of the drug in various tissues or non-target organs; the major consequences are the reduction of the therapeutic index of the drug, more doses necessary to obtain efficacy and several unwanted side effects. PNPs carrying drug or other moieties can penetrate deep into tissue through capillaries and reach merely the target tissue, where they can be taken up by the cells, limiting simultaneously fast clearance and side effects.[56] Having seen all the benefits and advantages in the use of PNPs, many efforts have been made in the last decades to fulfil several requirements necessary for the application of these systems *in vivo*: scientists investigated numerous physical and biochemical properties,

like size, nature of the surface, and kind of the polymers used for the preparation of PNPs; new synthetic methods and purification processes were developed to ensure those unavoidable properties for nanomedicine devices. To be specific, materials used for nanomedicine application are required to possess several characteristics, such as high biocompatibility, great biodegradability, low toxicity, predictable release profile in body, good mechanical properties and body metabolites' elimination.[57]

Materials that were found suitable for the preparation of PNPs can be both synthetic and natural polymers. Synthetic biodegradable polymers were firstly used for nanomedicine applications in virtue of their properties of flexibility if compared to natural materials. Indeed, the preparation of synthetic polymers can be tailored to give a wide range of desired properties to the final product, such as presence of specific functional groups, appropriate polymer's length and weight, desired degree of hydrophobicity; in addition synthetic polymers show a pronounced uniformity between different batches rather than materials from natural sources, avoiding in these way irreproducible results in the final nanoparticles. These advantages, together with the fact that they frequently show good biocompatibility and biodegradability, have played a crucial role in synthetic polymers preference among scientific community.[58] Polyamides, polyesters, polyurethanes, polyacrylamides and poly(amino acids) were used to prepare various nanoparticles for nanomedicine scopes.[59]

1.4.2 Polylactic-co-glycolic acid and polyethylene glycol

Among all the other synthetic polymers, aliphatic polyesters have been widely investigated and exploited for the production of drug delivery nanocarriers, and in particular great attention have attracted polylactic and polyglicolic acids.[60] A copolymer made of the two of them in various ratio, the poly(lactic-*co*-glicolic) acid (PLGA) weas approved by Food and Drug Administration (FDA) for drug delivery and biomedical applications due to its attested biocompatibility and biodegradability (**Figure 1.4.2.1**). In fact, this copolymer undergoes complete and time-predictable biodegradation in physiological medium or *in vivo* systems, due to the enzymatic or non-enzymatic hydrolytic degradation of the ester bond present in the polymer chain and with uniform degree in all the polymeric matrix. Furthermore, this degradation process leads to two original monomers, lactic and glycolic acids, as products, that in body are rapidly metabolized in the Krebs cycle and again degraded in carbon dioxide and water or excreted unchanged by kidneys and urinary system.[61] Knowing how the degradation of this polyester happens in body has made the process's rate controllable and

tunable by simply changing copolymer length, weight and monomers ratio during the synthetic steps. PLGA is actually synthesized by ring-opening copolymerization of the two monomers lactic and glycolic acids that are not in a linear form but are used as cyclic dimers: they are linked in a random order during the copolymerization process but their total amount as well as ratio can be easily controlled to bestowed desired properties on the final product.[62] As a matter of fact, the molar ratio of two monomers directly influences important characteristics of the final polyester: the most important one is the degree of crystallinity, which brings to a different mechanical strength, swelling behaviour and finally hydrolization and biodegradation rate. It is well proved that a molar ratio of 50:50 in the two monomers leads to a faster biodegradation than any other molar ratio with higher quantity of either lactic or glycolic acid.[63]
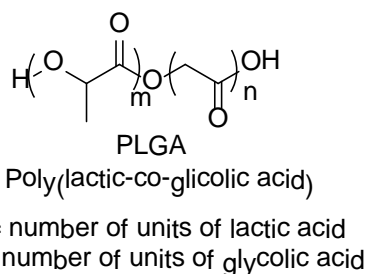

PLGA
Poly(lactic-co-glicolic acid)
m = number of units of lactic acid
n = number of units of glycolic acid

Figure 1.4.2.1: chemical structure of PLGA copolymer.

Owing to these properties, PLGA was the most utilized copolymer in medicine since 1970: firstly it found application as material for resorbable sutures, stunts and fibres due to its good mechanical strength and biodegradation, but recently it arose as favoured material for production of nanoparticles with drug delivery purpose. Indeed PLGA possesses the ability to form polymeric nanoparticles, nanocapsules or nanospheres suitable for drug delivery systems fabrication in view of the fact that they can host a wide variety of moieties (drugs, proteins, other nanoparticles) in their core, but they can be water redispersable, hence simply administrable intravenously or orally or parenterally in body, where they release those moieties in a well-defined time dependent manner.[60b]

Despite many advantages, nanoparticles made of PLGA present also some problematic disadvantages. They are in fact not very stable, but tend to aggregate in time, and for this reason it is necessary to introduce an auxiliary surfactant and stabilizing agents during the formation process that are not always biocompatible and not cytotoxic: the most used is generally poly(vinyl alcohol), which makes PLGA nanoparticles more stable in water, easier

to form and of smaller diameter compared to PLGA nanoparticles formed without surfactant. Moreover, PLGA nanoparticles easily undergo reticulo-endothelial system recognition, with a consequent fast removal from the bloodstream and a reduced residence time in body, which can lead in turn to a failure in drug delivery to the selected organs or tissues.

During the last ten years, many studies proposed the use of polyethylene glycol (PEG), instead of common surfactants agents, for the stabilization and quality improvement of different kinds of polymeric nanoparticles. PEG is an aliphatic polyether (**Figure 1.4.2.2**), worldwide synthesized by polymerization of ethylene glycol monomer in a large range of molecular weights.
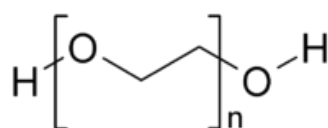
Figure 1.4.2.2: chemical structure of PEG.

PEG is found in many products of everyday life such as laxatives, drug excipients, additive in creams and toothpastes, ink solvents, anti-foaming agents in food.[64] Besides, PEG has been firstly used with drug delivery purpose in 1977,[65] coupled with proteins in order to enhance their permeation in body, and in 1990 the first PEG-protein conjugated was approved and commercially available.[66] During these studies, PEG arose as an impressive stealth polymer, able to solve many problems related to drug delivery inefficacy, so that the interest in its use grew exponentially. Indeed, PEG possesses a good hydrophilicity and it can be used to increase water-solubility of polymeric nanoparticles and also to stabilize them against aggregation by steric hindrance. Unfortunately, it is not possible to consider PEG as a biodegradable polymer, because experimental evidence clearly shows that it is eliminated by the kidneys without undergoing any biodegradation process. On the other hand, PEG with low molecular weight (less than 5 kDa) does not accumulate in organs even at high concentrations and it is extremely biocompatible, with no or few side effects after administration. Among all its advantages, the most important one remains the capacity of PEG to reduce opsonisation phenomenon of nanoparticles or small molecules at which it is anchored through a sort of "masking" ability: this effect is known as stealth effect and it has been experimentally demonstrated. More specifically, the presence of PEG on the surface of a nanoparticle avoids the recognition by the immune system of the same as a foreign moiety, with the consequent impossibility to be attacked by macrophages and taken up by RES organs such as liver and

spleen. This can bring to a dramatic increase in blood circulation time: it has been shown that PEGylated nanosystems could reach an extension in bloodstream residence up to 63% after intravenous administration compared to the non-PEGyalted ones. The outcome of this prolonged *in vivo* lifetime is the possibility for a drug delivery system to reach easier its site of action, where to take advantage of the enhanced permeability and retention effect or of an eventually present active targeting.[67]

The use of PEG in combination with PLGA occurred in 1994 when Gref developed PLGA microparticles coated with PEG in their external surface that showed an increased life time directly dependent on the amount of PEG used for the coating.[68] The coating with PEG is nowadays still exploited, but a covalently bind of PEG onto the nanoparticles surface has demonstrated to be much more efficient due to PEG impossible desorption in physiological medium, and increased surface density.[69] Following this suggestion, different kinds of copolymers based on PLGA and PEG were synthesized: they could be random or multi-block copolymers, linear or branched, with or without ending functional groups, and they have been all investigated in order to find the best candidate for drug delivery aim. To be specific, the di-block copolymer PLGA-*b*-PEG (**Figure 1.4.2.3**) has attracted great interest among scientific community.
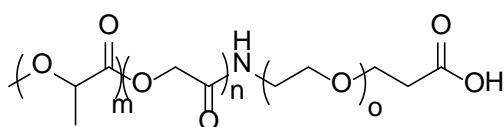

Figure 1.4.2.3: chemical structure of PLGA-*b*-PEG di-block copolymer

This copolymer presents several advantages compared to all the other kinds of similar copolymers. First of all, despite being a new material with proper and unique properties, it maintains the biodegradability of PLGA and the biocompatibility of PEG, as well as PEG stealth effect, that is also enhanced by the presence of a covalent, strong amide bond between the two constituting polymers, which guarantee a high and stable PEG surface's density to the corresponding nanoparticles. Anyhow, the real amazing characteristic of this copolymer is its ability to self-assemble into micelles of nanometric size without the assistance of any surfactants. Indeed, PLGA-*b*-PEG presents a well-distinct lipophilic portion (PLGA) and a hydrophilic one (PEG) which, once conjoined, transform the resulting product in an amphiphilic copolymer; the presence of these two portions allows the self-assembling of the system into micelles, in a way similar to common surfactant behaviour: when put in contact

with a non-solvent (typically water) the copolymer directs its lipophilic chains inward while the hydrophilic ones outward to the water environment. By doing this the PLGA remains inside the micelles forming a lipophilic core which can entrap and keep well-protected lipophilic moieties such as drugs, small nanoparticles, molecules, while the PEG goes outside creating a shell which confers stability in aqueous media, stealth effect to the entire system and, finally, the possibility to anchor several entities for active targeting exploiting the residual functional groups deriving from a previous functionalization of the PEG chains.

Being so, the use of amphiphilic block copolymers, especially PLGA-*b*-PEG, have continually grown up for their ability to form various types of nanoparticles. For this reason several PEGs were made commercially available, with the possibility to choose various lengths, molecular weight and in particular different ending reactive groups, such as amino, carboxylic acid, methoxy, maleimido, azido, alkyne etc.

1.4.3. Preparation methods for polymeric nanoparticles

Several methods have been developed for the synthesis of PNPs. The choice of one instead of another depends upon several factors such as the polymer's nature, the solubility of the drug that must be encapsulated, and the kind of nanoparticles to be obtained. The preparation of nanoparticles starting from pre-formed polymers, instead of using monomers and exploiting the polymerization process itself, offers several advantages. Typically, micelles formed during a polymerization process may present a non-complete biodegradablility in addition to difficult purification from residual monomers or oligomers, which are frequently toxic.[70] Due to these reasons the preparation of polymeric nanoparticles starting from a preformed polymer, such as amphiphilic copolymers, is often preferred. The most common techniques in this field are well described in the review of Pinto-Reis et al.[71] At this stage only a description of the two most utilized methods for preparation of PNPs starting from amphiphilic polymers is provided (**Figure 1.4.3.1**).

The nanoprecipitation technique is also known as solvent displacement method; by using this technique, nanospheres or nanocapsules can be formed. During the nanoprecipitation process a non-ordered assembling of a polymer into a nanosized system occurs; this is attributable to a first nucleation of polymer in small aggregates followed by aggregation of these pre-formed nuclei. Due to the fact that the course is not an ordered assembling, no specific skills of the polymers involved are required: even if the use of this technique was focused mostly on polyesters and PEGylated polyesters, nanoprecipitation can be easily applied to amphiphilic

polymers as well as to homopolymers, charge or non-charge polymeric chains, synthetic polymers or natural ones.[72] The only restriction is that the polymer used for nanoprecipitation must be soluble in organic solvents that are miscible with water, such as acetone, acetonitrile, tetrahydrofuran, dimethylformamide and dimethylsulfoxide.[73] Practically, once dissolved the polymer and the desired lipophilic drug in the solvent, the obtained solution is put in contact with a huge amount of water, that acts as a non-solvent for the polymer: in a strongly mixed system, the fast diffusion of the solvent into the aqueous phase takes place and this leads to the instantaneous polymer deposition on the interface between the two phases, starting in this way the aggregation, and consequent precipitation, of the polymeric nuclei; the process spontaneously ends when the stability of the system is reached.[74] The water phase may contain a surfactant or a stabilizing agent in order to favour the stability of the colloidal solution; typical stabilizing agents are polyvinylalcohol (PVA), polyvinylpyrrolidone (PVP) and polaxamers, but the use of PEGylated copolymers allows avoiding their use.

During the process, the organic solvent remains entrapped into the polymeric matrix together with the eventually present hydrophobic moiety: this happens because there is a natural tendency to minimize the free energy of the final nanosystems. Once formed the nanoparticles, the organic solvent must be removed from the suspension: this is possible by evaporation under smooth reduced pressure for those solvents that are more volatile than water but not for dimethylformamide or dimethylsulfoxide that are high boiling solvents; in this case the solvent must be removed in the following purification steps, for example by using an ultrafiltration technique or dialysis.

The PNPs obtained with this technique generally present small diameters (50-250 nm) with narrow size distribution (polidispersity index, PDI lower than 0.2) and, depending of the polymer used, may be stable for long period. Several studies have been carried out in order to better understand the process, and to obtain tunable properties of the final nanoparticles; many parameters like polymer's concentration and molecular weight, water/oil ratio, solvent's polarity have been investigated and their effects on size, stability and morphology of the obtained polymeric nanoparticles have been elucidated. An increase in polymer's concentration, and a decreased miscibility of the solvent in water either leads to the formation of nanoparticles with large diameter; best results were obtained by using dimethylformamide and acetone, but the latter is usually chosen for its poor toxicity and lower boiling point.[75]

Differently from nanoprecipitation, the oil-in-water emulsion method is an ordered assembling process by which micelles can be formed. An amphiphilic polymer is usually required to obtain stable particles with nanometric size; the polymers must also possess high

mechanical strength due to the fact that high energy is usually involved in the process. PEGylated polyesters block copolymers, such as PLGA-*b*-PEG, are frequently exploited for this process, thanks to their high biocompatibility, good mechanical properties and amphiphilicity. For this technique, it is necessary to use an oil phase non-miscible with water, thus the polymers selected must present solubility in solvent like chloroform, dichloromethane, hexane, acetate or others. This means that, during the process, the oil phase containing the polymer, and possibly the lipophilic moieties that must be encapsulated, is emulsified and dispersed in the form of nanodroplets by using a high energy sonication into a huge aqueous phase, that acts also in this case as non-solvent phase; the amphiphilic polymer in this condition behaves as a surfactant, directing the hydrophobic potions towards the inner core while the hydrophilic ones remain oriented toward the surrounding aqueous environment, immediately forming micelles. In this way, the oil nanodroplets are captured in the micelles' inner core as well as any lipophilic drugs dispersed in them. The organic solvent is generally removed by evaporation under vacuum, stabilizing in this way the micelle structure while drugs remain entrapped in the hydrophobic polymer's chains matrix.

The micelles' diameters obtained with this technique are usually about 50-200 nm, and the size distribution is narrow in the same way of the one obtained in the case of nanoprecipitation. Also in the case of oil in water emulsion many parameters were studied to find correlation with the final obtained colloidal solutions, especially regarding the energy power involved.[76]
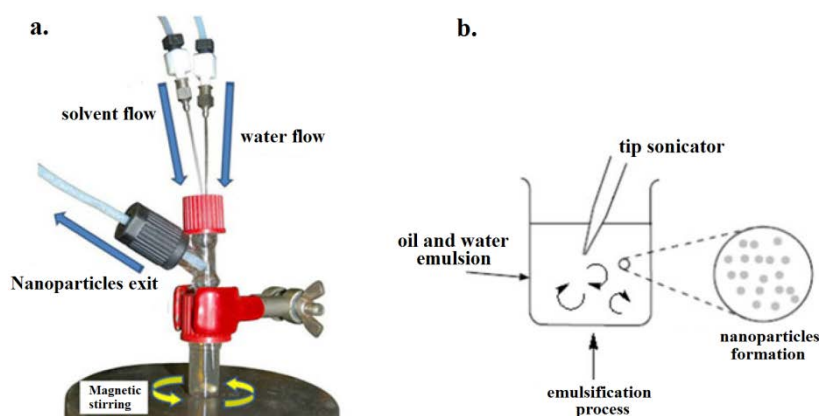

Figure 1.4.3.1: schematic representation of nanoprecipitation (a) and oil-in-water emulsion (b) processes. E. *Locatelli and M. Comes Franchini, (2012) J. Nanopart. Res. 14, 1316-1333.*

2. Aim

The present work aimed firstly at the development of multifunctional nanosystems whit drug delivery potentiality and secondarily at their preliminary evaluation as theranostic agents against glioblastoma multiforme.

More specifically, taking advantage by the state of the art, described in the Introduction, noble metal nanoparticles of silver and gold were synthesized in order to use them as active agents in the final multi-structured nanosystem. Particularly, gold nanorods (GNRs) and silver nanospheres (AgNPs) have been selected for their special properties. These nanoparticles were then capped onto the surface with specifically designed and synthesized organic ligands, able to create a self assembled monolayer thus stabilizing the nanoparticles and rendering them suitable for entrapment into polymeric nanocapsules.

Going towards the addressing of an efficient drug delivery, polymeric nanoparticles (PNPs) made of the promising poly(lactic-co-glycolic)-co-poly(ethylene glycol) acid (PLGA-*b*-PEG-COOH) were prepared: these would host, in their inner lipophilic core, gold and silver nanostructures or small molecules such as antitumor drugs.

GNRs were entrapped alone into the PNPs while AgNPs were entrapped both alone and simultaneously with the novel anti neoplastic drug Alisertib, in order to evaluate a possible synergistic effect between them.

Once obtained various kinds of PNPs, the targeting agent Chlorotoxin was conjugated on their outer shell, allowing in this way a more efficient and selective drug delivery against glioblastoma cells and tissues. The conjugation reaction has been possible thanks to the carboxylic acid groups exposed onto the PNPs' surface deriving from the free ending group of the PEG copolymer.

In addition, also the fluorescent dye Cyanine 5 or the radioisotope ^{99m}Tc were attached in order to allow common imaging techniques and follow nanosystems within the body.

Finally, all the obtained nanosystems were tested both *in vitro* and *in vivo* for preliminary proof of the concept of theranostic applications.

The possibility to exploit GNRs as contrast imaging agent was investigated, as well as their biocompatibility. Moreover, also the possibility to use them as therapeutic agents was investigated with *in vitro* studies of cells death thanks to localized hyperthermia and finally, a preliminary proof of concept for the importance of the targeting presence was addressed.

Similarly, in case of AgNPs the antitumor potentialities were investigated with *in vitro* studies, both for AgNPs alone and for the combined nanosystem containing AgNPs and Alisertib drug. Moreover, due to the encouraging results, also in vivo biodistribution studies and tumor regression investigation were successfully carried out.

Considering the promising results, a more step was made for the creation of a powerful theranostic device by linking together GNRs and AgNPs with click chemistry reaction between two reactive ligands coating the nanostructures: this approch allows the creation of a unique system and simultaneous maintenance of the properties of nanoparticles, thanks to the spacer that avoid touching between them.

Also this newly obtained complex system was successfully entrapped into the same polymeric nanocarrier and tested in order o check the properties' maintenance of the two nanostructures, thus opening the dream of multifunctional theranostic device for cancer fight and defeat.

3. Discussion

3.1. Synthesis of the precursors.

In this chapter, all the syntheses of the partners involved in the final nanosystems are described. These are the various organic ligands for nanoparticles surface coating, the copolymers for the assembling of the nanocarriers and, of course, the preparation of gold nanorods and silver nanoparticles.

3.1.1 Preparation of the organic ligands

First of all the organic ligand bearing an inert terminal group was prepared. The purpose of this ligand is the coating of surfaces of noble metal nanoparticles: the coating must ensure stability to the nanoparticles, complete removal of the previous surfactant agents, and solubility of the resulting nanoparticles into common organic solvents. Following the general rules to obtain a good self-assembled monolayer, described in Introduction-chapter 2, a ligand (**1**) with a thiol as head group, a long chain and an ester ending group were designed and synthesized.[77]

The synthesis of this ligand requires four steps. First of all the commercially available 4-mercaptobenzoic acid was oxidized with iodine in ethanol in order to obtain the corresponding disulphide (**Scheme 3.1.1.1**)
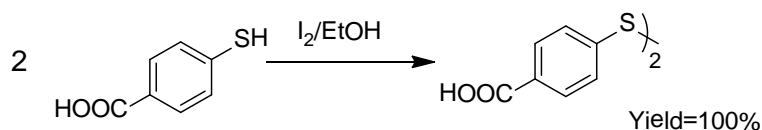
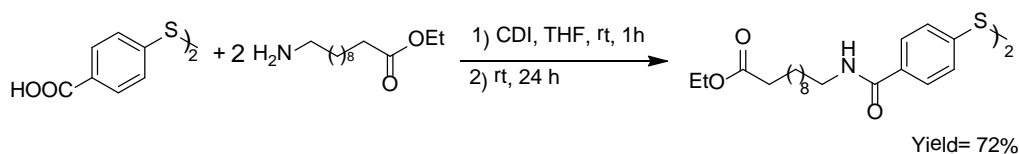**Scheme 3.1.1.1**: first step of the synthesis of ligand **1**.

This allows the protection of the thiol group and simultaneously it ensures the non-reactivity of the same as nucleophile during the following steps.

The second step of this synthesis consisted in esterification of the commercially available 11-aminoundecanoic acid with ethanol, giving in this way the corresponding ethyl ester (**Scheme 3.1.1.2**).
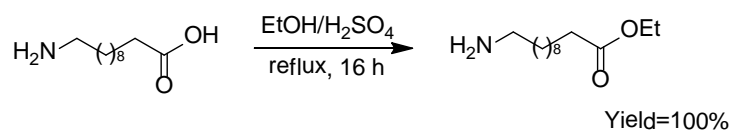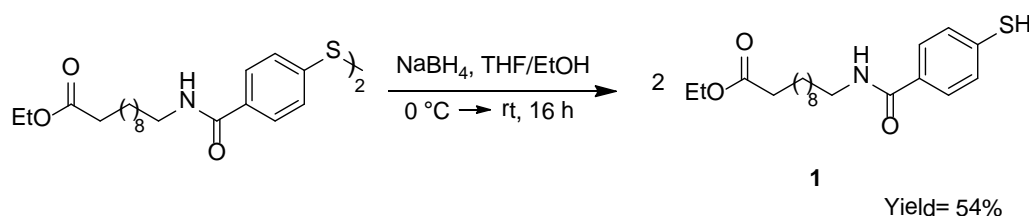
Scheme 3.1.1.2: second step of the synthesis of ligand **1**.

Once obtained, the two precursors were linked through an amide junction using 1,1-carbonyldiimidazole (CDI) as activating agent for the carboxylic acids present into the disulphide, and anhydrous tetrahydrofuran (THF) as solvent (**Scheme 3.1.1.3**).

Scheme 3.1.1.3: third step of the synthesis of ligand **1**.

Finally, the disulphide was reduced with sodium borohydride in order to restore the original thiol group and to obtain the final desired ligand (**Scheme 3.1.1.4**).

Scheme 3.1.1.4: last step of the synthesis of ligand **1**.

This ligand, having an ester ending group, will ensure great stability in organic solvents to the coated nanostructures; moreover it will not undergo side reactions in the following reaction conditions, necessary, for instance, during the polymeric nanoparticles formation or during click chemistry reaction between two nanostructures.

Next two ligands bearing an azido and an acetylene terminal group wew synthesized.[78] These two ligands must coat the same gold and silver nanoparticles as ligand **1**. In these cases the syntheses composed of two steps.

For the preparation of both ligand **2** and **3** the first step consisted in oxidation of the 11-mercaptoundecanoic acid with iodine, with the purpose of obtaining also in this case the corresponding disulphide (see **Scheme 3.1.1.5**).
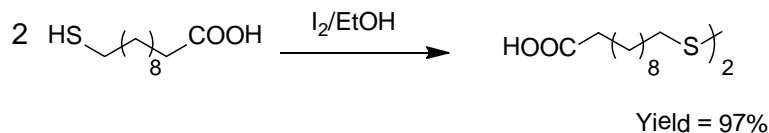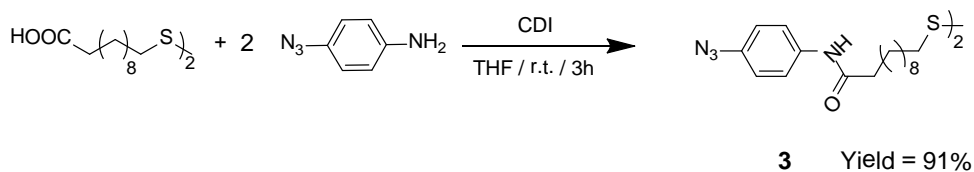

Scheme 3.1.1.5: first step of the synthesis of ligand **2** and **3**.

After this, for the synthesis of the acetylene-bearing ligand (**2**) the 4-ethynyl aniline was linked to the disulphide using CDI as activating agent for the carboxylic acids (**Scheme 3.1.1.6**).
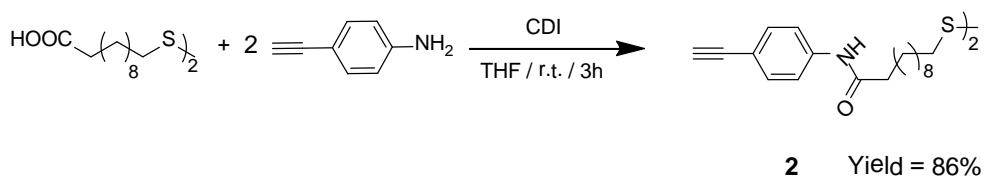
Scheme 3.1.1.6: second step of the synthesis of ligand **2**.

Similarly, for the preparation of the azido-bearing ligand (**3**) the second step was the linking of the reagent 4-azido aniline through an amide junction (**Scheme 3.1.1.7**).

Scheme 3.1.1.7: second step of the synthesis of ligand **3**.

As it possible to see, the ligands **2** and **3** still show the disulphide group instead of the thiol one. The choice not to restore the thiol group derived from the poor stability of acetylene and azido moieties under the reaction conditions required for the reduction and from the knowledge that also disulphides have strong affinity for gold and silver nanoparticles surface

as well as thiols. Thus the presence of a disulphide would, in most of the cases, lead to the same results obtained when a thiol is used.

All the obtained ligands were completely characterized by mean of ^{1}H-NMR, ^{13}C-NMR, infrared spectroscopy (IR), melting point (m.p.) and mass spectroscopy (ESI-MS).

### 3.1.2 Preparation of copolymer for nanocarrier.

A di-block copolymer constituted of PLGA and PEG presenting an ending functional group was synthesized for the obtainment of multi-functional nanosystem. PLGA with a carboxylic ending group (PLGA-COOH) is commercially available and, as already seen, it has been widely used for the preparation of safety and biodegradable polymeric nanoparticles. For the synthesis of PLGA-*b*-PEG di-block copolymer a PEG bi-functionalized at both the two end must be used; H$_2$N-PEG-COOH, as well as many other functionalized PEGs, are nowadays commercially available and suitable for the fabrication of various functionalized co-polymers. Using common activating agents, the carboxylic acids present at the end of the PLGA polymer could be linked with the free amino groups present at one end of the PEGs portion giving PLGA-*b*-PEG-COOH copolymer.

For the preparation of PLGA-*b*-PEG-COOH, the activating agents *N,N'*-dicyclohexylcarbodiimide (DCC) and *N*-hydroxysuccinimide (NHS) were added to a solution of PLGA-COOH in dichlorometane (DCM), and left to react for 24 hours (**Scheme 3.1.2.1**). The so-obtained PLGA-NHS is purified by filtration of dicyclohexylurea (DCU) and precipitation in diethylether.
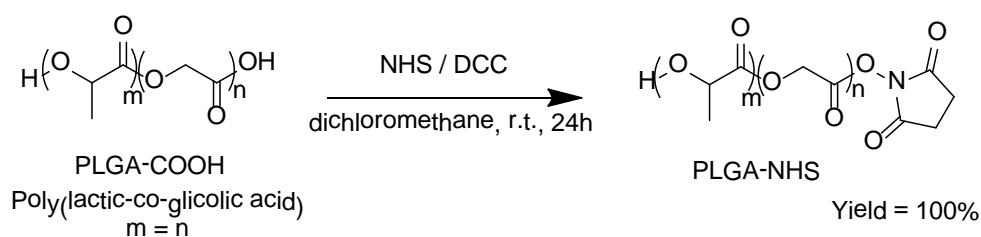
Scheme 3.1.2.1: first step of the synthesis of PLGA-*b*-PEG-COOH: activation of PLGA-COOH.

In a second step to a solution of the pre-activeted PLGA-NHS in chloroform, in the presence of an organic base like *N,N*-Diisopropylethylamine (DIPEA) the H$_2$N-PEG-COOH is added and left to react for one day (**Scheme 3.1.2.2**); the resulting co-polymer is purified by precipitation, washings firstly in diethylether and subsequently in water.
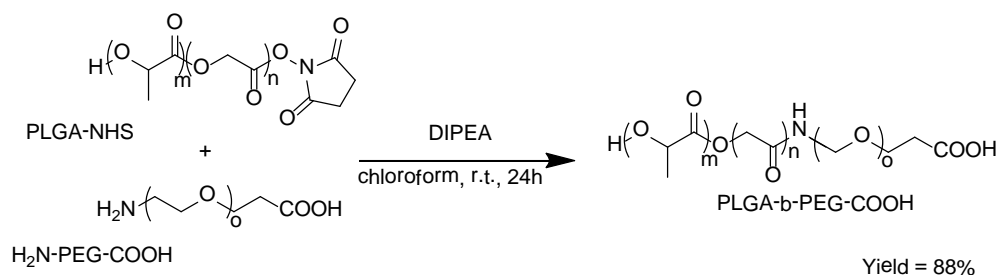
**Scheme 3.1.2.2**: second step of the synthesis of PLGA-*b*-PEG-COOH.

The copolymer was characterized by mean of ^{1}H-NMR. It must be stored in freezer at -18 °C, where it is stable for several months.

3.1.3 Synthesis of metal nanoparticles

Gold nanorods

For the synthesis of gold nanorods an already known methodology was employed. This technique was firstly adapted and applied to the synthesis of GNRs by Nikoobakht and El-Sayed in 2003, and is known as "seed-mediated and surfactant-assisted growth" method. By using this method, GNRs with different aspect ratio (length/width) can be obtained as well as a low amount of spherical particles, largely present when GNRs are synthesized with different techniques.

The procedure employs the use of a surfactant agent rather than a rigid templating one: the method consists in preparing the "seeds" of the nucleation by reducing a small amount of tetrachloroauric acid ($HAuCl_4$) in aqueous solution and also in the presence of the surfactant with a strong reducing agent, such as sodium borohydrate ($NaBH_4$), then in adding this seeds to the real growth solution, which contains ions of the adjuvant Ag^+, a substantial excess of the surfactant and a more abundant amount of $HAuCl_4$ partially reduced by Au^{3+} to Au^{1+} with ascorbic acid in order to facilitate the deposition of metal atoms to the seeds in growth (**Scheme 3.1.3.1**). The surfactant used during the synthesis is the hexadecyltrimethylammonium bromide, commonly known as CTAB. After 24 hours at controlled temperature (27-30 °C) a diluted solution of GNRs coated with surfactant is obtained, showing the typical red-purple coloration.
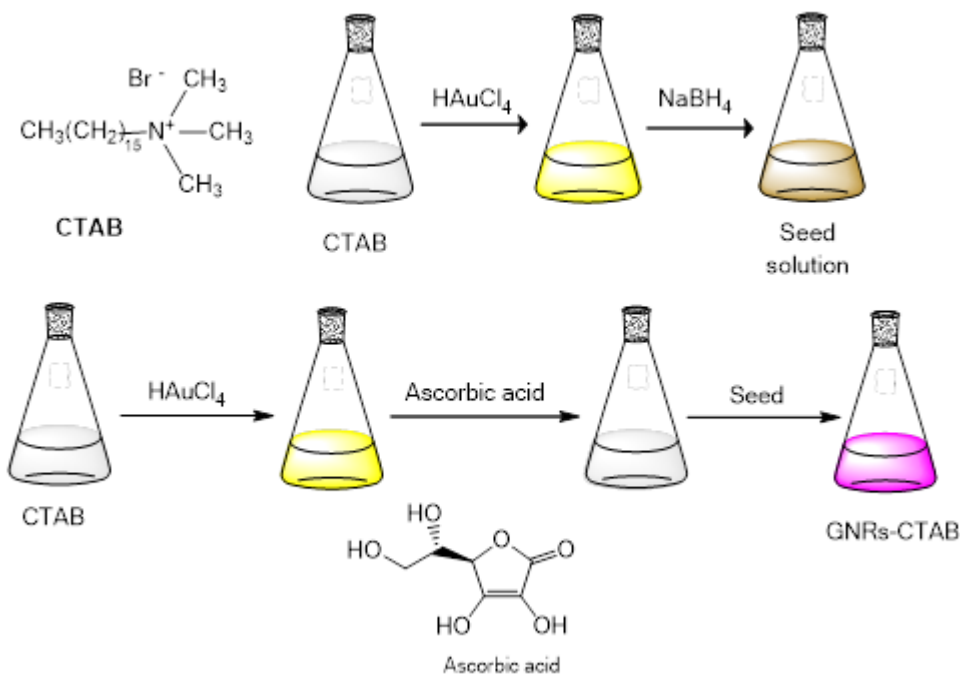
Scheme 3.1.3.1: representative procedure for the synthesis of GNRs

Regarding the mechanism, a great debate is still open to fully understand the role played especially by both the surfactant and the silver ions. Evidences showed that the CTAB is arranged in a bilayer structure around the GNRs, not only at the end of the synthesis, but also during the growing phase; more specificallythe head group of a first chain is oriented towards the surface of gold while a second is directed towards the water, leaving in the center the two hydrophobic tails. Silver ions seem to favor the proximity of more head-groups on the surface of the nanostructure, since being charged they tend to repel each other: silver ions can indeed come between them, and interact with Br^- ions present in the head groups, due to the fact that AgBr has a low Kps that behaves as driving force for this process. Probably for this reason, Ag^+ ions seem to promote the elongation of GNRs, and to increase their aspect ratio: evidences show, within certain limits, that the greater the amount of silver ions present in solution the greater the aspect ratio of GNRs obtained. This phenomenon was exploited to easily synthesize these nanostructures with controlled size and therefore specially designed properties.

The fact that the growth occurs preferentially in one direction rather than in all the others is to be attributed to the role played by the CTAB:[79] during the nucleation step, the seed that is formed, being already coated of surfactant, undergoes a first facial distinction phenomenon: this is the same that always occurs in the presence of impurities during the phases of

crystallization also of common organic and inorganic compounds. Once immersed in the growth solution, the seed undergoes the attack of the high concentrated surfactant preferentially on the most accessible {100} face and the formation of the bilayer in this direction prevents almost completely the growth of the structure, if not on the face {111} remained free from CTAB, thus leading to the rod-like structure desired: for the same reason, the {111} face remains in each following stage always more reactive than the {100} (**Scheme 1.3.2**).
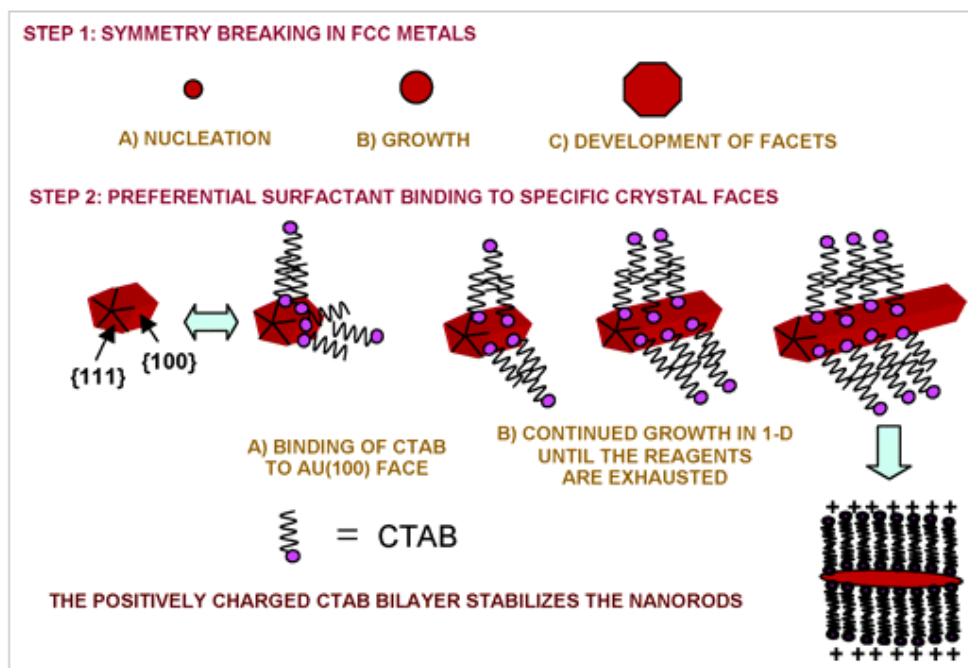
Scheme 1.3.2: growth mechanism and facial distinction in the synthesis of GNRs. *C. J. Murphy, J. Phys. Chem., 2005, 109, 13857.*

The presence of the surfactant is therefore essential for the synthesis of GNRs: indeed, several other surfactants were tested in addition to CTAB but results showed that both the nature of the head group, and the length of the chain of carbon atoms that constitute the hydrophobic tail may not be changed without irrevocably alter the process.[80] The major problem that arises with the use of CTAB is its high cytotoxicity: this was demonstrated in different studies and with various biological tests, which showed that the cell viability was always drastically reduced in the presence of CTAB or GNRs-CTAB, even at low concentrations. A complete elimination of CTAB from the GNRs surface would lead to aggregation of the same GNRs due to the lack of the agent stabilizer with consequent precipitation of the nanostructures. For this reason the replacement of CTAB instead of its removal must be preferred and exploited in order to reduce GNRs cytotoxicity.

Once obtained, GNRs-CTAB were purified and collected by high-speed centrifugation and washing with fresh water. After that they were completely characterized.

Transmission electron microscopy (TEM) analysis confirmed the obtainement of GNRs with no or low amount of gold nanospheres. The aspect ratio of this nanostructures resulted to be around 4, being length 50 nm and width 12-13 nm (**Figure 3.1.3.3 A**).

Uv-Vis spectroscopy showed the typical two absorption bands of GNRs, due to the longitudinal plasmon resonance (LPR) and to the transversal plasmon resonance (TPR). The first presented a maximum wavelength at 824 nm, while the latter a maximum at 518 nm, typical values for the obtained aspect ratio (**Figure 3.1.3.3 B**).
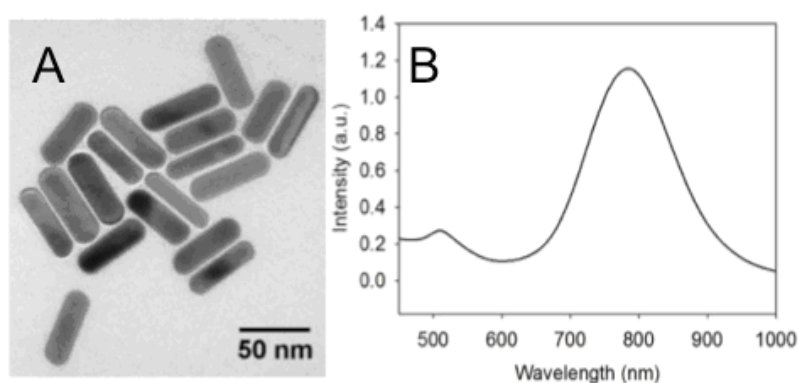

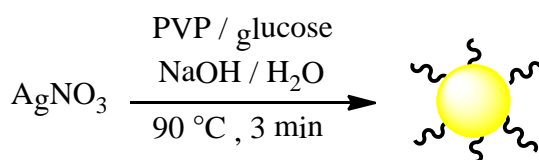**Figure 1.3.3**: TEM analysis (A) and UV-Vis spectroscopy (B) of GNRs-CTAB in water.

Silver nanoparticles

The synthesis of silver nanoparticles is formally more difficult than the one of gold nanoparticles: silver is more reactive than gold and this high reactivity could strongly interfere with the process of reduction, nucleation and deposition of neutral atoms into the nanoparticles' structure. Besides, the synthesis of nanospheres, instead of complex structures such as nanorods, is much easier thanks to the non-necessity to involve strongly shape control with template or surfactant agents.

Generally, in case of nanospheres' synthesis the so called "salt-reduction method" was used, which require only a sufficient strong reducing agent and the presence of a stabilizer. Most of the times the same reducing agent played also the role of stabilizing agent, consenting the nanoparticles synthesis and simultaneously avoiding aggregation of nanoparticles. Commonly used reducing agents were sodium borohydrate and citrate. Recently other reducing agents were tested in order to obtain always more concentrated solutions with homogeneous

particles. Among all the other surfactant agents, the polyvinylpyrrolidone (PVP) showed good ability to stabilize nanoparticles during their formation, avoiding aggregation phenomena, but consenting particles' growth with high uniformity. Moreover, PVP is less toxic than other surfactant positively charged: even in case of not complete removal PVP chains, which are neutral, it cannot interfere with DNA, which on the contrary presents a globally negative charge. Following the same guidelines, also the reducing agents were investigated: glucose was found to be able to completely reduce silver ions without interfering with nanoparticles' formation or affecting nanoparticles' growth.

Thus, the synthesis of silver nanoparticles was made dissolving PVP, glucose and NaOH in water, and rapidly adding at 90 °C an aqueous solution of silver nitrate (**Scheme 3.1.3.4**). After only three minutes at the same temperature, the nanoparticles formation was completed, and the colloidal solution was purified and concentrated with high-speed centrifugation washing with fresh water.

$$AgNO_3 \xrightarrow[\text{90 °C , 3 min}]{\substack{\text{PVP / glucose} \\ \text{NaOH / H}_2\text{O}}}$$

Scheme 3.1.3.4: synthesis of AgNPs-PVP.

Once purified, AgNPs-PVP were characterized by mean of UV-Vis spectroscopy, TEM analysis and dynamic light scattering (DLS), which was possible in this case due to the spherical nature of the particles (**Figure 3.1.3.5**).

UV-Vis spectroscopy revealed the typical absorption band of AgNPs at 410 nm: this was attributed to the surface plasmon resonance, and it conferred the intense yellow colour to these particles.TEM analysis confirmed the obtainement of silver nanospheres with great uniformity and in high concentration, without the presence of macro-aggregates. DLS analysis showed also that AgNPs have an average diameter of 5.5 ± 0.6 nm and a polydispersity index (PDI) value of 0.21 ± 0.011. Moreover, an elemental analysis by atomic absorption spectroscopy (AAS) gave an Ag value of 34064 ppm (315.8 mM).
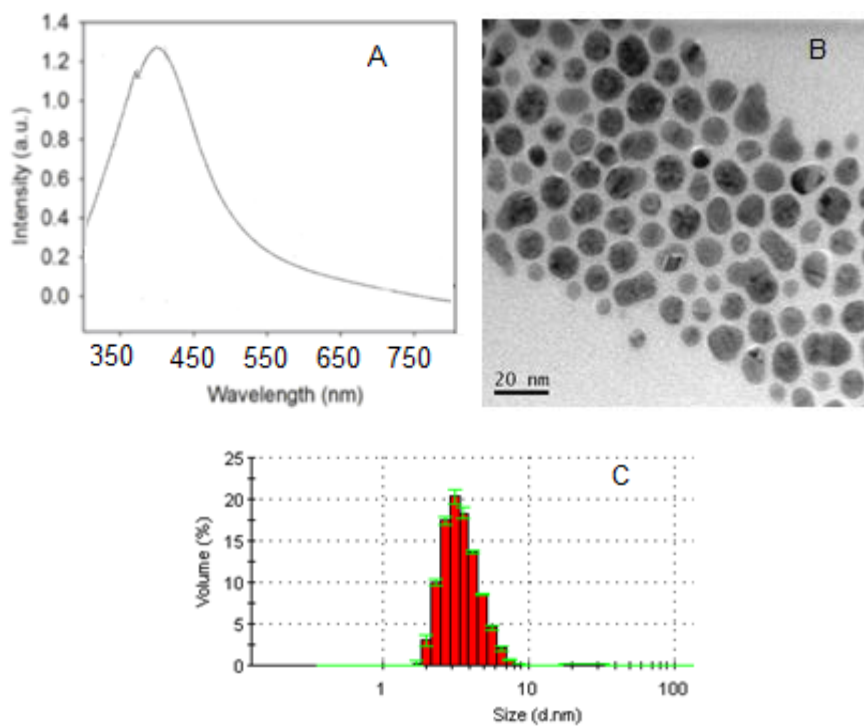
Figure 3.1.3.5: UV-Vis spectroscopy (A), TEM analysis (B) and DLS analysis (C) of AgNPs-PVP in water.

3.2. GNRs into polymeric nanoparticles: a theranostic tool against Glioblastoma Multiforme.

In this chapter, all the syntheses, preparations, characterizations and results obtained with GNRs are described. This means surface modification with organic ligand **1**, micelles formation and GNRs entrapment, decoration of the micelles' outer shell and all the *in vitro* and *in vivo* biological, physical and imaging tests.

All the procedures and results here described are part of- and can be found in-:

- M. Comes Franchini. J. Ponti, R. Lemor, M. Fournelle, F. Broggi, E. Locatelli: "Polymeric entrapped thiol-coated gold nanorods: cytotoxicity and suitability as molecular optoacoustic contrast agent", *J. Mater. Chem.*, **2010**, *20*, 10908–10914.

- E. Locatelli, W. Bost, M. Fournelle, J. Llop, L. Gil, F. Arena, V. Lorusso, M. Comes Franchini: "Targeted Polymeric Nanoparticles containing Gold Nanorods: A Therapeutic approach against Glioblastoma", *J. Nanopart. Res.*, **2014**, *16*, 2304-2313.

This chapter does not include surface modification with ligand **2** and **3**, as well as click chemistry reaction between GNRs and AgNPs: for that see Discussion-Chapter 4.

3.2.1 GNRs surface modification

As already discussed in Discussion-Chapter 1, water soluble GNRs can be synthesized in an easy and reproducible manner, also tuning their final aspect ratio and properties by the "seed-mediated growth method". Unfortunately, a high concentration of the surfactant and of the stabilizing agent CTAB is necessary in order to permit GNRs formation and simultaneously to avoid GNRs aggregation and precipitation once synthesized. It has been demonstrated several times that free CTAB molecules have a strong cytotoxic effect on healthy cells,[81] attributable to its ionic nature, which leads to a strong interaction with DNA and RNA molecules. In addition to this, it is also true that their complete removal always gives an immediate irreversible aggregation of GNRs. CTAB replacement, instead of simple removal, has also been tried with almost unsuccessful results, because complete ligand's shift and new functionalization is much more challenging for GNRs than for gold nanospheres, due to the differentreactivity of the {111} and {100} nanoparticles' faces.[82] The only procedures present in literature involved the use of ionic resins or adsorption of electrolytes, which result both not suitable for biological application because of their cytotoxicity.[83] In the last few years many effort were done to address this issue, but nowadays few easy, reproducible and robust protocols were developed.

In our laboratories, a procedure for an efficient CTAB removal and exchange with a non-cytotoxic organic ligand has been recently developed: thanks to a one-step reaction, a complete replacement of CTAB without affect GNRs stability can be performed, obtaining simultaneously lipophilic GNRs, suitable for the entrapment in polymeric micelles.

The ligand chosen for this purpose is the ligand **1**: the choice was based on the SAM's general rules and on the strong affinity of the thiol group with the gold surface.

The ligand's exchange reaction (**Figure 3.2.1.1**) requires the preparation of a hydro-alcoholic mixture: the acqueous phase contains GNRs-CTAB while the alcoholic phase is a solution of the ligand **1** in ethanol.
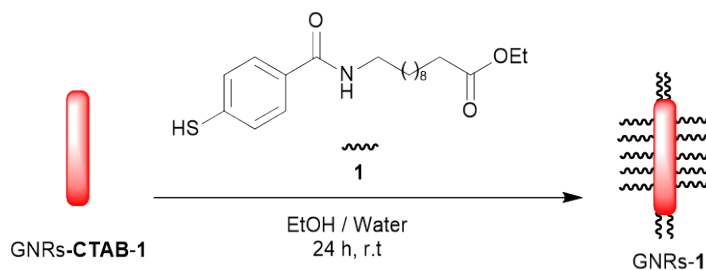

Figure 3.2.1.1: schematic representation of the ligand exchange reaction

After mixing the two solutions an ultrasound sonication lasting one hour is performed in order to allow the first process of the SAM[84]: this is a kinetically regulated step in which the head of the ligands interact with the metal surface replacing CTAB, though with a not yet ordered structure. After this first process 24 hour of incubation under slight mechanical stirring are necessary for the success of the second process of the SAM: this is a thermodynamically regulated step in which the tails of the ligands reach the minimum energy, that consists in a highly ordered structure, with all the chains oriented at 30° to the surface. This monolayer made of ligand's molecules attached to the metal surface confers high stability to the nanoparticles and a drastical change in the solubility of the same, thus leading to the obtainment of lipophilic GNRs.

After completing the ligand exchange, purification by several washes with ethanol, where CTAB is highly soluble, is necessary for the removal of unreacted ligand molecules and of replaced CTAB .The so-modified CTAB-free GNRs-**1** can be easily re-dispersed in common organic solvents such as chloroform, dichloromethane, acetone, tetrahydrofuran or dimethylformamide. Besides, the highest solubility and stability was observed in chloroform and dichloromethane, for this reason these solvents were chosen for the following steps (**Figure 3.2.1.2**).
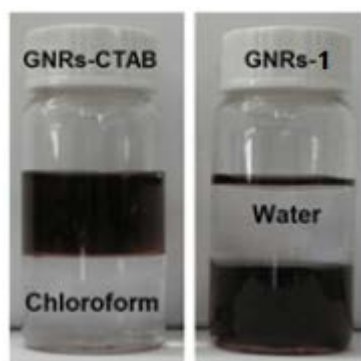

Figure 3.2.1.2: different solubility of GNRs-CTAB (water) and GNRs-**1** (chloroform)

GNRs-**1** were characterized by mean of several techniques in order to quantify the ligand exchange and to certify the effective removal of the CTAB molecules. UV-Vis spectroscopy was carried out showing maintenance of the properties of GNRs: indeed, the two absorption bands typical of rod-shaped nanostructures were still present, with no broadening and shape variation confirming the preservation of the metal nanostructures. Furthermore, a slightly red shift is observed in the LPR band (from 760 nm in water to790 nm in chloroform), which is generally more sensitive to the refractive index of the surrounding medium: this is in

accordance with literature feedback.[85] This was also confirmed by TEM images (**Figure 3.2.1.3**).
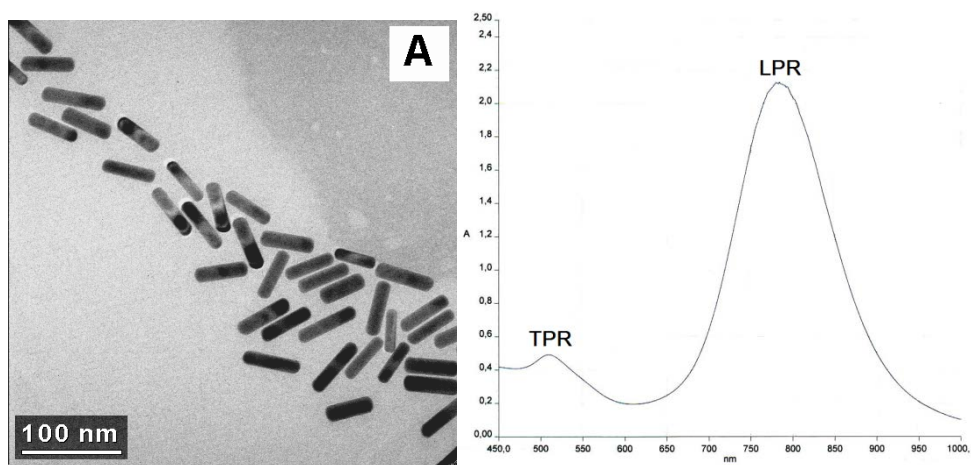

Figure 3.2.1.3: TEM image and UV-Vis spectroscopy of GNRs-**1** in chloroform.

^{1}H-NMR analysis was also performed: the comparison of the spectra of the ligand and free CTAB with the spectrum of GNRs-**1** clearly showed that CTAB molecules remained present neither on the metal surface nor among the ligand chains; besides, ligand **1** is clearly attached onto the metal surface, as demonstrated by the presence of all the significant ligand signals, and the disappear of the -SH hydrogen, meaning that the link with the metal surface has been effective (**Figure 3.2.1.4**).
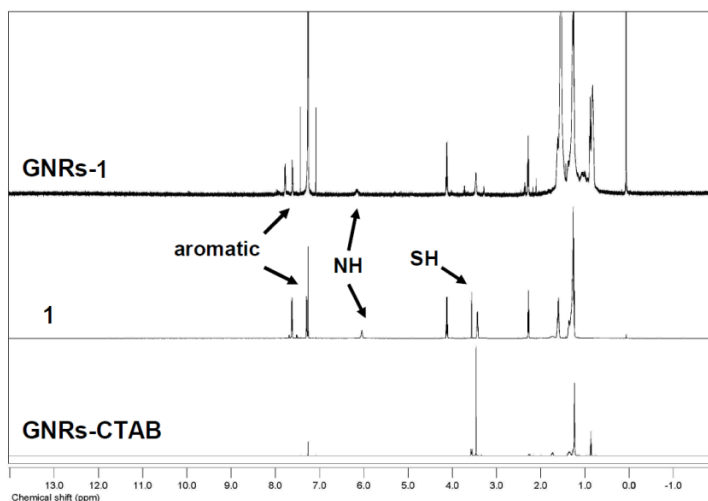

Figure 3.2.1.4: ^{1}H-NMR analysis of GNRs-**1**, ligand **1** and GNRs-CTAB in CDCl$_3$

Inductively coupled plasma atomic emission spectroscopy (ICP-AES) was exploited for the estimation of the metal content into the solution and showed a reaction yield of about 80% meaning that a good amount of nanoparticles can be recovered after the ligand exchange.

Gravimetric analysis revealed, by difference with the metal amount, that the ligand anchored to the surface is about the 35-40% of the entire system, which is satisfactorily high and surely high enough to ensure stability to GNRs during the following steps. IR spectroscopy confirmed once again the effective ligand exchange and the removal of CTAB (**Figure 3.2.1.5**).
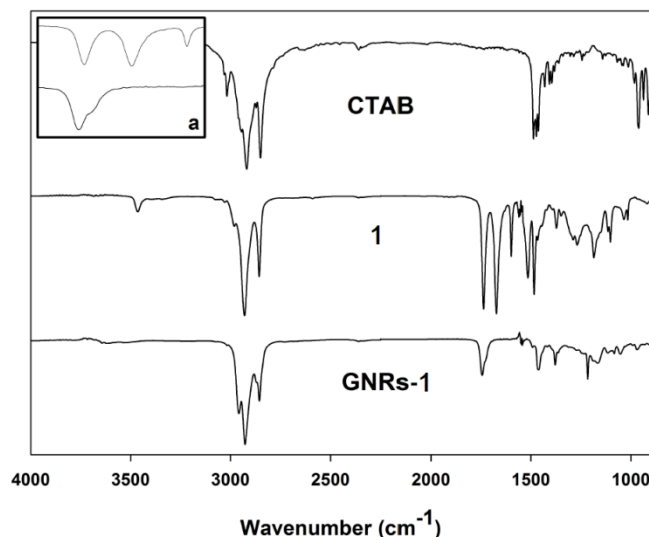

Figure 3.2.1.5: FTIRspectra of CTAB, ligand **1** and GNRs-**1** in KBr. Ligand **1** and GNRs-**1** comparison between 1800 and 1500 cm^{-1} (a).

3.2.2 Entrapment of GNRs into polymeric nanoparticles

Once obtained lipophilic nanostructures, they can be easily embedded into a polymeric core which shows the same lipophilic characteristic. This is the case of PLGA copolymer (see Introduction Chapter 4) and even better of PLGA-*b*-PEG copolymer. The latter of these can be exploited for the obtainment of polymeric micelles or nanocapsules (depending on the assembling technique involved), that possess a well-protected biodegradable lipophilc core, which can host not only small molecules but also nanostructures, provided they are lipophilic as well.

In case of GNRs-**1**, due to the higher solubility they showed in chloroform or dichloromethane, it is preferable to apply the oil-in-water technique, since it requires a non-miscible water solvent: more specifically, the use of dichloromethane instead of chloroform must be preferred when possible because of its lower evaporation point, which allows easier solvent removal at the end of the synthesis. Therefore, in a general procedure, PLGA-*b*-PEG-COOH was dissolved into a freshly prepared dichloromethane solution containing GNRs-**1**.

An aqueous phase was then slowly added on the top of the organic one and, after mutual separation of the two phases, a sonication with a trip probe sonicator was provided, in order to furnish the necessary energy to the system for the self-assembling process (**Figure 3.2.2.1**).

Figure 3.2.2.1: The two phases (solvent on the bottom and water on the top) just before the sonication process

After a short time (1-2 minutes), the two phases resulted completely mixed and an opal, pale pink colloidal solution was formed. The micelles formed were immediately stable and they did not require any incubation time; anyway, the solvent used remained entrapped in the lipophilic core as well as the GNRs-**1**, so it must be removed by evaporation under vacuum or by stirring the solution for a few hours. After solvent removal, the solution appeared more limpid and violet but a slight opalescence can be still visible due to the Tyndall effect typical of the polymeric nanoparticles.

Purification of the so-obtained solution is necessary for elimination of small un-reacted molecules, such as polymer chains, but also for removal of bigger aggregates, such as some GNRs collapsed during the step. Thus, two purification processes were performed. The first was intended to eliminate small particles and molecules and it was achieved by exploiting centrifugal filter devices that possess membranes with well-defined cut-off: particles smaller than 6-7 nm pass through the membranes and are eliminated with water, thus allowing concentration and simultaneous purification (**Figure 3.2.2.2**).
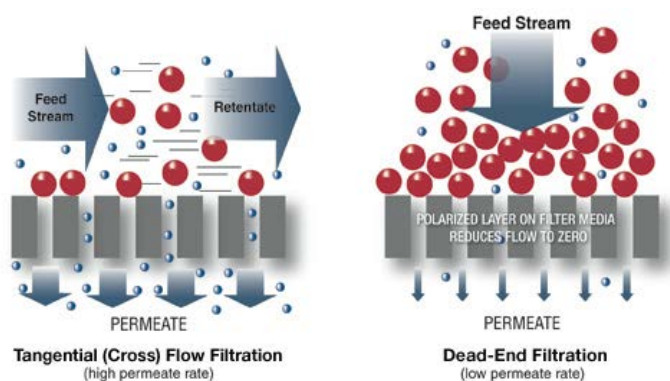
Figure 3.2.2.2: two different way of PNPs purification from small molecules: tangential flow filtration (left) and low speed centrifugation (right).

The retained volume, containing GNRs-**1**-PNPs, was subjected to the second purification step, which consisted in filtration through a syringe filter with cut-off of 0.22 µm that allows passage to GNRs-**1**-PNPs but not to bigger aggregates. Moreover, this kind of filtration left the material completely sterile since no bacteria are smaller than 250 nm. The so-purified solution can be used for biological test and all the other necessary steps.

GNRs-**1**-PNPs were completely characterized in order to furnish collaborators with all the useful information (**Figure 3.2.2.3**). TEM analysis clearly revealed the presence of GNRs embedded in a polymeric matrix of size around 100-120 nm. Dynamic light scattering (DLS) analysis showed a hydrodynamic diameter of 140.5 ± 1.40 nm and a polydispersity index (PDI) of 0.248 ± 0.013, meaning that the PNPs have a narrow size distribution. The ζ-potential value was found to be highly negative (-65.3 mV): this is due to the presence of free carboxylic acid groups on the micelles' outer shell, deriving from the free-end of the PEG chains used in the copolymer synthesis, that are deprotonated at physiological pH.
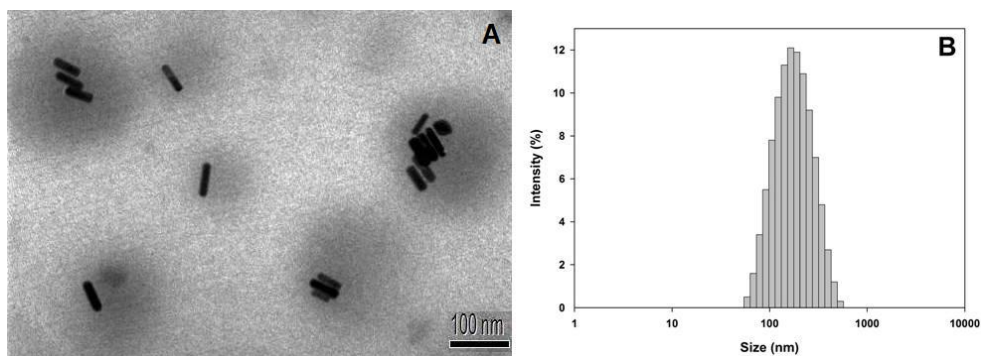

Figure 3.2.2.3: TEM image (A) and DLS analysis of GNRs-**1**-PNPs (B).

63

Atomic absorption analysis (AAS) was also performed for gold amount determination, which was found to be 0.21 mg/mL corresponding to a final solution of 1.07 mM. Total concentration of the nanoparticles in the final solution was estimated by weighting the dry matter after water evaporation and found to be 5.6 mg/mL.

3.2.3 GNRs-1-PNPs surface conjugation with active agents

One of the most challenging goals in the field of nanotechnology is the controlled modification of the surface of PNPs. Surface modification has gained increasing interest during the last few years, because it opens the possibility to modify the final properties of the prepared nanosystems, widening in this way their potential applications as discussed in Introduction. For surface modification of PNPs, covalent bonding of agents is generally preferable to physical adsorption or ionic interaction, due to its stronger nature, which prevents leaching from the nanoparticles' surface under physiologic conditions, and consequent random dispersion within the body. A covalent bonding requires the presence of a free terminal group on the nanoparticles' surface, able to react with the corresponding opposite group present on the agent to be attached. Several reactive groups have been exploited for this purpose. Carboxylic acids and amino groups are the most commonly used, because they can be easily introduced in the polymeric chains, and can react with one another under mild reaction conditions; maleimide group has also been exploited for surface conjugation reactions with amino or thiol groups as well as Huisgen 1,3-dipolar cycloaddition- click chemistry reactions between azido groups and alkynes.[86]

In our case, the conjugation reaction took advantage of the free carboxylic acids groups present in the micelles' outer shell: they derived from the free-end of the PEG chains, thus they can react with nucleophile groups, such as amino or alcohol groups, after pre-activation with water-soluble common activating agents. Generally, the carboxylic acids are activated using 1-ethyl-3-(3-dimethylaminopropyl) carbodiimide (EDC) hydrochloride and *N*-hydroxysulfosuccinimide (sulfo-NHS) in water for 1 hour. EDC reacts with carboxylic acids to form an active O-acylisourea intermediate; this intermediate is unstable in water and is subjected to hydrolysis, with restoration of the carboxylic acid and the consequent release of urea by-products. Therefore, O-acylisourea must react immediately with a primary amino group, which easily displaces the activating agent by a nucleophilic attack, with subsequent

formation of an amide bond, and release of the EDC by-product as a soluble urea derivative (**Figure 3.2.3.1**).
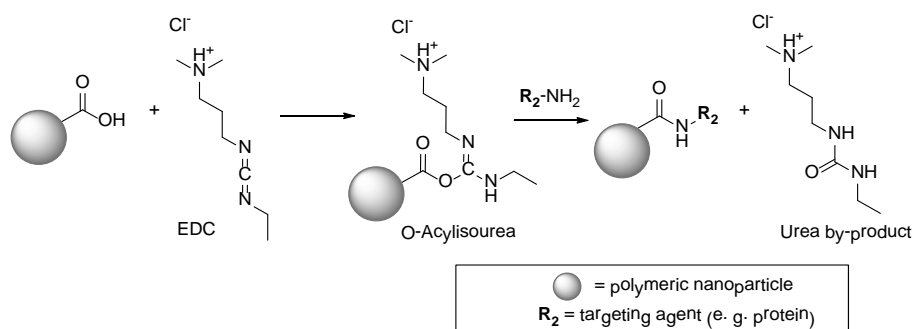

Figure 3.2.3.1: EDC activation of carboxylic acids on the surface of PNPs.

Although EDC can be used in neutral conditions, optimal effectiveness is achieved under moderate acidic media (pH = 4-6). When a phosphate buffer (pH 7.2) or simple water is used, the efficiency of EDC is reduced, and a water-soluble N-hydroxysuccinimide (Sulfo-NHS) has to be added in the reaction mixture. The formation of an NHS ester instead of O-acylisourea increases the stability of the system also at neutral pH values.

Following this procedure, GNRs-**1**-PNPs have been decorated in the outer shell with different types of targeting or imaging moieties, in order to allow either active drug delivery or common imaging techniques. As a first thing, the peptide Chlorotoxin was conjugated on the micelles' outer shell, because it is particularly suitable for glioma malignant cells targeting as described in Introduction. Fortunately, Chlorotoxin, as well as many other peptides, presents a free-amino group at one end, which can be exploited for amidation reaction with carboxylic acids. After 24 hours of reaction, purification by small molecules and aggregates is necessary as before, for this reason we repeated both the two process described in Chapter 3.2.2.

The so-obtained GNRs-**1**-PNPs-Cltx were then completely characterized. DLS analysis showed a hydrodynamic diameter of 155.1 ± 0.85 nm, with a narrow size distribution (PDI value of 0.180 ± 0.004), thus meaning that PNPs are not affected during the conjugation reaction. The ζ-potential value was equal to -21.4 mV, showing a slight increase if compared to GNRs-PNPs due to partial loss of free carboxylic acids, now involved in the amide bond. The concentration of gold, estimated with AAS analysis was found to be 195 ppm, corresponding to a solution 0.99 mM. ^{1}H-NMR analysis, performed on dried washing aqueous solution re-dispersed in D_2O, showed no signal for Cltx (diagnostic signal at 2.81 ppm),

meaning that the conjugation yield can be considered quantitative, thus the concentration of Cltx in the final sample was estimated to be 6.2 µM.

Then we also conjugated the fluorescent dye Cyanine5.5 (Excitation wavelength 675 nm, Emission wavelength 694 nm), in order to allow common imaging techniques and simplify biological investigations. Unfortunately, Cyanine5.5 can be purchased only with an ending NHS group, so a previous modification to transform –NHS group into an amino one must be performed to permit the coupling reaction. Because of this reason, Cyanine5.5-NHS ester was modified with diaminobutane (DAB): after 24 hours of incubation the amino-bearing Cyanine5.5 was obtained. Then the micelles were conjugated and purified following the previously described procedure. Even in this case the nanosystem was completely characterized. DLS analysis showed a mean diameter of 157.0 ± 2.4 nm with a PDI value of 0.327 ± 0.007 and a ζ-potential value of -28.4 mV. AAS analysis showed a gold concentration of 594 ppm, corresponding to 3.02 mM in the final concentrated solution. Uv-Vis analysis of washing aqueous solution was carried out to determine the Cyanine5.5 concentration in the sample solution, which resulted to be 2.9 mM.

Finally the same nanosystem decorated with both Chlorotoxin and the amino bearing Cyanine5.5, GNRs-**1**-PNPs-Cltx/Cy5.5, was obtained using the standard described procedure and purification. Characterization of the final nanosystem was carried out; DLS analysis showed a mean diameter of 122.5 ± 0.79 nm with a PDI value of 0.238 ± 0.014 and a ζ-potential value of -26.8 mV. AAS analysis showed a gold concentration of 1200 ppm, corresponding to 6.0 mM in the final concentrated sample. Uv-Vis analysis of washing aqueous solution showed a Cyanine5.5 concentration in the sample solution of 3.2mM, while the concentration of Cltx was estimated through ^{1}H-NMR analysis as previously described to be 6.2 µM.

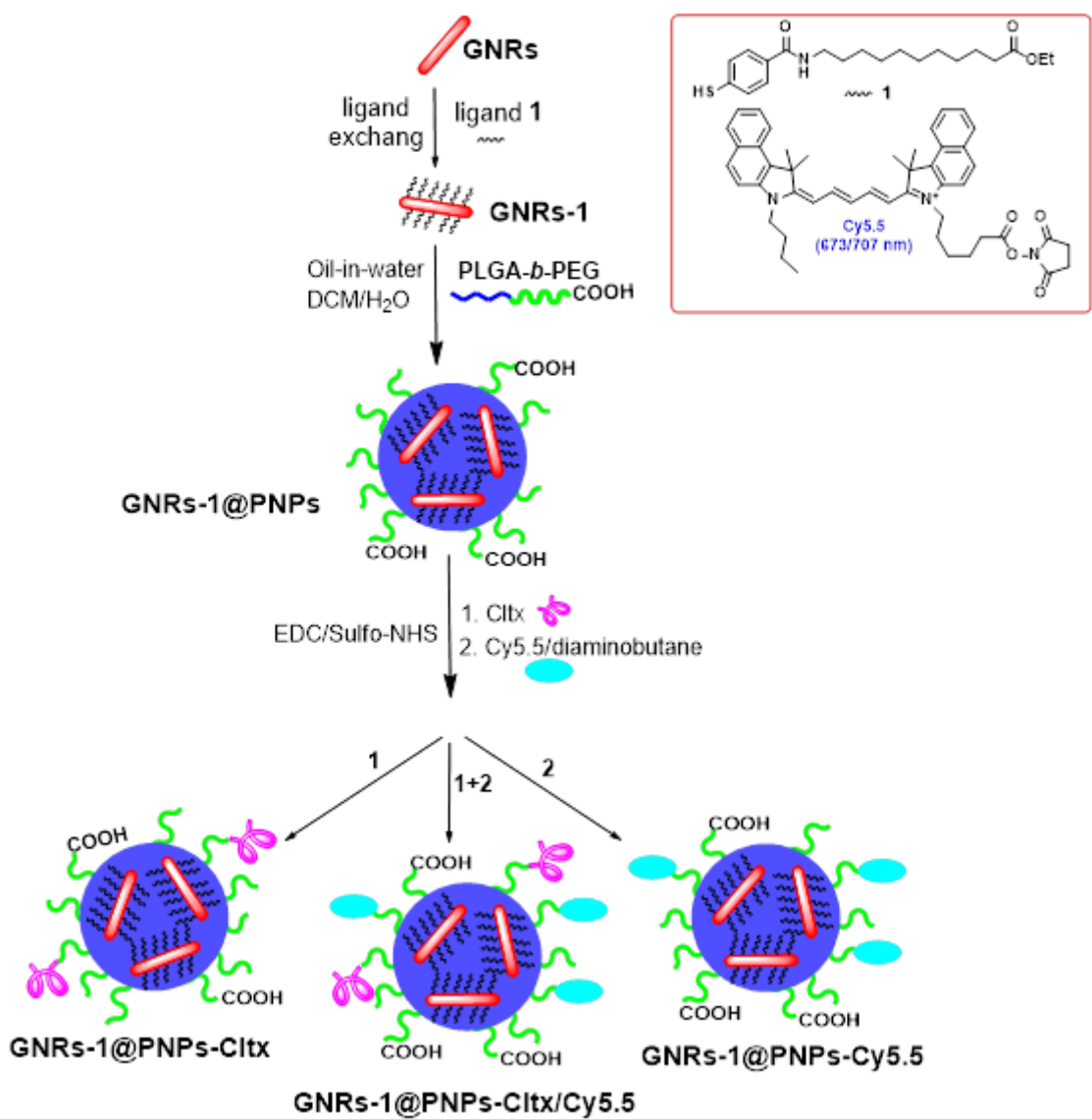Figure **3.2.3.2** shows a summary of the entire procedure described above.

Figure 3.2.3.2: schematic representation of the entire procedure for the preparation of the three GNRs-containing nanosystems.

3.2.4 In vitro and in vivo tests

The biological and physical investigations were carried out in collaboration with the European Commission, Joint Research Centre, Institute for Health and Consumer Protection Nanobiosciences, of Varese (Italy), with the Fraunhofer IBMT, Group Biomedical Ultrasound Research, of Sankt Ingbert (Germany) and with the Ephoran Multi Imaging Solutions of Colleretto Giacosa (Italy).

As a result of the special properties and biocompatibility of GNRs, the studies described below aimed to the evaluation of the final nanosystem as a theranostic tool: this means that the diagnostic capability was tested together with the non-cytotoxicity, but also with the possibility to exploit GNRs entrapped into the polymeric matrix as a therapeutic agent thanks to localized and highly selected hyperthermia.

First of all the stability of the suspension of GNRs-**1**-PNPs in biological medium was tested: for this purpose the two parameters of size and ion leakage were defined and checked to determine the behaviour of the nanosystems in the culture medium. This experimental set-up was considered due to the importance in understanding the behaviour of nanomaterials in culture medium, under different biological conditions (e.g. serum concentrations). In fact, it is of crucial importance to know the physic-chemical characteristics (e.g. aggregation state, stability, morphology, ion leakage, etc.) of nanomaterials also after they are put in contact with cells, and not only in water. The results showed a substantial stability of the nanosystem and were considered positive. Indeed, concerning the size distribution measurements in culture medium under different serum concentrations (from 0.1 to 10% v/v) low aggregation was observed comparing the size at time 0 and after 72 h of incubation without significant differences among the serum concentrations. Moreover, ICP-MS analysis showed that the GNRs-**1**-PNPs dispersants contained only traces of Au ions corresponding to 0.004% w/v of the tested concentration, meaning that no leaching occurred in time; in addition the amount of Au ions released from GNRs-1-PNPs, suspended in culture medium and incubated for 72 h under standard cell culture conditions (95% humidity, 37 °C, 5% CO_2) was too low to be detected by the analysis.

For a first citotoxicity evaluation Balb/3T3 (mouse embryonic fibroblasts cell line) were incubated with our nanosystem. This cell line is sensitive to chemicals/nanoparticles, and is therefore recognized as one of the most promising *in vitro* models for the study of the

carcinogenic potential induced by chemicals or nanomaterials. After seeding the cells, GNRs-**1**-PNPs suspensions were directly added to the cell culture, in order to obtain the appropriate final concentration of 1, 10, 20, 40, 60 and 80 μM. After 72 h of exposure, cell viability was studied by a Colony Forming Efficiency assay. Each experiment included a negative control (untreated cells in culture medium), a positive control (cells exposed to sodium chromate 1000 mM) and a blank control (cells exposed to the suspension containing only PNPs without GNRs). The results obtained on Balb/3T3 after 72 h of exposure to GNRs-**1**-PNPs showed for all the concentrations tested, except for 1 μM, a statistically significant toxicity versus the corresponding Blank-PNPs, meaning that a dose–effect relationship is present (**Figure 3.2.4.1**). The half-inhibitory concentration (IC50) was calculated to be 20.3 μM. The observed toxicity was not due to Blank-PNPs, in fact the corresponding volume, added to reach the highest tested concentration (80 μM) of this nanosystem did not produce any toxicity. In addition, since no Au free ions content was measured in the culture medium, after 72 h of incubation under standard cell culture conditions, we also excluded toxicity related to Au ions.
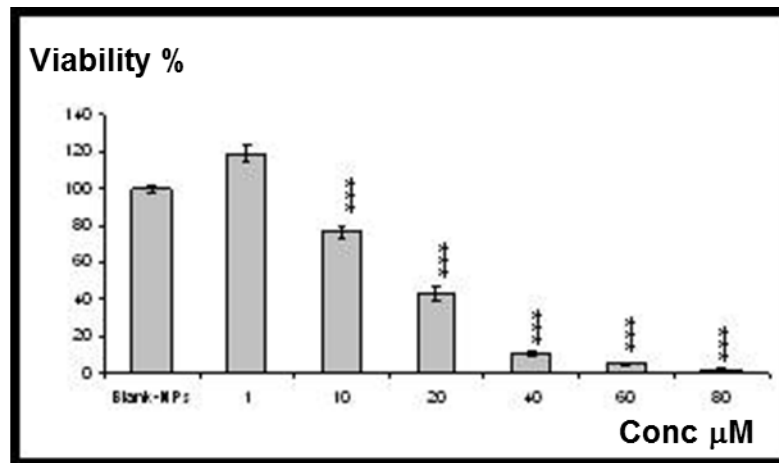

Figure 3.2.4.1: Cytotoxicity induced by GNRs-**1**-PNPs on Balb/3T3 cells after 72 h of exposure to concentrations ranging from 1 to 80 mM.

Therefore, a concentration of gold equal to 20-25 μM must be considered the limit in all the following studies.

After this, with respect to the possible future application of the particles as optoacoustic molecular contrast agents, the detectability of spherical tumor-mimicking gel phantoms, loaded with different concentrations of GNRs-**1**-PNPs was evaluated. For this purpose, three different concentrations of GNRs-**1**-PNPs (550, 110 and 11 μM) contained into alginate

spheres, were prepared as well as a blank control (PNPs without GNRs). The alginate spheres were prepared by adding alginate homogenized with the nanosystem into a solution of $CaCl_2$, where the spheres phantoms solidified instantaneously. For the imaging tests, the laser wavelength was set to 778 nm for single wavelength optoacoustic imaging, according to the particle absorption spectrum. Optoacoustic detectability of GNRs-**1**-PNPs was proved, as it is possible to see in **Figure 3.2.4.2**, since the gel pad is optically transparent and no optoacoustic signals could be generated.
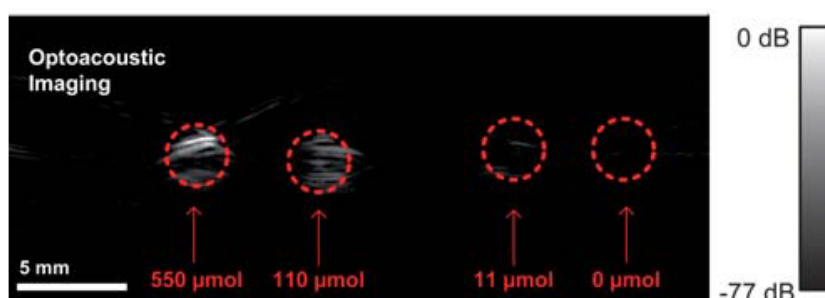

Figure 3.2.4.2: Optoacoustic image taken at 780 nm from three alginate spheres of GNRs-**1**-PNPs and for blank-PNPs

The image contrast of the gel spheres is clearly correlated to the concentration of the GNRs-**1**-PNPs in the optoacoustic image. While the sphere with a gold concentration of 11 µM can be recognized, no signal at all is generated by the control phantom consisting of blank-PNPs: the measurements clearly showed that phantom gel spheres containing GNRs-**1**-PNPs at a concentration as low as 11 µM can be detected with satisfying signal to noise ratio in the range of 10 dB. It has also to be mentioned that a laser fluence of 10 mJ/cm^2, corresponding to about 30% of the safety threshold for diagnostic imaging was used in all measurements. For this reason, GNRs nanosystems can be considered suitable contrast agents for diagnosis with optoacoustic technique.

Encouraged by this results, the binding affinity of GNRs-**1**-PNPs-Cltx towards glioblastoma cells was investigated using conventional optical phase contrast microscopy (**Figures 3.2.4.3** a, d and g) and optoacoustic microscopy (**Figures 3.2.4.3** b, e and h). GNRs-**1**-PNPs-Cltx were incubated for 20 h with U87MG (Human glioblastoma-astrocytoma, epithelial-like cell line) at a concentration of 25µM of gold, value chosen after evaluation of IC50 found on Balb/T3 cell line, and imaged using a system, consisting in an inverted optical microscope, a

laser source, a single element transducer, and an electronics system.[87] This system set-up allows intrinsic 3D imaging of samples with optical contrast based on an acoustical detection mechanism. For control experiments, U87MG cells without NPs-incubation and U87MG cells incubated with GNRs-**1**-PNPs (without chlorotoxin) at a concentration of 25 µM of gold were used. The results showed that no differences between untreated cells (Fig. g), cells incubated with GNRs-**1**-PNPs (Fig. d) and cells incubated with GNRs-**1**-PNPs-Cltx (Fig. a) can be observed in optical mode. On the contrary, a clear difference was recognizable using optoacoustic microscopy. Control cells that were not incubated with GNRs did not show any optoacoustic signal (Fig. h), and a pure noise image was obtained. Incubation with GNRs-**1**-PNPs led to a minor signal (Fig. e), while for cells incubated with GNRs-**1**-PNPs-Cltx, stronger and more abundant signals were detected (Fig. b). It must be underlined that optoacoustic signal amplitude is directly proportional to the local absorption coefficient of the sample: given that the contrast agents used have a much higher absorption cross section at the wavelength of interest than the native cells, it is clear that the enhanced signal amplitude in the samples incubated with GNRs-**1**-PNPs-Cltx indicates an effective binding of the particles to the cells. The lack of signal in figure h confirms that no optoacoustic signal is induced by the cells themselves; therefore, all measured signals in Figs. b and e rely on the presence of GNRs-**1**-PNPs-Cltx and GNRs-**1**-PNPs, respectively.

The surface density of bound PNPs was estimated from the images, by calculating the ratio between the area where PNPs have bounded (bright pixels), and the total area of the cells in the investigated sample. Values of 30%, 0.3% and 0.003% were obtained for cells incubated with GNRs-**1**-PNPs-Cltx, cells incubated with GNRs-**1**-PNPs and non-incubated cells, respectively. The considerably higher value obtained for cells incubated with GNRs-**1**-PNPs-Cltx confirms the suitability of Cltx as a binding agent towards U87MG glioblastoma cells.
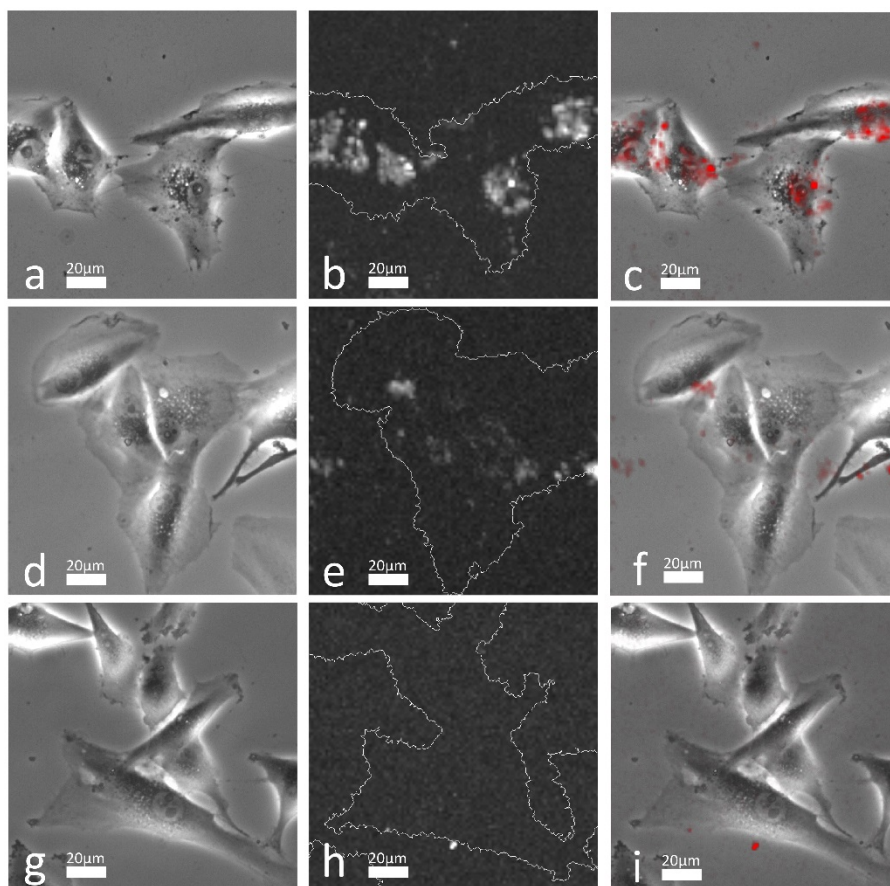
Figure 3.2.4.3: Optical microscopy (a, d and g) and optoacoustic microscopy (b, e and h) images of U87MG cells after incubation with GNRs-**1**-PNPs-Cltx (a, b), after incubation with GNRs-**1**-PNPs (d, e) and control cells (g, h). An overlay of the optical images and the optoacoustic images is shown on the right (c, f and i, optoacoustic data shown in red) to easily localize the actual distribution of NPs in target cells.

The above-described experiments confirmed the possibility to exploit GNRs-**1**-PNPs-Cltx as a powerful diagnostic tool. Besides, for a real theranostic agent, it must be demonstrate also its potentiality as therapeutic device. In case of GNRs hyperthermia and consequent termo-ablation of tissues after laser irradiation can be obtained and exploited for therapeutic approach against cancer. Thereofore, to demonstrate a preliminary proof of concept of selective laser induced cell death, glioblastoma cells incubated with GNRs-**1**-PNPs-Cltx were irradiated with the described microscopic imaging system (**Figure 3.2.4.4**).
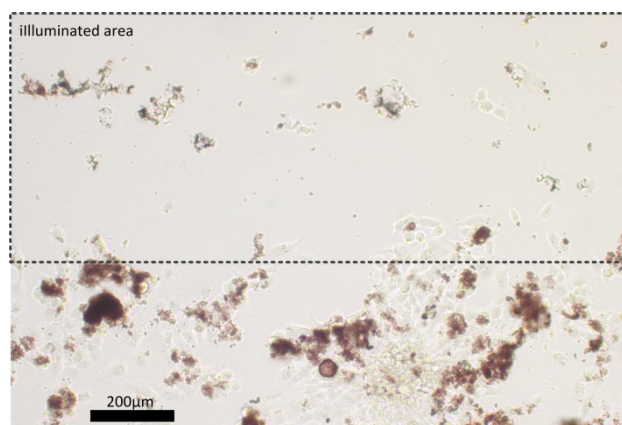
Figure 3.2.4.4: U87MG glioblastoma cells incubated with GNR-**1**-PNP-Cltx. The part of the cell chamber that has been illuminated with laser is surrounded by a dotted line.

First, control experiments using cells without any particles were conducted. Illumination of these cells did not show any influence on cell morphology or vitality because cells present in this spectral range are rather trasparent. Therefore, no effect was induced. In a second experiment, cells were incubated with GNRs-**1**-PNPs and even in this case no significant alterations on cell morphology were observed. In contrast, after incubation with GNRs-**1**-PNPs-Cltx, a short exposition to the laser resulted in cell death, as can be seen in Figure **3.2.4.4**. In the irradiated area (surrounded by the dotted line), only a few cells can be observed, confirming cell death and subsequent detachment from the substrate as a result of irradiation. Interestingly, colonies of living cells can be recognized in the lower part of the image, corresponding to the non-irradiated area. As a consequence, the viability of the non-irradiated cells was investigated after the experiments and confirmed that no effect was inferred due to exposition to GNRs-**1**-PNPs-Cltx without laser irradiation.

The so-obtained results are extremely encouraging and clearly demonstrate the possibility to apply GNRs-based nanosystems not only as diagnostic but also as therapeutic agents, in line with the theranostic aim of this work.

Finally, a first proof of the concept of *in vivo* tumor retention and elimination has been addressed. In this case, optical imaging was exploited for a better visualization of the nanosystem into tumor or healthy organs, and for an easier quantification in *ex-vivo* experiments. The distribution and tumour retention of GNRs-**1**-PNPs-Cltx/Cy5.5 after intratumoural injection was investigated in subcutaneous tumor bearing mice at 5 min, 4h, and 24h post injection. GNRs-**1**-PNPs-Cy5.5 (non-targeted nanosystem) were used as control (Figure **3.2.4.5**). The images showed that for GNRs-**1**-PNPs-Cltx/Cy5.5, the *in vivo* signal into the tumour was very intense at 5 min after injection, and still persisted at 24 h after

injection (Figs. a-d), although slow leak from the tumour and accumulation into the kidneys was observed. Images of *ex-vivo* scans recorded on organs and tissues at mice' sacrifice showed intense signal into the tumour and into the kidneys and very weak signal into other organs. No signal was present in typical RES organs, such as liver and spleen (Fig. i). On the other hand, in the case of GNRs-**1**@PNPs-Cy5.5, *in vivo* images showed lower signal into the tumour at 5 min after injection, and the signal decreased rapidly with time and was very weak at 4 and 24 h after injection (Figs. e-h). *Ex-vivo* images in this case showed significant accumulation in the liver and in the kidneys meaning that the non-targeted nanosystem is recognized by macrophages or cells of the reticuloendothelial system (RES) more easily respect to the targeted one. A quantitative analysis performed on the fluorescence signal recorded in the tumor of mice after intratumor injection of GNRs-**1**-PNPs-Cy5.5/Cltx demonstrated that at 4h about 48% of the initial fluorescence was recovered in the tumor and it was still of 22% at 24 h. The same analysis performed on the fluorescence signal recorded in the tumor of mice after intratumor injection of GNRs-**1**-PNPs-Cy5.5 demonstrated that only ~18 % of the initial fluorescence was recovered in the tumor after 4 h post administration; this value decreased up to 2.5% at 24 h. These results confirmed a slower washout of the targeted nanoparticles from the tumour compared to the non-targeted one, underlining the importance of Cltx for a good retention of the nanosystems into the tumour.
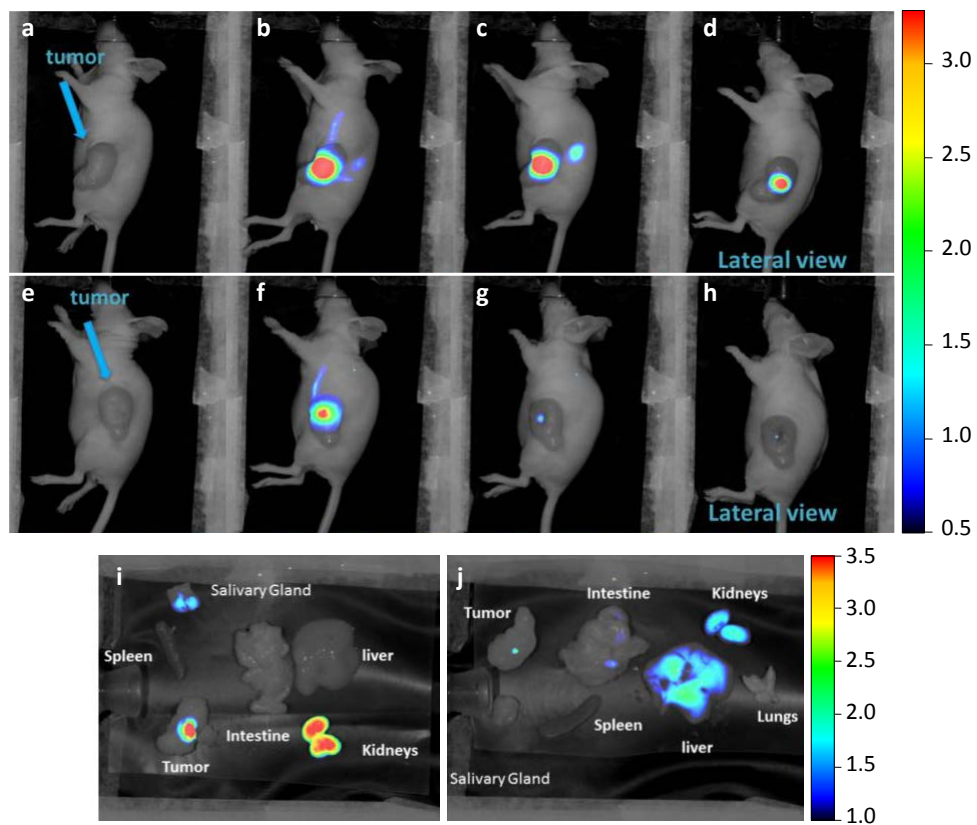
Figure 3.2.4.5: Optical Imaging (OI) scans recorded for GNRs-**1**-PNPs-Cltx/Cy5.5 (a-d) and GNRs-**1**-PNPs-Cy5.5 (e-h) after intratumour administration in U87MG bearing mouse; Images recorded on harvested organs and tissues after sacrifice for GNRs-**1**-PNPs-Cltx/Cy5.5 (i) and GNRs-**1**-PNPs-Cy5.5 (j).

3.3 AgNPs into polymeric nanoparticles and synergistic effects with antineoplastic drug: towards therapy against Glioblastoma Multiforme.

In this chapter, all the syntheses, preparations, characterizations and results obtained with AgNPs are described. This means surface modification with organic ligand **1**, micelles formation and AgNPs entrapment, double-entrapment of AgNPs and Alisertib drug, decoration of the micelles' outer shell and all the *in vitro* and *in vivo* biological tests.

All the procedures and results here described are part of- and can be found in-:

- E. Locatelli, F. Broggi, J. Ponti, P. Marmorato, F. Franchini, S. Lena, M. Comes Franchini: "Lipophilic Silver Nanoparticles and Their Polymeric Entrapment into Targeted-PEG-Based Micelles for the Treatment of Glioblastoma", *Adv. Healthcare Mater.*, **2012**, *1*, 342–347.

- E. Locatelli, M. Naddaka, C. Uboldi, G. Loudos, E. Fragogeorgi, V. Molinari, A. Pucci, T. Tsotakos, D. Psimadas, J. Ponti, M. Comes Franchini: "Targeted Delivery of Silver Nanoparticles and Alisertib. *In Vitro* and *In Vivo* Synergistic Effect Against Glioblastoma", *Nanomedicine*, **2014**, doi:10.2217/NNM.14.1

This chapter does not include surface modification with ligand **2** and **3** as well as click chemistry reaction between GNRs and AgNPs: for that see Discussion-Chapter 4.

3.3.1 AgNPs surface modification

AgNPs synthesized with the salt reduction method, in presence of PVP resulted dispersed in water. As already discussed for GNRs, it is important to remove the water-soluble stabilizer agents, and to replace them with organo-soluble ligands. This step is of major importance in case of GNRs, due to the high CTAB citotoxicity, while not so strong problems in biological studies were underlined in case of PVP use, but it is also mandatory in order to modify solubility of the final resulted nanosystems towards an organic phase instead an aqueous one. For this reason, the same ligand exchange reaction performed for GNRs was provided in case of AgNPs. Also in this case the ligand used was ligand **1**, because it presents strong affinity, not only with gold surface but also for silver one, thanks to the presence of a thiol group. As well as CTAB, PVP presents a weak affinity and no covalent bind with silver surface, thus is replacement can be obtained without excessive efforts, using that particular ligand. Following the already described procedure, a hydroalcoholic mixture consisting in an aqueous phase with AgNPs-PVP ethanol with ligand **1**, was left to react under slight sonication for one hour, then 24 hour under mechanical stirring. Purification of the coated AgNPs was achieved by using centrifugation and by washing with ethanol for the removal of un-reacted reagent and PVP; the so-obtained AgNPs-**1** were easily redispersed in common organic solvent, such as chloroform, dimethylformamide or dimethylsulfoxide. AgNPs-**1** were completely characterized in order to confirm the coating and the complete removal of PVP.

UV-Vis analysis showed that the SPR absorption band was still present, meaning that the nanoparticles' intrinsic properties were not affected during the process. The red shift (from 404 to 411 nm) in this case is less evident if compared to the one observed for GNRs-**1**, because of the lower influence of the surrounding medium on this band (comparable to the TPR of GNRs). TEM analysis also confirmed the maintaining of size and shape of the nanoparticles, while DLS analysis showed a slight increase in the hydrodynamic diameter, from 12 nm for AgNPs to 22 nm for AgNPs-**1**, in any case in line with a solvent change (**Figure 3.3.1.1**).
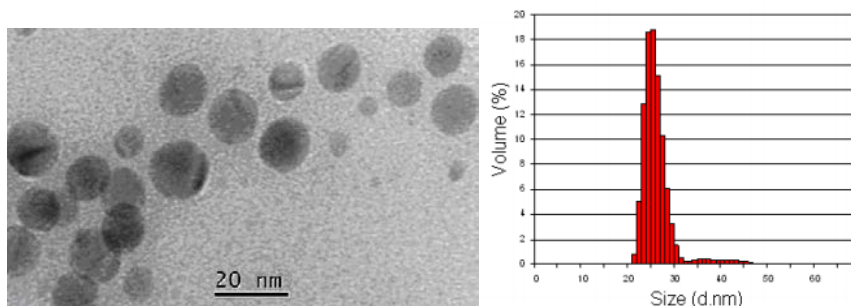
Figure 3.3.1.1: TEM (left) and DLS (right) analysis of AgNPs-**1**

AAS analysis was performed for the quantification of the silver quantity, and showed that a good amount of silver can be recovered after the ligand exchange procedure, with a yield of 80%.

Termogravimetric analysis (TGA) was registered for an accurate determination of the ligand **1** anchored onto the metal surface (**Figure 3.3.1.2**): in line with what obtained for GNRs-**1**, even in this case the ligand amount was found to be equal to 16% of the total matter, an amount sufficient for a good stabilization of the nanoparticles during the following steps.
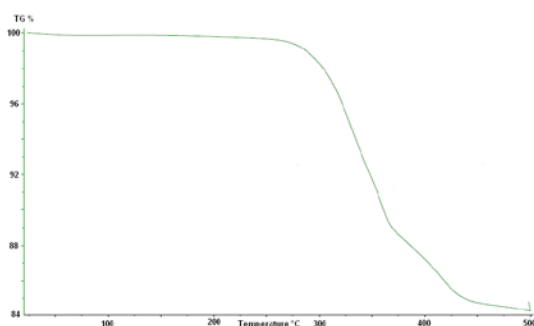
Figure 3.3.1.2: TGA analysis of AgNPs-1

^{1}H-NMR analysis registered both for AgNPs-**1** and free ligand **1** confirmed the covalent bind formed between the thiol groups and the Ag atoms onto the metal surface: indeed, all the diagnostic signal of ligand **1** were recovered in the NMR spectrum of AgNPs-**1**, except for the –SH signal, whom disappearance suggested the formation of a strong covalent Ag-S- bond (**Figure 3.3.2.3**).
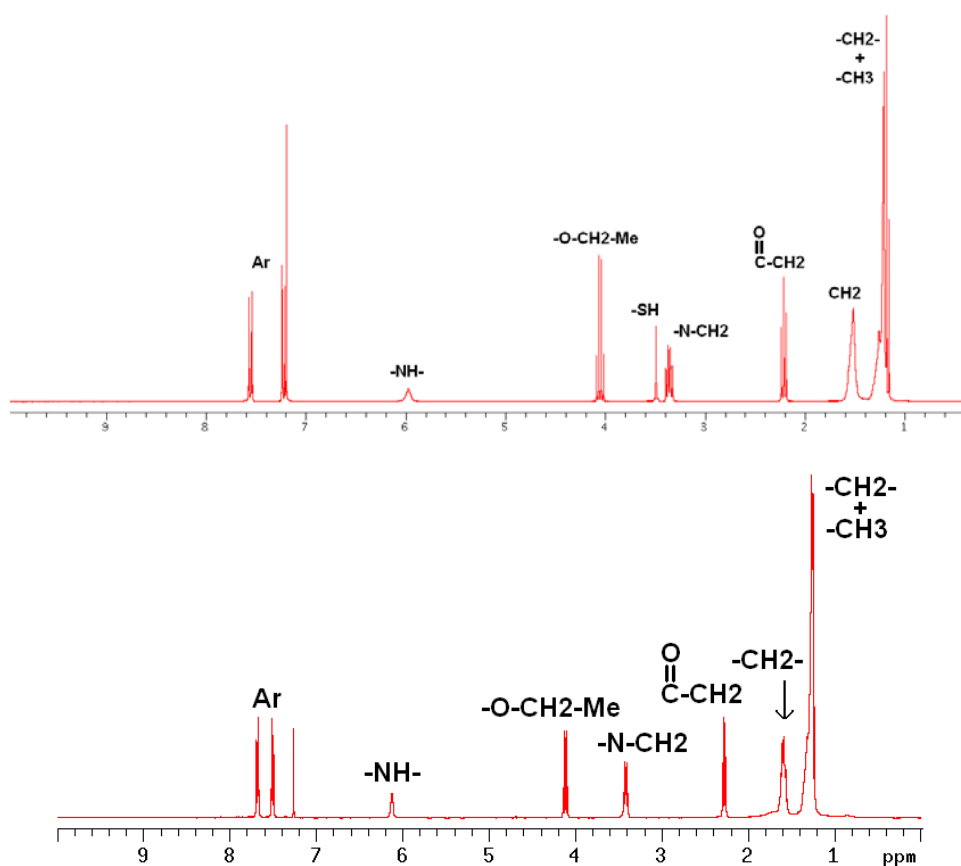
Figure 3.3.1.3: ^{1}H-NMR analysis of ligand 1 (above) and AgNPs-1 (below) in chloroform.

3.3.2 Entrapment of AgNPs and/or Alisertib into polymeric nanoparticles

Once obtained lipophilic silver nanoparticles, it was possible to entrap them into the same nanocarriers described for GNRs. Also in this case PLGA-b-PEG was used for the creation of the micelles, but the nanoprecipitation technique was preferred to the oil-in-water one, because of the higher solubility of AgNPs-**1** in dimethylsulfoxide than in chloroform. In a general procedure the organic phase, consisting in dimethylsulfoxide with AgNPs-**1** dispersed in it, was mixed with an aqueous phase in a vigorously stirred reactor, maintaining the water/organic ratio constantly 10/1 with removal of the resulting colloidal solution. This system is suitable also for large amount of solutions and eventually scaling-up of the process, because it works continuously and not batch after batch (**Figure 3.3.2.1**). The resulting solution contained AgNPs-**1**-PNPs, though an incubation time of 30 minutes was necessary, in order to allow the system to reach the stability; indeed, the nanoprecipitation process provides PNPs through interfacial desolvation of the polymer and subsequent aggregation of small

nuclei into nanometric particles, not so highly ordered as the ones obtained with oil-in-water technique: this aggregation requires more time than few seconds to form and reach a stable state, thus the system must be left to incubate until this process is completely ended.
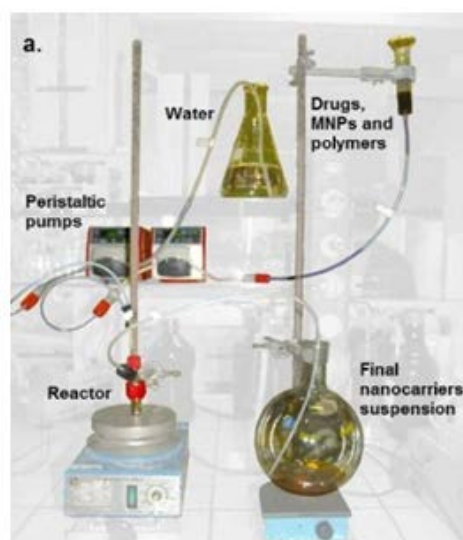

Figure 3.3.2.1: Entire flow system for the nanoprecipitation technique

After the necessary time, the colloidal solution resulted completely stable and with an opal, yellow-brownish colouration. The so formed PNPs maintained the solvent used and the AgNPs-**1** entrapped in the lipophilic core just as in the case of GNRs-**1**; unfortunately in this occasion it was impossible to remove dimethylsulfoxide by evaporation, due to the high boiling point: this goal was achieved thanks to the first step of the purification technique, and by washing several times with fresh water. After solvent removal, the solution appeared more limpid and yellowish, even though the typical opalescence of PNPs remained visible.

The so-obtained AgNPs-**1**-PNPs were completely characterized (**Figure 3.3.2.2**).

TEM analysis showed the presence of numerous AgNPs of diameter around 10-20 nm entrapped into a spherical polymeric matrix of size around 80-100 nm. Differently from GNRs, the amount of AgNPs entrapped results particularly high, so that the polymer is slightly visible, meaning that the entrapment of spherical small nanoparticles is easier than the one of non-spherical moieties such as GNRs.

DLS analysis revealed that the obtained PNPs present a hydrodynamic diameter of 71.01 ± 0.41 nm and a narrow size distribution (PDI value of 0.19 ± 0.006).Also in this case the ζ-potential value was found to be highly negative (-51.5 mV), due to the presence of deprotonated carboxylic acid groups on the PNPs' outer shell.
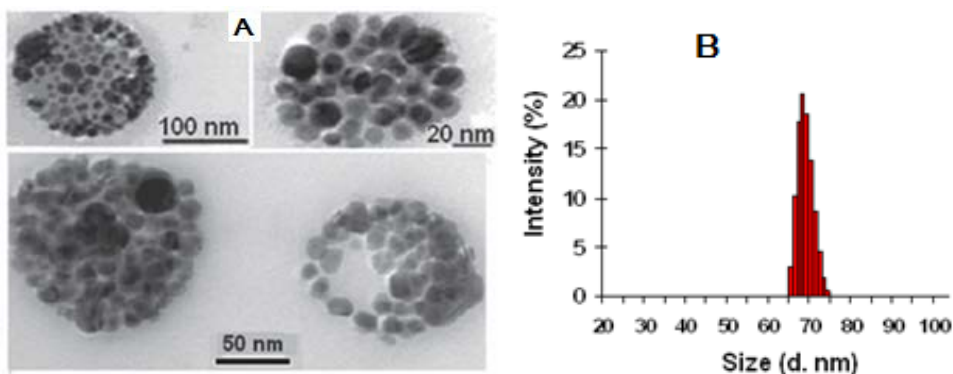
Figure 3.3.2.2: TEM image (A) and DLS analysis of AgNPs-1-PNPs (B).

AAS analysis was also performed for silver amount determination, which was found to be 1.05 mg/mL, corresponding to a final solution of 9.7 mM. Total concentration of the nanoparticles in the final solution was estimated by weighting the dry matter after water evaporation, and found to be 16.8 mg/mL.

In order to evaluate a possible synergistic effect between AgNPs and the promising antitumor drug Alisertib (Ali), two more nanosystems were prepared using the same methodology described above.

First of all a nanocarrier made of PLGA-*b*-PEG copolymer and containing Alisertib alone was obtained; the entrapment of a small molecule was possible by simply dissolving both the copolymer and the drug into a common solvent, as in this case dimethylsulfoxide. After nanoprecipitation of Alisertib-loaded PNPs (Ali-PNPs), the resulted colloidal solution was left to incubate, and reached stability for 30 minutes, then it was purified and completely characterized.

DLS analysis showed the obtainment of PNPs with a diameter of 80.5 ± 0.94 nm, and a very narrow size distribution (PDI value of 0.12 ± 0.004). The ζ-potential was found to be of -51.6 mV. In this case high performance liquid chromatography (HPLC) was used in order to determine the Alisertib amount entrapped into the PNPs. To do this a first treatment of the sample was necessary, aimed to the release of drug from the core of PNPs, where it cannot be visible with HPLC analysis, nor be injected into small diameter capillary column of the instrument. Thus, PNPs were re-opened adding to an aliquot of the solution a huge amount of a polymer solvent, for example in this case acetonitrile, which was also the eluent of the analysis, and ultrasonicating for one hour. The so-obtained solution, where the copolymer and the drug are now separated and dissolved, was analyzed, and the concentration of Alisertib

was determined by comparison of peak's integration value with previously analyzed standards at different drug concentration. The Alisetib value was found significantly high, with a concentration of 785 µM. Dry matter of the solution gave a total PNPs concentration of 9.8 mg/mL.

Finally, also a nanocarrier containing both AgNPs and Alisertib was provided, which would show the real synergistic effect. In order to obtain the simultaneous entrapment of two different moieties into the same nanocarrier, it is mandatory to find a suitable solvent, able to dissolve both of them. In this case, dimethylsulfoxide well suited the purpose, and because of this it was the solvent chosen for this preparation. Indeed AgNPs-**1**, Alisertib and the copolymer were all dissolved into this solvent, then by using also in this case the nanoprecipitation technique, both Alisertib and AgNPs were entrapped into PNPs. After the usual 30 minutes, the so-obtained Ag/Ali-PNPs were purified, concentrated and completely characterized.

DLS analysis showed an increase in the generally obtained hydrodynamic diameter, which in this case resulted to be 190.6 ± 0.80 nm, meaning that the entrapment of two moieties instead of a single one was more challenging than what expected, and surely leaded to an enlargement of the nanocarrier's core. However, these dimensions are worldwide considered suitable for biomedical applications, thus the nanosystem obtained underwent all the necessary following steps and studies. The PDI value (0.09 ± 0.03) confirmed the narrow size distribution of the nanosystems, while ζ-potential value resulted as expected to be highly negative (-47.8 mV).

AAS analysis was necessary in order to determinate silver conten: the concentration was found equal to 2.28 mg/mL (21 mM) for silver, confirming the obtainment of a nanocarrier with a suitable amount of AgNPs. Dry matter value resulted to be in line with what obtained previously (10.4 mg/mL).

3.3.3 Nanosystems' surface conjugation with active agents

Following the same procedure exploited for GNRs-**1**-PNPs, also all the above-described nanosystems were decorated in the outer shell with active agents.

In this case, Chlorotoxin was used to target glioblastoma cancer cells as for GNRs; anyway the radioisotope [99mTc] was preferred as imaging agent, due to the possibility of Positron Emission Tomography (PET) imaging that it can allow.

As already described, Chlorotoxin was conjugated thanks to its free-amino group at one end, in an amidation reaction with the carboxylic acids on the micelles' outer shell. After 24 hours

of reaction and purification, AgNPs-**1**-PNPs-Cltx were obtained and once again completely characterized.

DLS analysis showed a hydrodynamic diameter of 117.4 ± 14.4 nm, with a narrow size distribution (PDI value of 0.22 ± 0.013), thus meaning that the PNPs were not affected during the conjugation reaction. The ζ-potential value was equal to -16.2 mV, showing, as previously observed, a slight increase if compared to AgNPs-**1**-PNPs because of the partial loss of free carboxylic acids, now involved in the amide bond. The concentration of silver, estimated with AAS analysis, was found to be 1.40 mg/mL, corresponding to a solution 13.0 mM.^{1}H-NMR analysis, performed on dried washing aqueous solution re-dispersed in D_2O, showed no signal for Cltx, meaning that the conjugation yield can be considered quantitative, thus the concentration of Cltx in the final sample was estimated to be 6.2 μM.

Following the same procedure, also Ali-PNPs were conjugated with Chlorotoxin, and the obtained Ali-PNPs-Cltx were purified and characterized.

In this case, DLS analysis showed a mean diameter of 98.2 ± 3.8 nm with a PDI value of 0.16 ± 0.009 and a ζ-potential value of -23.2 mV. HPLC analysis showed an Alisertib concentration of 120.8 μM. Thanks to ^{1}H-NMR analysis Chlorotoxin concentration was estimated to be 6.2 μM. Finally, the nanosystem loaded with both AgNPs-**1** and Alisertib was conjugated with Chlorotoxin; characterization of the final nanosystem was carried out: DLS analysis showed a mean diameter of 199.1 ± 0.6 nm with a PDI value of 0.21 ± 0.02 and a ζ-potential value of -15.4 mV. AAS analysis showed a silver concentration of 0.23 mg/mL, corresponding to 2.17 mM in the final concentrated sample. HPLC analysis showed an Alisertib concentration in the sample solution of 41.8 μM, while the concentration of Cltx was estimated through ^{1}H-NMR analysis as previously described to be 6.2 μM.

All the obtained nanosystems were also radiolabelled by co-workers with ^{99m}Tc, in order to allow PET imaging. The direct labeling of NPs with ^{99m}Tc is the most commonly used method for radiotracking, applied to various types of NPs. With this technique, the generator eluate (Na[99m]TcO$_4$) is mixed with an acidic stannous chloride ($SnCl_2$) solution for reduction of ^{99m}Tc from the heptavalent oxidation state to lower oxidation states, in order to facilitate the formation of radiometal complexes with random groups that are present on the surface of the NPs, such as in our case the carboxylic one.[88]

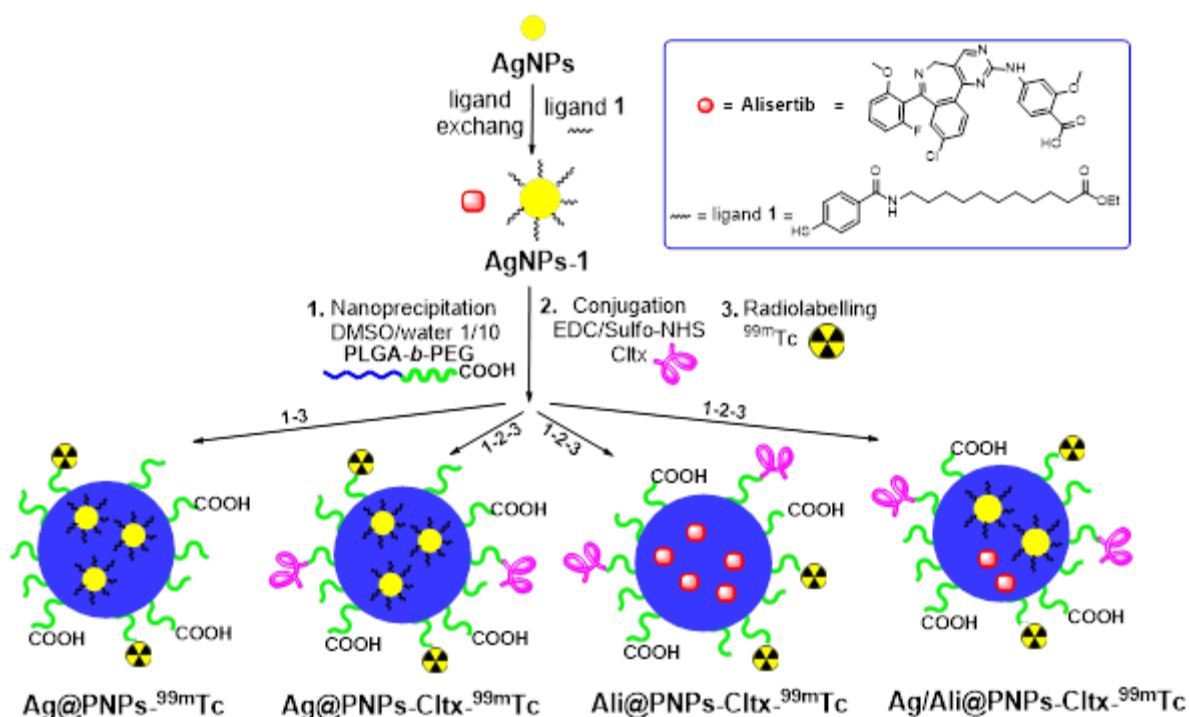In Figure **3.3.3.1** it is possible to see a summary of the entire procedure described above.

Figure 3.3.3.1: schematic representation of the entire procedure for the preparation of the three AgNPs and/or Alisertib containing nanosystems.

3.3.4 In vitro and in vivo tests

The biological and physical investigations were carried out in collaboration with the European Commission, Joint Research Centre, Institute for Health and Consumer Protection Nanobiosciences, of Varese (Italy), and with the Technological Educational Institute of Athens (Greece).

Due to the well-known antibacterial activity of AgNPs, the studies described below aimed to the evaluation of the final nanosystem as a therapeutic tool against glioblastoma multiforme; for this reason the cytotoxicity of all the obtained nanosystems was tested together with the possible synergistic effect with Alisertib drug against glioblastoma cell lines, such as U87MG. Firstly, an in vitro evaluation of the biological activity and cytotoxicity of silver nanoparticles alone was carried out, in order to verify the real possibility to use AgNPs-based nanosystems as therapy against glioblastoma multiforme. For this reason not only the final nanocarrier AgNPs-PNPs-Cltx was tested, but also all the components alone with the aim of excluding cytotoxic effects due to them: thus AgNPs, ligand **1**, PNPs, PNPs-Cltx, simple Cltx, AgNPs-**1**-PNPs, and the final AgNPs-**1**-PNPs-Cltx were all evaluated on U87MG after an incubation

84

period of both 24 h and 72 h (**Figure 3.3.4.1**). The test selected for cell viability verification was the trypan blue exclusion dye test, which allows distinguishing and consequently counting living cells from died ones. The same assay was used also to assess cytotoxicity of AgNPs-1-PNPs and AgNPs-1-PNPs-Cltx on healthy Balb/3T3 cell line after 24 h of exposure, as already tested for GNRs-based nanocarrier, in order to better understand the possible effects of their administration on non-cancerous cells. The concentrations tested ranged from 0.1 to 200 μM of silver in case of U87MG, while Balb/3T3 were exposed to a median value of 100 μM of silver. The results showed that a significant dose-effect relationship and cell death was observed for U87MG line, exposed to AgNPs-**1**-PNPs-Cltx both for 24 and 72 h. The IC50 value in silver of AgNPs-**1**-PNPs-Cltx was obtained after graphical interpolation and was found to be equal to 80 μM after 24 h, and interesting 45 μM after 72 h of exposure. Furthermore, no toxicity and significant cell death was observed after exposure of U87MG to only AgNPs-**1**-PNPs, AgNPs or Cltx, meaning that, differently from the complete nanocarrier, the single components were not able to induce cell damage. Equally, the exposure to PNPs-Cltx and to ligand **1** at the same amount, present in the final nanosystem, showed good cell viability of 80% and 84% on U87MG and 85% and 89% on Balb/3T3. These two last experiments ruled out possible cytotoxic effects for the simple organic coating and for the polymeric part of the nanocarrier. The viability of Balb/3T3 after exposure to AgNPs-**1**-PNPs and AgNPs-**1**-PNPs-Cltx for 24 h showed that the nanomaterials did not induce any statistically significant toxicity in healthy cell line, confirming the specificity of Cltx for cells deriving from glioblastoma.
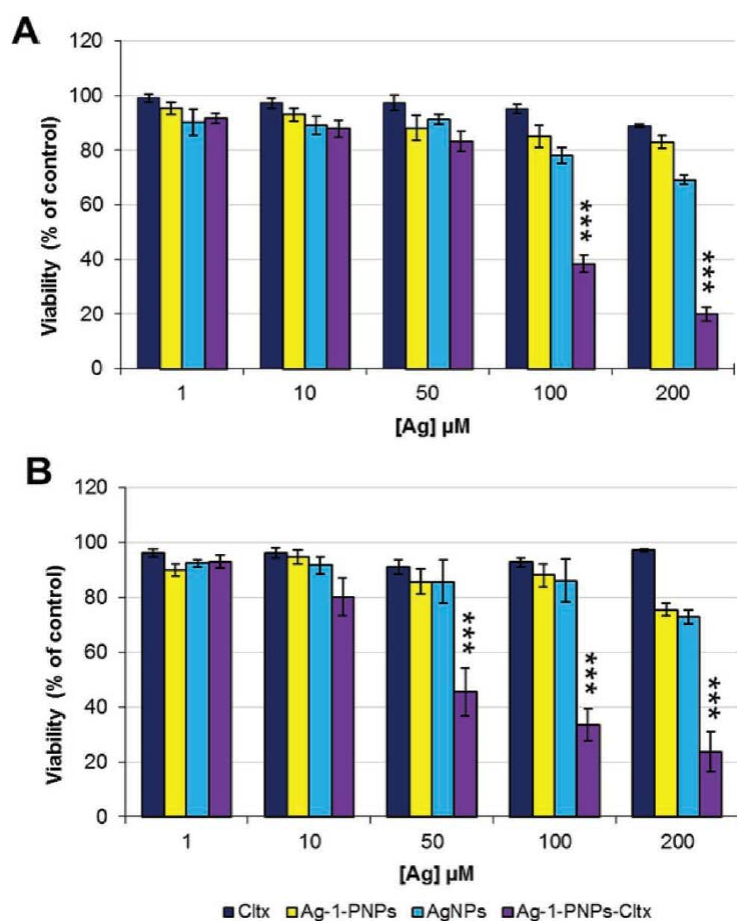
Figure 3.3.4.1: Dose-effect relationship induced by Cltx, AgNPs, AgNPs-**1**-PNPs, AgNPs-**1**-PNPs-Cltx on U87MG after 24 h (A) and 72 h (B) of exposure.

After this process, in order to demonstrate the real effect of Cltx targeting for the delivery of silver inside cells, and to better understand the relationship between silver amount administration and real active agent obtained into cells, the Ag uptake into the U87MG cells was examined by using the ICP-MS technique onto cells lysates after incubation with three of the prepared nanocarriers.

The results showed that after exposing cells for 24 h to 80 μM (the value of IC50) of AgNPs-**1**-PNPs-Cltx, AgNPs-**1**-PNPs and AgNPs, the amount of silver found in each cell was in the range of a few picograms, but significantly higher for the final nanocarrier bearing Cltx (3.97 pg/cell) (**Figure 3.3.4.2**). Likewise, exposing cells for 72 h to 45 μM (the value of IC50) of the same nanomaterials, the amount of silver found in each cell was more than 8 times higher for AgNPs-**1**-PNPs-Cltx than for the other two nanosystems. This investigation clarified that the cytotoxicity effect saw in the previous experiment was uptake-dependent, and that AgNPs can act as real antitumor drugs. Furthermore, these results demonstrated that the presence of Cltx, specifically enhanced the uptake into cancer glioma cells because it acts as a targeting

peptide for cell specific internalisation of AgNPs, thus increasing the cytotoxicity of silver included in the nanocarrier. The results obtained in these first two in vitro tests clearly gave evidence of the cytotoxic effect of AgNPs, since the ligand **1** itself and the polymer did not have any effect on cells viability despite their entrapment into the same nanocarrier having the clorotoxin in the outer surface.
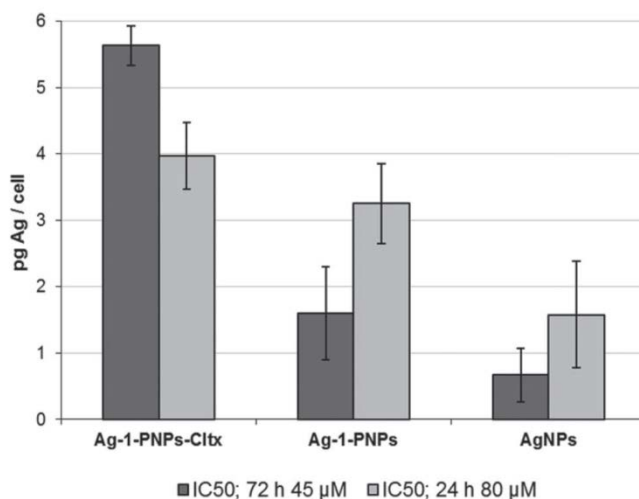

Figure 3.3.4.2: silver uptake deriving from three different nanosystemsintoU87MG cells after exposure of 80μM and 45 μM of silver for 24 and 72 h respectively. Results are expressed as picograms/cell (pg/cell).

Once demonstrated the possibility to exploit silver as real antitumor drug, a comparison of these results with Alisertib alone and Alisertib loaded NPs (Ali-PNPs-Cltx), and the evaluation of the synergistic effect between AgNPs and Alisertib, both loaded in the same nanosystem (Ag/Ali-PNPs-Cltx), was carried out. U87MG cell line was consequently incubated for 48 h and 72 h with all the above cited compounds, and the cell viability was checked.

For these tests, the range of concentrations tested was 1 nM - 10 μM for Alisertib, corresponding to concentrations of 0.05 nM - 0.5 μM of silver in Ag/Ali@PNPs-Cltx. Dimethylsulfoxide (DMSO) was used to dissolve Alisertib alone and for this reason it was also tested, as solvent control, at the concentration of 0.2 % v/v.

By increasing concentrations and exposure times, a statistically significant decrease of cell viability was observed for all the compounds tested (**Figure 3.3.4.3**), while DMSO did not show any statistical significant toxicity. At each examined time point, Ali-PNPs-Cltx resulted more toxic than Alisertib alone, meaning that its entrapment into a polymeric matrix and the presence of Cltx allowed easier permeation of the membrane cell. By interpolating and comparing the IC50 of Ali-PNPs-Cltx (20 nM) and Ag/Ali@PNPs-Cltx (10 nM of Alisertib

and 0.5 nM of Ag), it resulted clear that the nanocarrier containing both the two agents was more toxic even if this effect became evident only after 72 h of incubation. A real synergistic effect between AgNPs and Alisertib drug was obtained and the IC50 value of the combined nanosystem was extremely promising, being strongly lower than common antitumor drugs.
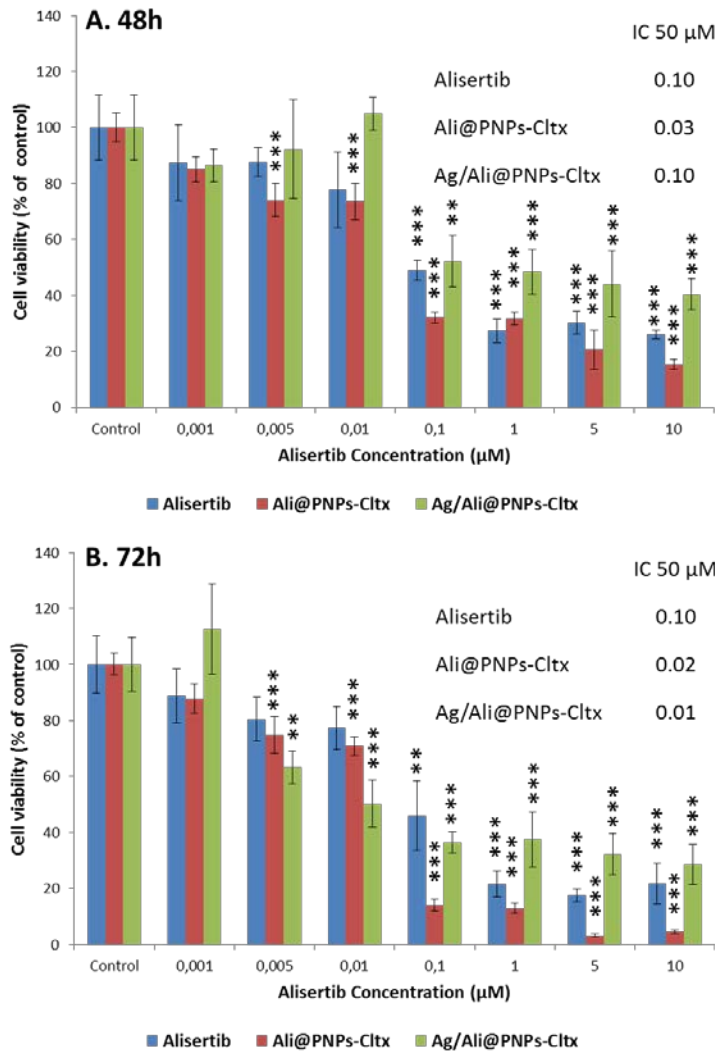
Figure 3.3.4.3: U87MG cells exposed for 48 h (A) and 72 h (B) to Alisertib, Ali-PNPs-Cltx and Ag/Ali-PNPs-Cltx at different concentrations.

Once completed this first preliminary evaluation *in vitro*, some *in vivo* tests were also performed.

In vivo studies were executed after subcutaneous inoculation of U87MG cell in mice, and after a consequently sufficient tumor growth. Firstly the biodistribution and consequent tumor uptake of AgNPs-**1**-PNPs-^{99m}Tc and AgNPs-1-PNPs-Cltx/^{99m}Tc administered by intravenous injection was evaluated (**Figure 3.3.4.4**). All imaging studies *in vivo* indicated, as expected, a huge concentration of nanoparticles in liver, the organ mostly involved in clearance of foreign objects, as well as a slow -but continuous- increase of the concentration in bladder, meaning

that nanosystems can be excreted during time by urinary system. Besides, it must be specified that concentration in liver dropped from 80% for the nanosystem without Cltx, to 60% for the one possessing Cltx, meaning that lower unspecific body elimination occurred thanks to the presence of an active drug delivery. The overall results showed that tumor bearing mice presented noticeable accumulation in tumor 80 minutes post injection of nanosystems. Among all tested products, the highest concentration was observed for the nanosystem bearing the targeting agent Ag/Ali-PNP-Cltx/^{99m}Tc. More specifically, the quantitative analysis showed a silver concentration in tumor of 0.6% of the overall administered dose for the nanosystem without Cltx, certainly due to the enhanced permeability and retention (EPR) effect; this value must be compared to the 5% one obtained for the nanosystem bearing the targeting agent: this concentration is considered rather significant, because of the fact that normal healthy tissues showed unspecific accumulation lower than 2% for the same nanocarrier. This result, combined with the increased concentration in bladder (from 3% to 7%), provides strong evidence that Ag/Ali-PNP-Cltx/^{99m}Tc has favorable kinetic *in vivo* properties, when compared to non-targeted nanosystems, thus is likely to be more effective as drug delivery device.
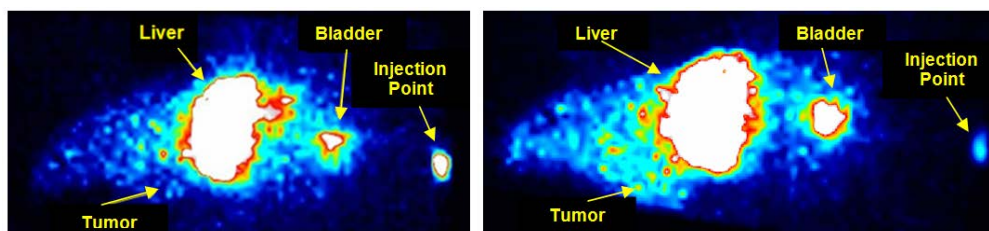

Figure 3.3.4.4: Comparative images of a tumor bearing mouse injected with AgNPs-**1**-PNPs-^{99m}Tc (left) and Ag/Ali-PNP-Cltx -^{99m}Tc (right)

With these preliminary investigations *in vivo*, the possibility to significantly deliver drugs and nanoparticles to the tumor site has emerged as a reality.

Due to these encouraging evidences, a real therapeutic effect was assessed. For this experiment 20 mice were inoculated, as previously, with U87MG cells, and the resulting tumor was left to grow for 24 days. Tumor size was monitored every day and until it became evident. At day 24 the mice were divided into 4 groups, each one consisting of five animals, and to each group a treatment was administered through a single intravenous injection. The first group represent the control, so no nanosystems were given to these animals, but only physiological solution; the second group received 100 µL of AgNPs-**1**-PNPs-Cltx at a dose of 5.97 mM in silver; the third group received 100 µL of Ali-PNPs-Cltx at a dose of 0.11 mM in

Alisertib, and finally the fourth group received the complete nanocarrier Ag/Ali-PNPs-Cltx at a comparable dose of silver and Alisertib. After this treatment at day 24, no more administrations were given to the mice, but the tumor size was daily monitored. The comparative measurements of the average tumor size for the 4 groups are given in Figure **3.3.4.5.**
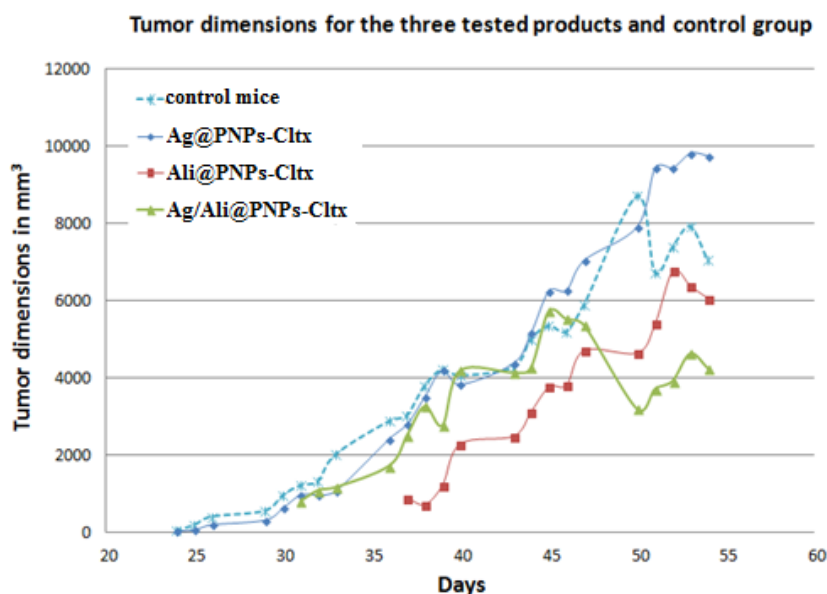

Figure 3.3.4.5: Tumor dimensions for the four tested mice groups: Control (pale blue line), AgNPs-**1**-PNPs-Cltx (blue line), Ali-PNPs-Cltx (red line) and Ag/Ali-PNPs-Cltx (green line)

The evaluation of results for tumor decrease showed that, treating the mice with AgNPs-**1**-PNPs-Cltx, did not have significant effect on tumor size. On the other hand, Ali-PNPs-Cltx resulted in a slowdown in tumor size compared to the control group and AgNPs-**1**-PNPs-Cltx group. Surprisingly, when Ag/Ali-PNPs-Cltx was injected the development of the tumor was strongly altered compared to the 3 other groups, and a tumor size decrease was noticeable from day 48 on. The weight of the mice remained constant for all groups, except for the Ag/Ali@PNPs-Cltx, where a weight loss was observed following Day 48, which is correlated to the observed tumor decrease, which was quantified to be equal to -22 % of the entire mass.

This data supported the argument that a synergistic effect with Ag/Ali-PNPs-Cltx took place: the *in vitro* results at 72 hours and the *in vivo* effects after day 48 showed a greater tumor decrease in comparison with the other nanosystems.

These results are extremely encouraging in supporting the idea of using silver nanoparticles in synergist effect with antitumor drugs as real therapeutic agent against cancer. In addition, the radiolabeling of the nanocarrier allowed *in vivo* imaging, satisfying in this way also the diagnostic purpose of theranostic field.

3.4 Click chemistry on the surface of GNRs and AgNPs

In this chapter the assembly of GNRs and AgNPs into a single nanosystem is described. This means surface modification with organic ligand **2** and **3** of GNRs and AgNPs respectively, click chemistry reaction between the two obtained nanostructures, and final entrapment into polymeric nanoparticles.

All the procedures and results here described are part of- and could be found in-:

- E. Locatelli, G. Ori, M. Fournelle, R. Lemor, M. Montorsi, M. Comes Franchini: "Click Chemistry for the Assembly of Gold Nanorods and Silver Nanoparticles", *Chem. Eur. J.,* **2011***, 17,* 9052-9056.

3.4.1 Surface modification of GNRs and AgNPs with ligands 2 and 3

The synthesis of multifunctional nanostructures with co-existing functionalities and properties is of particularly interest especially in the emerging field of theranostic.

One of the biggest issues, nowadays still to be addressed is how to combine individual nanostructures into a single device without losing their original properties. Indeed, most studies arose in the last decades aimed to the development of a single type of nanoparticle, which combains two or more materials: those were generally assembled by using polydentate ligands[89] or synthesizing heterodymer structurescomposed for instance of quantum dots, or magnetic and metallic nanoparticles together. One example of this approach is given by the numerous catalysts based on gold and copper, or gold and platinum nanoparticles prepared in the last few years.[90]

However, with this approach several of the optical, magnetic, or electronic properties are often altered or lost, since the different components are touching each other, or are mixed togheter. A potential solution is to not modify intrinsic structure of nanoparticles but to link them through an organic framework obtained with simple reaction, in order to obtain multifunctional nanoparticles in which the individual components are maintained distant by a spacer. Nowadays only few examples of this approach have been reported due to the challenging aim that a covalent link between nanoobjects represents.[47] The possibility to bind together GNRs and AgNPs could open the door to a real, powerful, theranostic device able to combine different therapeutic capability as well as imaging ones.

To address this exciting possibility, a quick and simple organic reaction for the linkage of two metallic nanostructures would be preferable to preserve the properties of the two of them. The click chemistry reaction, with its unique characteristics, seems to be the ideal case for this scope. As already discussed in Introduction, the azide/alkyne Huisgen cycloaddition is the perfect example of click chemistry, thus it represents the best candidate for this purpose.

In order to allow this reaction between GNRs and AgNPs it is mandatory to modify their surfaces with specifically designed ligands: these ligands must confer stability to both the two nanostructures and simultaneously present the two orthogonal free, reactive terminal groups azido and acetylene.

As already discuss in Discussion-Chapter 1, the synthesis of acetylene and azido ending groups bearing ligands (ligand 2 and 3) has been performed, thus at this point it was possible to proceed with the coating of GNRs and AgNPs with the ligands synthesized, thanks to their thiol groups.

It was arbitrarily decided to functionalize GNRs with the acetylenic ligand **2**, while AgNPs were coated with the azides ligand **3**. For the coating the same procedure already described in Chapter 3.2 and 3.3 has been used. This methodology requires the dissolution of the organic ligand in an alcoholic solution and then its addition to an equal volume of aqueous solution containing the nanoparticles yet coated with surfactant agents.

However, the ligands **2** and **3** were characterized by a high insolubility in alcohols, thus it was not possible to use ethanol, but it was necessary to use dimethylformamide (DMF), where the ligands are perfectly solubilised, and which is however a solvent miscible with water.

For this reason, two DMF solutions were prepared, one containing ligand **2** and one containing ligand **3**: to the first solution GNRs-CTAB were added, while to the second AgNPs-PVP. As previously described the mixture that is obtained by mixing the two phases must be left to react one hour under sonication and 24 hours under mechanical stirring in order to lead to the exchange completeness. After the necessary purification, aimed to the removal of supernatant, surfactants agents (CTAB or PVP) and unreacted ligands, GNRs-**2** and AgNPs-**3** have been obtained.

All the coatings tried both on gold and on silver gave excellent results, thus demonstrating once again the remarkable affinity of the disulphide group for noble metal nanostructures.

The success of the exchange reaction was indicated by the fact that it was possible at this point to re-disperse the functionalized nanoparticles in organic solvents such as DMF, THF, and DMSO: these solvents are all excellent for the subsequent click reaction.

The functionalized nanoparticles were characterized by ^{1}H-NMR after redispersion in deuterated DMSO;: the analysis confirmed the success of the exchange reaction and the complete removal of CTAB and PVP (**Figure 3.4.1.1**).
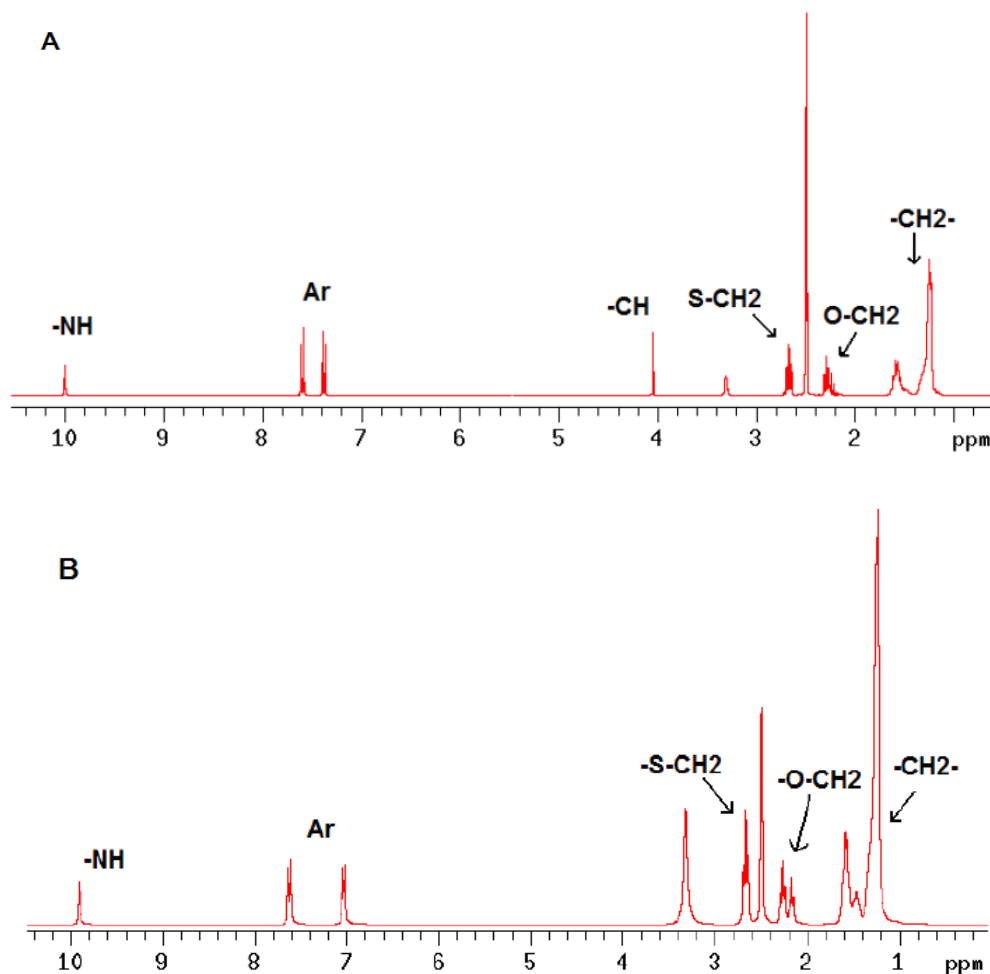
Figure 3.4.1.1: ^{1}H-NMR of GNRs-**2** (A) and AgNPs-**3** (B) in DMSO-d6 (600 MHz)

Anyway, once verified the possibility of anchoring also these two ligands to the nanostructures, a different approach was selected due to the more interesting scenario. Indeed, it was known from the work of O' Brien[47] that during the reaction between two nanostructures it is preferable to work at very high dilution, for the reason that many cross-linking are possible onto a fully coated surface, leading to the formation of big aggregates.

To prevent this side effect, but without wishing to extremely dilute the two solutions containing the nanoparticles, it was instead attempted to dilute the functional groups directly onto the particle surface. This is a challenging purpose, because of the necessity to maintain stability during and after the process, thus is not simply possible to reduce the amount of organic ligand involved in the exchange. On the other hand, this was possible by performing mixed coatings of the nanostructures, using not only the ligand which possesses the reactive termination, but simultaneously also another ligand, which has a similar internal structure but instead a non- reactive terminal functionality (**Figure 3.4.1.2**).
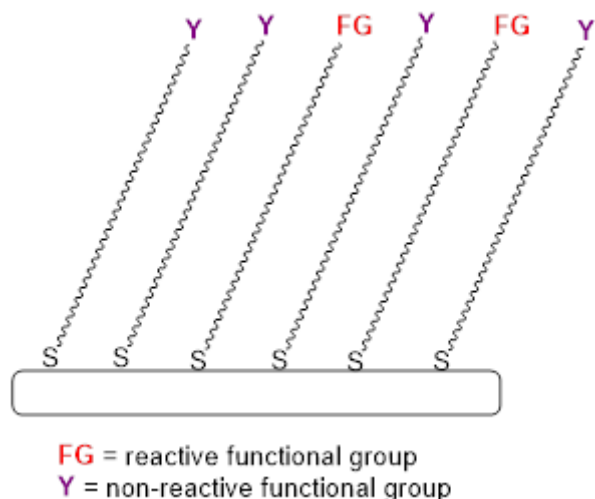
Figure 3.4.1.2: example of mixed SAM onto a metal surface.

As non-reactive ligand suitable for the coating of these nanoparticles, the ligand **1** was chosen, because it present an identical internal structure to the azido and acetylene ones, it had already given excellent results in the previous attempted exchange reaction and also because owning an ester termination it would not undergo parasitic reactions in subsequent steps.

Therefore, two solutions constituted of a mixture of ethanol and DMF in equal ratio were prepared: this is ideal for dissolving both the two reactive ligands and the non-reactive one. To the first solution containing ligand **1** and **2** in a molar ratio 1/ 1 an aqueous solution of GNRs-CTAB was added, while to the second, containing ligand **1** and **3**, AgNPs-PVP was mixed.

During the 24 hours required for the reaction, both the nanostructures underwent a mixed capping by the two ligands: indeed, the kinetic and thermodynamic of the process is slightly affect by the different nature of the terminal end of the ligands, while it is strongly dependent upon the nature of the head group and the internal chain structure: thus ligand **2** and **3** provided no-preferential attach onto the metal surface compared to ligand **1**, a well-mixed coating was obtained.

The same procedure used for the previous described ligand exchange was used also in this case; washings were always performed with mixture of DMF/EtOH, in order to allow removal of all the un-reacted ligands. The so-coated nanoparticles were soluble in the same solvents as before (for instance DMF and DMSO), but a partial solubility in other solvents such as chloroform, typically given by the presence of the ligand **1** begun to emerge.

To ensure that both the desired ligands were present onto the metal surface, but most importantly, in order to determine the ratio between the two of them, ^{1}H- NMR analysis was

performed for each of the two nanoparticles prepared. With this technique it was also possible to extimate the ratio beteween the two organic ligands presented onto the surface by integration of two diagnostic signals. The results showed that, a mixed coating was really obtained but especially for AgNPs, the relationship obtained onto the surface was not equal to the initial ligands ratio used, but it varied depending on the binder used. It was noted in particular, that the azido ligand, which was used onto AgNPs was especially un-favoured during the exchange with respect to the non-reactive ligand **1**, while with the acetylene ligands onto GNRs there was not this effect and quite a perfect 1/1 ratio was recovered onto the surface. The result suggested that the functional groups azides are too much diluted on the surface of the nanoparticles in order to conduct a good coupling reaction. Therefore to rebalance the relationship between ligands **3** and **1** onto AgNPs, the exchange reaction was repeated, but using an initial ratio between the two ligands equal to 1/5 in favour of the azido one. By doing this, a final ratio onto the surface much more balanced than before was achieved (**Figure 3.4.1.3**).
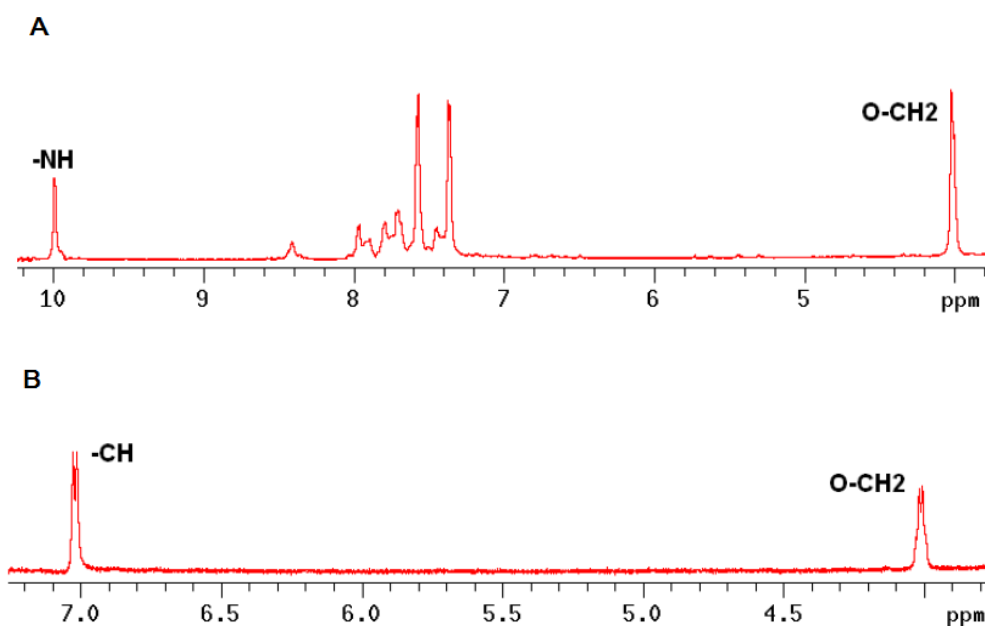
Figure 3.4.1.3: ^{1}H-NMR of GNRs-**1**/**2** (A) and AgNPs-**1**/**3** (B) in DMSO-d6 (600 MHz). Diagnostic signals were showed.

To further complete the nanostructures characterization also UV/Vis spectroscopy and TEM images of GNRs-**1**/**2** and AgNPs-**1**/**3** were performed (**Figure 3.4.1.4**): these techniques confirmed that the shape of GNRs has been retained as well as their optical properties (λ max at 756 nm).

Also in the case of AgNPs-**2/3** the same morphology of the starting water soluble AgNPs was retained after the ligand exchange. DLS measurements, which are possible in case of silver due to the spheric shape, indicated that the mixture of ligands produced stable and not aggregated dispersions showing a uniform size distribution with average diameter of 12.0 nm, in line with what obtained by the ligand exchange with ligand **1** only.
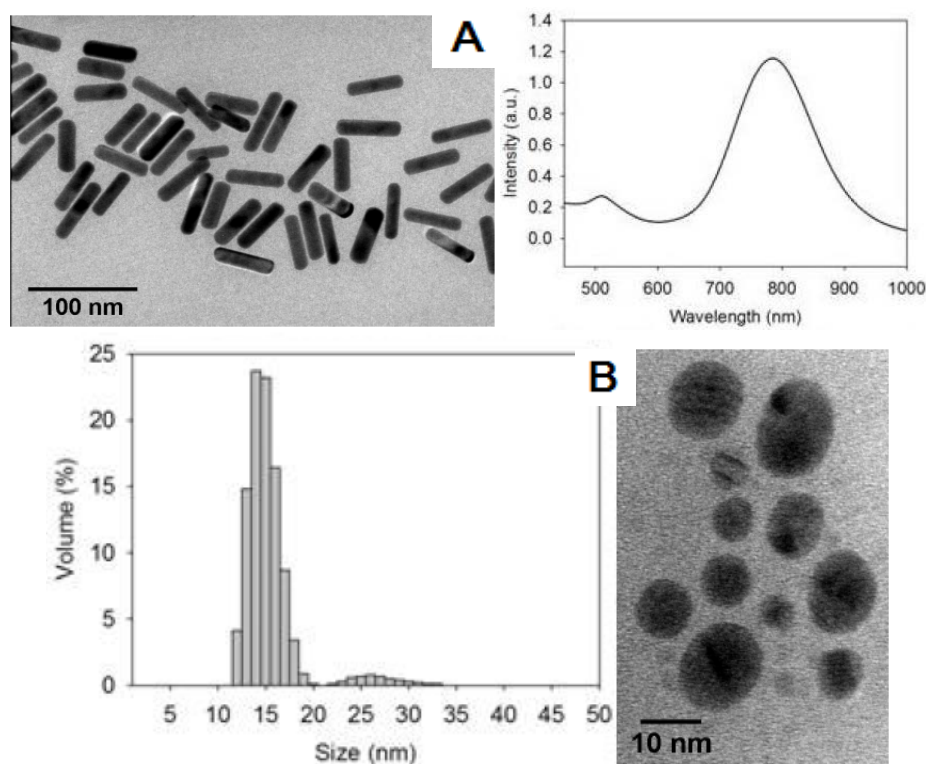
Figure 3.4.1.4: A. TEM image and UV-Vis spectra of GNRs-**1/2**. B. DLS analysis and TEM image of AgNPs-**1/3**.

3.4.2 Cycloaddition reaction between the functionalized nanostructures

At this point the cycloaddition reaction between the two nanostructures presenting the acetylene and the azido groups was attempted. The chosen azide/alkyne Huisgen cycloaddition would lead to the formation of a triazole ring, which could be formed in two different regioisomers: the 1,4-sobstituted and the 1,5-sobstituted.

It was decided to conduct the cycloaddition reaction in the three ways described in the Introduction: a not-catalyzed reaction at high temperature, a copper catalysed one (CuAAC), and finally a ruthenium catalyzed (RuAAC) reaction. In this way the formation of different regioisomers, depending on the conditions used would be observed and monitored.

For the reaction without catalysts GNRs-**1**/**2** and AgNPs-**1**/**3** were dissolved in DMF, because of its high boiling point, in order to reach sufficiently high temperatures (at list 100 °C) for the conducting of the reaction. The reaction mixture, consisting of an equal volume of solution of GNRs and AgNPS, was then left under magnetic stirring and heating for 72 h.

After that, also the copper catalyzed reaction was performed (CuAAC): to do this high temperature is not necessary, thus it is preferable to use a solvent such as THF, due to its easier removal at the end of the reaction. In a general procedure, the nanoparticles were first redispersed in this solvent, and mixed also in this case in equal volume, then copper iodide (CuI) was added to the mixture as well as a base, such as triethylamine, necessary for the catalytic cycle. The reaction was allowed to procede at room temperature for 24 h.

Finally, also ruthenium catalyzed reaction (RuAAC) was attempted: in this case it is preferable to use again the DMF solvent, where the catalyst results more active. Therefore, identical volumes of the two solutions containing the nanoparticles in DMF were mixed, the ruthenium catalyst (chloro(pentamethylcyclopentadienyl)ruthenium(II) tetramer) commercially available, was added and the mixture was left to react for 24 h at room temperature. Differently from the copper catalyzed reaction, in this case the use of a base is not necessary.

All the resulted solution obtained were dried, redispersed in deutereted DMSO, and analyzed by ^{1}H-NMR of the crude in order to accurately determine the presence of the triazole ring and the possible formation of different regioisomers.

By literature review it is known that the two signals relative to the heteroaromatic hydrogen of the two regioisomers of the 1,2,3-triazole ring fall around 8 and 9 ppm and that the signal at higher fields can likely belong to the 1,5-sobstituted regioisomer, and vice versa.

In all the crudes analyzed at list one of these two signals was detected, meaning that all the three reactions performed leaded to the formation of the triazole ring. As expected, in the case of the reaction carried out without the catalyst it is possible to see the appearance of both signals mentioned above, at 8.96 and 9.16 ppm respectively, and therefore the formation of both regioisomers can be supposed: by integration of these signals an almost equal ratio of the two of them was revealed (**Figure 3.4.2.1**). In the case of the copper catalyzed reaction only the appearance of the signal at 9.16 ppm was observed: the reaction was therefore regioselective given only one regioisomer, probably the 1,4 -substituted, as expected from literature feedback. On the contrary, in the case of catalysis with ruthenium the appearance of only the signal at 8.96 ppm was observed: indeed, the reaction was regioselective but led to the formation of the opposite regioisomer that corresponds likely to the 1,5-substituted one.
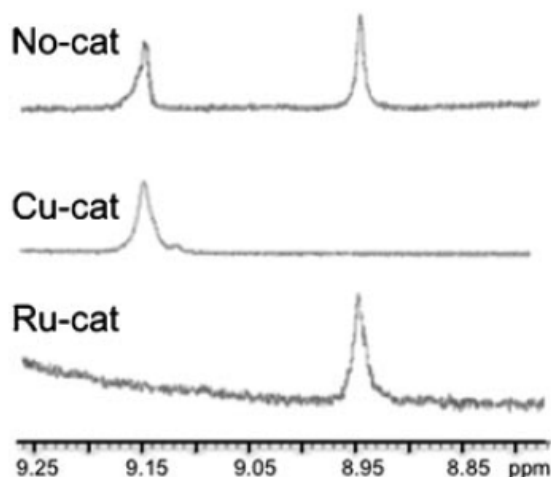
Figure 3.4.2.1: ¹H-NMR analysis in the range 8.80-9.25 ppm of the three crudes of reaction. From top to down: not-catalyzed, copper catalyzed and ruthenium catalyzed.

These results were extremely encouraging because they confirmed the possibility to obtain reaction between two ligands anchored to the metal surface and at the end between the two nanostructures. In order to have ulterior confirmations about the occurred reaction, the cycloadducts obtained were characterized by IR spectroscopy and TEM analysis (**Figure 3.4.2.2**), which definitely showed the assemblies of GNRs-**1/2** and AgNPs-**1/3** from a click linkage, where GNRs can be easily identify by their peculiar shape while silver is in the form of spheres.

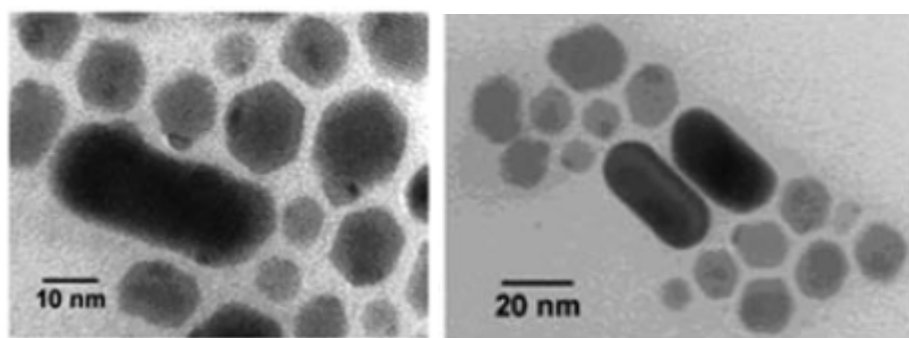**Figure 3.4.2.2**: TEM images of GNRs-click-AgNPs

The nature of the two different nanostructures (Au and Ag) was analyzed and confirmed by energy dispersive analysis (EDS). Moreover, by an accurate TEM images observation a spatial distance between GNRs and AgNPs in the range of 2–3 nm was obtained, which is in quite good accordance with the value expected for the linker length (ca. 3 nm), also

considering that the organic ligands between the metallic surfaces could be slightly constrained (**Figure 3.4.2.3**).
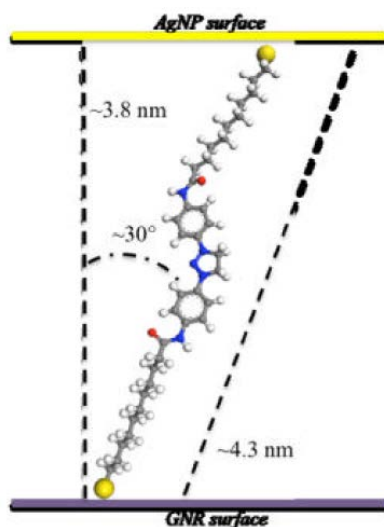

Figure 3.4.2.3: schematic representation of the possible disposition of the ligands between the two nanostructures and consequent expected distance.

3.4.3 Entrapment of GNRs-click-AgNPs into polymeric nanocarrier

As a final stage of this research work the entrapment of the above obtained cycloadducts into a polymeric nanocarrier was achieved. For this extremely challenging attempt the nanoprecipitation technique was preferred due to the final solubility of the click product in DMF, a solvent miscible with water.

In addition, the cycloadducts obtained from the non-catalyzed reaction were chosen, since it was not necessary the purification of the reaction mixture, given the absence of catalysts or other reagents. Following the general procedure already described, GNRs-click-AgNPs were entrapped into PNPs made of PLGA-*b*-PEG-COOH copolymer. The so-obtained GNRs-click-AgNPs-PNPs were purified with the previously described two methods, but using in this case filters with a cut-off of 450 nm instead of 220 nm, due to the bigger size of the particles obtained. After that, a complete characterization was carried out. ICP analysis showed a gold concentration in the final sample of 15 ppm and simultaneously a silver concentration of 18 ppm, confirming the entrapment of both the two moieties into the nanocarriers. DLS analysis showed that GNRs-click-AgNPs-PNPs presented an average diameter of 287.0 ± 3.1 nm with a uniform size distribution and a PDI value of 0.100 ± 0.012; ζ-potential analysis indicated a value of -37 mV, attesting the presence of free carboxylic acid groups onto the surface. The obtained rather high diameter found justification in the encapsulation of the cycloadduct,

especially if compared with an empty PNPs obtained with the same solvent and technique (blank-PNPs), which presented an average diameter of 87.3 ± 0.4 nm. This increase of size clearly demonstrates the entrapment of GNRs-click-AgNPs into polymeric nanoparticles (**Figure 3.4.3.1**).
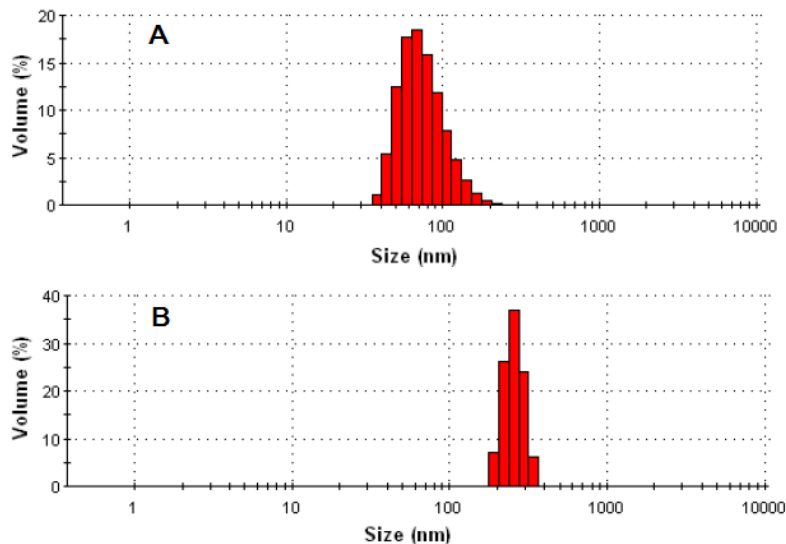
Figure 3.4.3.1: DLS analysis showing comparison between size of blank-PNPs (A) and GNRs-click-AgNPs-PNPs

3.4.4 In vitro evaluation of optoacoustic imaging capability

For proving the suitability of the GNRs-click-AgNPs-PNPs as contrast agent for optoacoustic imaging, a phantom study using particle-loaded alginate structures was performed. As already discussed in Chapter 3.2.4, GNRs-**1**-PNPs demonstrated their suitability as contrast agent for optoacoustic imaging both in phantom studies and in *in vitro* ones. Thus, this experiment aimed in particular at the demonstration of real maintenance of the peculiar nanostructure's properties after covalent linkage with another one. For this experiment conventional GNRs-**1**-PNPs were used as reference. Two phantoms alginate spheres containing either GNRs-**1**-PNPs or GNRs-click-AgNPs-PNPs at the same concentration were prepared and investigated for optoacoustic signal amplitudes ability: encouragingly the acquired data showed that PNPs containing the cycloadduct led to similar optoacoustic signal amplitudes than conventional GNRs-**1**-PNPs without AgNPs (**Figure 3.4.4.1**).
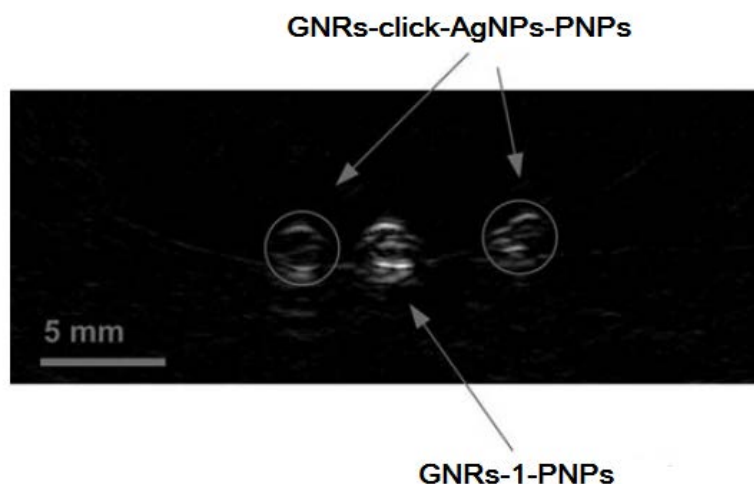
Figure 3.4.4.1: optoacoustic image obtaine for two alginate spheres containing GNRs-click-AgNPs-PNPs and one containing only GNRs-1-PNPs.

More specifically, both the two alginate spheres are detectable with optoacoustic imaging with a signal-to-noise ratio of 45 dB for the GNRs-click-AgNPs-PNPs and 55 dB for the GNRs-1-PNPs. Although replacing GNR by the cycloadduct in the phantoms resulted in a loss of signal to noise ratio of 10 dB, both the two systems are well suitable as optoacoustic contrast agents due to the high signal to noise ratio, which was observable with this technique. Therefore it is possible to state that the chemical linkage between the two nanostructures does not affect the excellent optical and optoacoustical properties of the GNRs entrapped into the polymeric matrix.

This multifunctional device, since the demonstrated toxicity of AgNPs against cancer cells is highly suitable for the new emerging concept of theranostic applications for cancer treatment.

4. Conclusion

In conclusion, during these three years of work, multifunctional nanosystems that present potentiality for drug delivery and theranostic applications were successfully synthesized and tested against glioblastoma multiforme *in vitro* and *in vivo*.

After a preliminary huge investigation in the past literatures, gold nanorods (GNRs) and silver nanoparticles (AgNPs) were chosen for their special and promising properties: GNRs could be exploited both as contrast agent in optoacoustic imaging and as therapeutic localized-hyperthermia generator, while AgNPs could be promising as therapeutic antitumor agent. Both the two nanostructures were synthesized with modified and adjusted salt-reduction methods and completely characterized by mean of several techniques. Surface modifications with specifically designed organic ligands of these metal nanostructures were provided in an easy, robust and reproducible protocol, with losing neither stability nor peculiar properties of the nanoparticles. Thanks to this process organo-soluble, surfactant-free, metal nanoparticles could be obtained and their final solubility or reactivity tuned as desired by simply changing the terminal groups of the ligands anchored to the surface. Indeed, three suitable organic ligands were synthesized with the same head thiol group, highly similar internal chain but different terminal groups: an ester group in order to confer solubility but not reactivity to the nanoparticles (ligand 1), an acetylene (ligand 2) and an azido (ligand 3) group in order to confer reactivity towards click chemistry azido-alkyne Huisgen cycloaddition to both the two nanostructures.

The huge characterization, especially by mean of ^{1}H-NMR, of the obtained lipophilic metal nanoparticles demonstrated the efficiency of the ligand exchange reaction as well as their properties' maintenance.

In order to address the challenging issue of an efficient delivery of this particles within the body, polymeric nanoparticles (PNPs) constituted of the FDA-approved poly(lactic-*co*-glycolic) acid covalently linked to a chain of poly(ethylene glycol), known as PLGA-*b*-PEG-COOH, were selected as nanocarriers for the metal nanostructures. Indeed, PNPs are known for their capability to host, in their inner lipophilic core, small molecules but also rather large nanoparticles, provided that they are lipophilic as well. Therefore, the entrapment of the above described, surface-modified metal nanoparticles can be achieved. By using two

different techniques, the nanoprecipitation or the oil-in-water, both GNRs and AgNPs, as well as the novel anti neoplastic drug Alisertib were entrapped into the PNPs: more specifically, GNRs were entrapped alone, while AgNPs were entrapped both alone and simultaneously with the Alisertib, in order to evaluate a possible synergistic antitumor effect between them. All the nanosystems obtained were completely characterized by mean of several techniques such as DLS, AAS, UV-Vis, TEM, TGA etc.

Finally, to all the nanosystems prepared the peptide Chlorotoxin, a targeting agent able to specifically recognized glioma cancer cells, was conjugated onto the outer shell: the conjugation reaction was achieved taking advantage of the carboxylic acid groups exposed onto the PNPs' surface, deriving from the free ending group of the PEG copolymer, and it exploited common organic amidation reaction with water soluble carboxylic acids activator.

In this way an efficient and selective drug delivery against glioblastoma cells and tissues could became a reality.

When necessary for the biological tests, and visualization within the body, also the fluorescent dye Cyanine 5 or the radioisotope ^{99m}Tc were anchored to the PNPs surface.

All the obtained nanosystems were tested both *in vitro* and *in vivo* for preliminary proof of concept of theranostic applications.

More specifically, GNRs were tested as contrast imaging agent in optoacoustic technique firstly in phantom studies then *in vitro* onto a glioblastoma cell line: both the results were extremely encouraging because GNRs were definetly able to act as contrast agent for this kind of imaging. GNRs were also tested as therapeutic agents thanks to localized hyperthermia phenomenon that they could allow: the *in vitro* tests clearly showed an almost complete cells death after laser irradiation of cell line exposed to GNRs at a safe and non toxic concentration. Moreover, the targeting with chlorotoxin revealed to be of foundamental importance for tumor up-take and retainment of the entire nanosystem as demonstrated by *in vivo* test in tumor bearing mice.

AgNPs were investigated as therapeutic agent against glioblastoma multifome firstly *in vitro* and then also *in vivo*. An interesting cytotoxic effect has emerged from preliminary in vitro evaluation; this effect was definetly enhanced when AgNPs and Alisertib drug co-exhist into the same nanocarrier: a synergistic effect between the two of them was clearly revealed, leading to an exceptional IC50 value of 10 nM after 72 hours of incubation. Also in this case, the necessity of the targeting agent chlorotoxin was clearly demonstared, not only by IC50 values but also thanks to up-take studies. Moreover, this promising nanosystem containing

both Alisertib and AgNPs was tested *in vivo* in tumor bearing mice: the effect on only one administration was extremely successful because a tumor mass reduction of 22% was obtained.

Finally, a covalent linkage between GNRs and AgNPs with the click chemistry reaction azido/alkyne Huisgen cycloaddition was attempet and achieved: thanks to the two reactive ligands 2 and 3 anchored to the surface of the metal nanostructures the reaction can be performed obtaining linked nanoparticles but with a spacer in the middle, meaning that no-quenching of the properties occurred. The complex nanosystem obtained was completely characterized in order to confirm the formation of the triazole ring by ^{1}H-NMR analysis and TEM images.

The creation of a unique nanosystem constituted of two different nanoparticles and simultaneous maintenance of their properties is a purpose considered still nowadays extremely challenging.

Also these complex nanosystem was entrapped into a PNPs and a preliminary evaluation of the maintenace optoacoustic ability of GNRs was performed in phantom experiments.

In conclusion, powerful and promising multifunctional nanosystems for drug delivery aim and gliblastoma treatment have been developed, characterized and tested: the encouraging results obtained the hope of a real cancer defeat.

5. Experimental section

5.1 Materials and Methods

All chemicals were purchased from Sigma-Aldrich (St. Louis, MO) and used as received. Poly(D,L-lactide–*co*–glycolide) (50/50) with carboxylic acid end group (PLGA-COOH, inherent viscosity 0.12 dL/g, MW~7 kDa) was purchased from Lakeshore Biomaterials (Birmingham, AL, USA). Polyethylene glycol with amino and carboxylic acid end groups (NH_2-PEG-COOH and H_2N-PEG-NH_2MW~3 kDa) was purchased from Rapp Polymere GmbH (Tübingen, Germany). All aqueous solutions were prepared with deionized water obtained using an ultrafiltration system (Milli-Q, Millipore) with a measured resistivity above 18 MΩ/cm. Dichloromethane (DCM) and chloroform ($CHCl_3$) were passed through basic alumina prior to use. THF was distilled from sodium/benzophenone just prior to use and stored under Ar. Other solvents were purified by standard procedures. Light petroleum ether refers to the fraction with bp 40-60°C. The reactions were monitored by TLC performed on silica gelplates (Baker-flex IB2-F).^{1}H NMR and ^{13}C NMR spectra were recorded using $CDCl_3$ or DMSO solutions at 300, 400 and 600 MHz for ^{1}H and 75.46, 100.6 and 150.92 MHz for [13]C. Chemical shifts (δ) are reported in ppm relative to $CHCl_3$ (δ = 7.26 for ^{1}H and δ = 77.0 for ^{13}C).

Mass spectra were obtained with an electrospray ionization source (ESIMS). All the ESIMS spectra were performed using MeOH as the solvent. Melting points were determined with a Büchi melting point apparatus. Transmission Electron Microscopy (TEM) was conducted on a JeolJEM 2010 at 200 keV. Samples for TEM analyses were prepared by spreading a small drop of the nanoparticle dispersion on amorphous carbon-coated copper grids (Formvar carbon 400 mesh grids) followed by air-drying. Fourier transform infrared (FTIR) spectra were recorded on a Perkin-Elmer Spectrum 2000. DLS measurements were performed on a Malvern Zetasizernano-S working with a 532 nm laser beam. ζ potential measurements were conducted in DTS1060C-Clear disposable zeta cells at 25 °C. SpectraAA 100 Varian was used for atomic absorption spectroscopy (AAS) analyses. Inductively Coupled Plasma Atomic Emission Spectroscopy(ICP-AES) was performed on a Liberty 200 Varian. High-performance liquid chromatography (HPLC) analyses were performed using a L-6200 liquid chromatograph (Merck – Hitachi, Darmstadt, Germany) equipped with a L-4200 variable Merck-Hitachi UV-VIS detector

(Merck – Hitachi, Darmstadt, Germany). Data acquisition and peak area integration were carried out with a Merck-Hitachi D-2500 Chromato-integrator - D-6000 (v.2.03) HPLC Manager data system (Merck-Hitachi, Darmstadt, Germany). Chromatographic separations were carried out on a (C18) Supelcosil LC-18DB 250 x 4.6 mm (5 µm) column (Supelco, Bellefonte, PA,USA) at room temperature. The samples were eluted with a mobile phase of CH_3CN – H_2O (50:50, v/v) under isocratic conditions at a flow rate of 1 mL/min. The detector wavelength was set at 300 nm. Identification of the compounds in the analyzed samples was achieved by comparison with the authentic specimens. Retention time under various chromatographic conditions constituted the comparison criteria. The samples (0.5 mL) were diluted with 2 mL of CH_3CN and analyzed by HPLC (20 μL injections; the amount injected was chosen so as to maintain the peak area counts in the linear range 1,000 - 600,000) after sonication (15 min) and filtration on syringe filter SterivexTM-GP 0.22 μm of polyether sulfone (Millipore, USA) to remove metals and polymers from the sample to inject.

Cell culture procedures: U87MG stabilized cell line deriving from human glioblastoma was supplied by the American Type Culture Collection (ATCC), mycoplasma free certified. Cells were prepared from deep-frozen stock vials and maintained in complete culture medium composed by Modified Eagle Medium low glucose added with 10% (v/v) Fetal bovine serum (Australian origin, Gibco Invitrogen, Italy) and 1% (v/v) penicillin/streptomycin (Invitrogen, Italy) under standard cell culture conditions (37 °C, 5% CO2 and 95% humidity, HERAEUS incubator, Germany). Cells were kept in culture at sub-confluent state. ITLC-SG coated fibre sheets were purchased from Gelman Sciences (Ann Arbor, MI). Sodium pertechnetate was eluted from a ^{99}Mo-^{99m}Tc generator. (DRYTEC, GE Healthcare). Radioactivity was measured on a Capintec CRC-15 dose calibrator (Ramsey, NJ). Radio-TLC analysis was performed on a Packard Imager (Canberra, Meriden, CT).

All the animals were maintained and handled in accordance with the Guidelines for Accommodation and Care of Animals (European Convention for the Protection of Vertebrate Animals Used for Experimental and Other Scientific Purposes) and internal guidelines and experimental procedures were approved by local authorities.

5.2 Organic synthesis

Synthesis of 4,4'-disulfanediyldibenzoic acid.
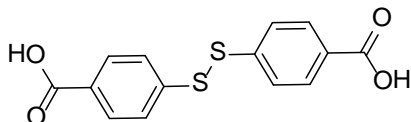
To a stirred solution of 4-mercaptobenzoic acid (1.00 g, 6.48 mmol) in ethanol (20 mL) a saturated solution of iodine in ethanol (3.35 mL) was added drop wise. The reaction was left to react for 3 hours at room temperature then the precipitate was filtered and washed with cold ethanol (3x10 mL). 0.87 g (yield 87%) of product were recovered in the form of a white powder.
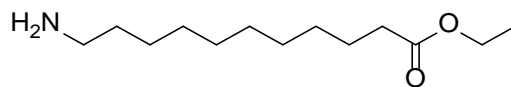
Data:

m.p.: 346 - 348 °C;
^{1}H-NMR (400 MHz, DMSO-*d6*): δ= 7.93 (d, 4H, CH), 7.64 (d, 4H, CH).
^{13}C-NMR: (100 MHz, DMSO-*d6*): δ= 166.6 (2C), 140.8 (2C), 130.3 (4CH), 129.7 (2C), 126.1 (4CH);
GC-MS ESI : ES⁻ 305 (M -1).

Synthesis of ethyl 11-aminododecanoate

To a suspension of 12-aminododecanoic acid (3.0 g, 13.2 mmol) in ethanol (50 mL) was added slowly concentrate sulfuric acid (0.8 mL). The mixture was refluxed for 18 h,cooled to room temperature, and the solvent was evaporated under reduced pressure. The crude wassuspended in ethyl acetate (200 mL), washed with 1 M ammonia aqueous solution (3 x 50 mL). The organic layer was dried over $MgSO_4$ and evaporated to yield 3.2 g (98 %) of product as a white solid.

Data:

m.p. = 56-58 °C;

^{1}H-NMR (400 MHz, CDCl3): δ = 4.10 (q, 3J(H,H) = 7.2 Hz, 2H), 2.67 (t, 3J(H,H) =7.1 Hz, 2H), 2.26 (t, 3J(H,H) = 7.6 Hz, 2H), 1.64-1.55 (m, 2H), 1.47-1.38 (m, 2H), 1.33-1.19 (m, 17H);

^{13}C-NMR (100.6 MHz, CDCl3): δ = 173.8, 60.1, 42.1, 34.3, 33.5, 29.6, 29.5, 29.4, 29.3, 29.2, 29.1,5 26.9, 24.9, 14.2;

FTIR (CCl4): ν = 3441, 2979, 2929, 2855, 1737, 1655, 1550, 1465, 1192, 1127, 1040,1012 cm-1;

GC-MS ESI: 244 (M+1).

Synthesis of bis-ethyl 11-(4-benzamido)dodecanoatedisulfide
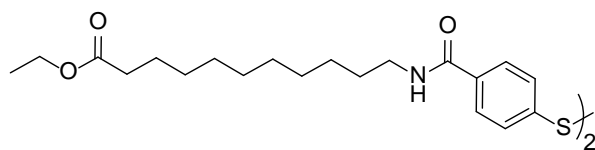
To a stirred solution, of 4,4'-disulfanediyldibenzoic acid (1.8 g, 2.47 mmol) under nitrogen, in 25 mL of anhydrous THF, *N,N'*-carbonyldiimidazole (595 mg, 3.70 mmol) was slowly added. The reaction was stirred for one hour at

room temperature and then ethyl 11-aminododecanoate (1.13 g, 4.94 mmol) in 5 mL of anhydrous THF were added. The reaction mixture was stirred for additional 3 hours at room temperature, then the solvent was removed under reduced pressure and EtOAc (10 mL) was added. The solution was washed three times (3x10 mL) with water and the organic layer was dried over $MgSO_4$ and dried giving 2.31 g (78.8%) of product as a white solid.

Data:

m.p. = 145-146 °C;

^{1}H-NMR (300MHz, CDCl3): δ = 7.68 (d, 3J(H,H) = 8.4 Hz, 4H), 7.50 (d, 3J(H,H) = 8.4 Hz, 4H), 6.12 (t, 3J(H,H) =5.6 Hz, 2H), 4.11 (q, 3J(H,H) = 7.1 Hz, 4H), 3.42 (q, 3J(H,H) = 6.9 Hz, 4H), 2.28 (t, 3J(H,H) = 7.8 Hz,4H), 1.70-1.52 (m, 8H), 1.41-1.21 (m, 34H);

^{13}C-NMR (100.6 MHz, CDCl3): δ = 173.9 (2C), 166.6(2C), 140.1 (2C), 133.7 (2C), 127.7 (4CH), 126.6 (4CH), 60.1 (2CH2), 40.1 (2CH2), 34.3 (2CH2), 29.6(2CH2), 29.5 (2CH2), 29.4 (2CH2), 29.3 (2CH2), 29.2 (2CH2), 29.1 (2CH2), 29.0 (2CH2), 26.9 (2CH2),24.9 (2CH2), 14.2 (2CH3);

FTIR (CCl4): ν = 3443, 2981, 2921, 2852, 1740, 1678, 1629, 1595, 1532, 1397, 1128, 1012 cm-1;

[M+Na]+: 752;

Synthesis of ethyl 12-(4-mercaptobenzamido)dodecanoate(**1**)
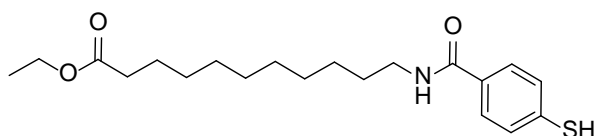
After cooling at 0°C, to a stirred suspension of bis-ethyl 11-(4-benzamido)dodecanoatedisulfide (0.91 g, 1.2 mmol) in a mixture of ethanol/THF (1:1, 50 mL)was added slowly NaBH$_4$ (0.17 g, 4.4 mmol). After complete addition, the mixture was allowed toreach room temperature and react for 4 h. Afterwards, the solvents were evaporated under reduced pressure and the crude was suspended in ethyl acetate (40 mL), washed with diluted HCl aqueous solution (0.1 M, 3x15 mL) and water (3x15 mL). The organic layer was dried over MgSO$_4$, evaporated to yield 0.79 g (87 %) of compound **1** as a white solid.

Data:

m.p. = 86-87 °C;

^{1}H-NMR (300MHz, CDCl3): δ = 7.62 (d, 3J(H,H) = 8.4 Hz, 2H), 7.27 (d, 3J(H,H) = 8.4 Hz, 2H), 6.14 (s, brs, 1H),4.11 (q, 3J(H,H) = 7.2 Hz, 2H), 3.56 (s, 1H), 3.41 (q, 3J(H,H) = 6.8 Hz, 2H), 2.27 (t, 3J(H,H) = 7.5 Hz,2H), 1.64-1.53 (m, 4H), 1.39-1.21 (m, 17H);

^{13}C-NMR (100.6 MHz, CDCl3): δ = 173.9, 166.7, 135.8,131.8, 128.5 (2CH), 127.5 (2CH), 60.1, 40.1, 34.4, 29.6, 29.4, 29.3, 29.2, 29.2, 29.1, 29.0, 26.9, 24.9,14.2;

FTIR (CCl4): ν = 3457, 2979, 2930, 2856, 1736, 1673, 1598, 1515, 1484, 1372, 1240, 1186 cm-1;

[M+Na]+: 388;

Synthesis of 11,11'-disulfanediyldiundecanoic acid
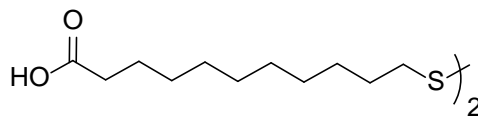
To a stirred solution, cooled at 0 °C and under nitrogen, of 11-mercaptoundecanoic acid (0.5 g, 2.29 mmol) in 10 ml of dichloromethane, was added slowly a solution of sulfuryl chloride (95 µL, 1.15 mmol) in dichloromethane (5 mL). After 30 minutes the solvent was removed under vacuum giving 465 mg (93%) of 11,11'-disulfanediyldiundecanoic acid as a white solid.

Data:

m.p : 92-93 °C.

^{1}H-NMR (300 MHz, DMSO-*d6*): d= 2.68 (t, 4H, -CH2-S), 2.36 (t, 4H, -CH2-C=O), 1.57-1.72 (m, 8H), 1.21-1.46 (m, 24H) ppm.

^{13}C-NMR (100 MHz, DMSO-*d6*): d= 175.14, 41.04, 40.76, 40.21, 39.93, 39.66, 38.61, 34.34, 29.55, 29.43, 29.25 ppm

IR (atr, cm-1): 2916.38, 2848.54, 1692.90, 1471.41, 1427.78, 1411.39, 1289.04, 1262.49, 1231,29, 1206.33, 1105.00, 945.24, 718.96.

GC-MS ESI: 433 (M - 1).

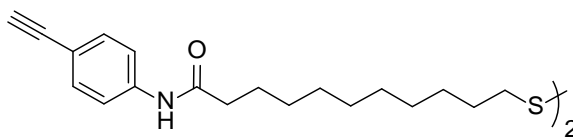*Synthesis of N-(4-ethynylphenyl)-11,11'-disulfanediyldiundecanoic amide:*

To a stirred solution, under nitrogen, of 11,11'-disulfanediyldiundecanoic acid (197 mg, 0.45 mmol) with 6 mL of anhydrousTHF, was slowly added N,N'-carbonyldiimidazole (191 mg, 1.18 mmol). The reaction was stirred for one hour at room temperature and then 4-ethynylaniline (105 mg, 0.9 mmol) in 5 mL of anhydrous THF were added. The reaction mixture was stirred for additional 2 hours at room temperature, then the solvent was removed under reduced pressure and EtOAc (10 mL) was added. The solution was washed three times (3x10 mL) with water and the organic layer was filtered and dried giving 1 (193 mg, 68%) as a pale yellow solid.

Data:

m.p. : 119-122 °C.

^{1}H-NMR (300 MHz, DMSO-d6): d= 10.0 (s, 2H, NH), 7.58 (d, 4H, CH), 7.37 (d, 4H, CH), 4.03 (s, 2H, CH), 2.68 (t, 4H, -CH2-S), 2.28 (t, 4H, -CH2-C=O), 1.41-1.63 (m, 8H), 1.15-1.39 (m, 24H) ppm.

^{13}C-NMR (100 MHz, DMSO-d6): d= 172.18, 140.57, 132.97, 119.46, 116.46, 84.12, 80.32, 41.05, 40.77, 40.22, 39.94, 39.66, 38.57, 29.54, 29.46, 29.33, 29.23 ppm.

IR (paraffin, cm-1): 4329.67, 3276.01, 2923.95, 2854.62, 1659.61, 1462.82, 1377.25.

GC-MS ES+ : 655 (M + Na).

Synthesis of N-(4-azidophenyl)-11,11'-disulfanediyldiundecanoic amide:
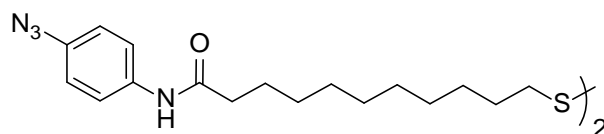
To a stirred solution, under nitrogen, of 11,11'-disulfanediyldiundecanoic acid (300 mg, 0.69 mmol) with 5 mL of anhydrousTHF, was slowly added N,N'-carbonyldiimidazole (290 mg, 1.79 mmol). The reaction was stirred for one hour at room temperature and then p-azidoaniline (255 mg, 1.5 mmol) in 6 mL of anhydrous THF were added. The reaction mixture was stirred for additional 2 hours at room temperature, then the solvent was removed under reduced pressure and chloroform (10 mL) was added. The solution was washed three times (3x10 mL) with water and the organic layer was filtered and dried giving 1 (358 mg, 78%) as a pale brown solid.

Data:

m.p. : 147-149 °C.

^{1}H-NMR (300 MHz, DMSO-d6): d= 9.91 (s, 2H, NH), 7.63 (d, 4H, CH), 7.02 (d, 4H, CH), 2.68 (t, 4H, -CH2-S), 2.28-2.13 (m, 4H, -CH2-C=O), 1.40-1.62 (m, 8H), 1.12-1.39 (m, 24H) ppm.

^{13}C-NMR (100 MHz, DMSO-d6): d= 171.95, 137.55, 121.14, 119.94, 117.39, 41.04, 40.76, 40.21, 39.93, 39.65, 39.37, 38.58, 36.98, 29.53, 29.21 ppm.

IR (paraffin, cm-1): 4330.16, 3289.83, 2923.08, 2854.33, 2360.35, 2133.53, 1655.24, 1461.18, 1377.14.

GC-MS ES+ : 689 (M + Na)

Synthesis of PLGA-NHS

PLGA-NHS
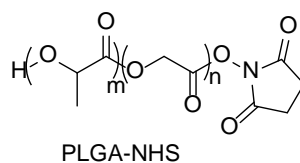
Poly(D,L-lactide–co–glycolide) (PLGA–COOH, 3 g, 0.43 mmol) and *N*-hydroxysuccinimide(NHS, 0.20 g, 1.7 mmol) were dissolved in dichloromethane (15 mL). After cooling at 0°C *N,N'*-dicyclohexylcarbodiimide (DCC, 0.38 mg, 1.8 mmol) was added and the mixture was left to warm up at room temperature and react for 24 h. Afterwards, dicyclohexylurea (DCU) was removed by filtration and PLGA–NHS was precipitated with cold diethylether (20 mL), and repeatedly washed with the same solvent (3 x 10 mL). After drying, the resulted white solid PLGA-NHS (2.91 g, 0.42 mmol) was collected. The product could be stock at -20 °C for no more than one week.

Data

^{1}H-NMR (300 MHz, CDCl3): δ = 5.11-5.31 (m, 1H), 4.63-4.92 (2H, m), 1.50-1.61 (m, 3H).

Synthesis of PLGA-b-PEG-COOH
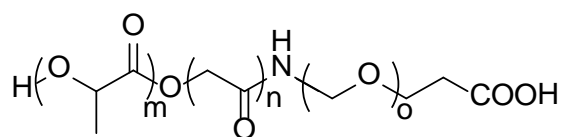
PLGA–NHS (2.91 g, 0.42 mmol) was dissolved in chloroform (20 mL) followed by addition of NH$_2$-PEG-COOH (1.24 g, 0.42 mmol) and *N,N*-diisopropylethylamine (0.21 mL, 1.20 mmol). After 24 h the copolymer was precipitated withcold diethyl ether (30 mL) and washed with the same solvent (3 x 10 mL) and cold water (3 x 20 mL) in order to remove the unreacted products. The resulting white solid PLGA-*b*-PEG-COOH (3.36 g, 0.33 mmol) was dried under vacuum and stored at -20 °C, where it is stable for more than one year.

Data

^{1}H-NMR (300 MHz, CDCl3): δ = 5.11-5.31 (NHS, m), 4.63-4.92 (1H, m), 3.63 (s,2H), 1.50-1.61 (m, 3H).

5.3. Nanothecnology

Chapter 2

Preparation of GNRs-1

GNRs-CTAB (2.5 mL, 20 mM) were diluted with 2.5 mL of water then added to a solution of ligand Ethyl 11-mercaptoundecanoate **1** (30 mg, 0.08 mmol) in 5 mL of ethanol. The mixture was left to react firstly one hour into a sonication bath then overnight at room temperature under mechanical stirring. After that GNRs-**1** were precipitated by centrifugation (6000 rpm, 30 min) and washed with ethanol (2x10 mL) in order to remove excess ligand and CTAB. GNRs-**1** were then redispersed in 3.5 mL of chloroform, dried under a stream of nitrogen and re-dispersed again in 7 mL of dichloromethane. Finally, the solution was sonicated for 30 minutes and use immediately for next step.

Synthesis of GNRs-1-PNPs

Gold nanorods polymeric nanoparticles (GNRs-**1**-PNPs) were prepared using the oil-in-water (O/W) emulsion-solvent evaporation technique. PLGA-*b*-PEG-COOH (7 kDa–3 kDa, 70 mg, 7 µmol) were added to 7 mL of GNRs-**1** in dichloromethane. 70 mL of ultrapure water were added to the oil phase and the mixture was emulsified for 2 minutes with a trip probe sonicator (input = 600 W, ampl = 80%). The solvent was evaporated under *vacuum* then the suspension was concentrated and purified from small molecules, washing with water (3 times), using centrifugal filter devices (Amicon Ultra, Ultracel membrane with 100.000 NMWL, Millipore, USA) to a final concentration of 5 mL. Finally, GNRs-**1**-PNPs were filtered in order to remove aggregates and bacteria using a syringe filter phenex-PES of polyether sulfone (26 mm, 0.20 µm, Phenomenex, Italy).

*Synthesis of GNRs-**1**@PNPs-Cltx*

To a stirred suspension of GNRs-**1**-PNPs (5 mL, 1.07mM) in phosphate buffer (PBS, 20 mL, 0.01 M) was added a solution of *N*-hydroxysulfosuccinimide (23 mM, 1.74 mL) and a solution of 1-ethyl-3-(3-dimethylaminopropyl) carbodiimide hydrochloride (2.8 M, 0.71 mL). The solution was left to react at room temperature for one hour then then the un-reacted EDC and Sulfo-NHS were removed by one fast filtration of the entire solution on centrifugal filter devices (Amicon Ultra, Ultra cell membrane with 100.000 NMWL, Millipore, USA) and the volume of the system restored with PBS.After that, 125 µg (0.031 µmol) of Chlorotoxin (MCMPCFTTDHQMARKCDDCCGGKGRGKCYGPQCLCR) dissolved in 1 mL of water was added and the system left to react overnight. The mixture was then concentrated and purified, washing with PBS (3 times) using centrifugal filter devices (Amicon Ultra, Ultra cell membrane with 100.000 NMWL, Millipore, USA), to a final volume of 5 mL. Finally GNRs-**1**-PNPs-Cltx was filtered using a syringe filters phenex-PES of polyether sulfone (26 mm, 0.20 µm, Phenomenex, Italy).

Modification of Cyanine5.5-NHS ester with 1,4-diaminobutane

To a stirred solution of Cyanine5.5-NHS ester (100 nmol) in water (10 mL), 1,4-diaminobutane (300 nmol, 26.4 µg) was added. The reaction was left to react under nitrogen flux and in dark for 24 hours. The so activated Cyanine5.5 with terminal amino group was used in the next step without purification.

*Synthesis of GNRs-**1**-PNPs-Cy5.5*

To a stirred suspension of GNRs-**1**@PNPs (5 mL, 1.07mM) in PBS (20 mL, 0.01 M) was added a solution of *N*-hydroxysulfosuccinimide (Sulfo-NHS, 23 mM, 1.74 mL) and a solution of 1-ethyl-3-(3-dimethylaminopropyl) carbodiimide hydrochloride (EDC, 2.8 M, 0.71 mL). The solution was left to react at room temperature for one hour then the un-reacted EDC and Sulfo-NHS were removed by one fast filtration of the entire solution on centrifugal filter devices (Amicon Ultra, Ultra cell membrane with 100.000 NMWL, Millipore, USA) and the volume of the system restored with PBS. After that, 6.4 nmol of Cyanine5.5, previously activated with terminal amino group as above reported, was added and the system left to react overnight. The mixture was then concentrated and purified, washing with PBS (3 times), using centrifugal filter devices (Amicon Ultra, Ultra cell membrane with 100.000 NMWL, Millipore, USA), to a final volume of 2 mL. Finally GNRs-**1**-PNPs-Cy5.5 were filtered using a syringe filters phenex-PES of polyether sulfone (26 mm, 0.20 µm, Phenomenex, Italy).

*Synthesis of GNRs-**1**-PNPs-Cltx/Cy5.5*

To a stirred suspension of GNRs-**1**-PNPs (5 mL, 1.07mM) in PBS (20 mL, 0.01 M) was added a solution of *N*-hydroxysulfosuccinimide (Sulfo-NHS, 23 mM, 1.74 mL) and a solution of 1-ethyl-3-(3-dimethylaminopropyl) carbodiimide hydrochloride (EDC, 2.8 M, 0.71 mL). The solution was left to react at room temperature for one hour then the un-reacted EDC and Sulfo-NHS were removed by one fast filtration of the entire solution on centrifugal filter devices (Amicon Ultra, Ultra cell membrane with 100.000 NMWL, Millipore, USA) and the volume of the system restored with PBS. After that, 125 µg (0.031 µmol) of Chlorotoxin (MCMPCFTTDHQMARKCDDCCGGKGRGKCYGPQCLCR) dissolved in 1 mL of water, and 6.4 nmol of Cyanine5.5, previously activated with terminal amino group, were added and the system left to react overnight. The mixture was then concentrated and purified, washing with PBS (3 times), using centrifugal filter devices (Amicon Ultra, Ultra cell membrane with 100.000 NMWL, Millipore, USA), to a final volume of 2 mL. Finally GNRs-**1**-PNPs-Cltx/Cy5.5 were filtered using a syringe filters phenex-PES of polyether sulfone (26 mm, 0.20 µm, Phenomenex, Italy).

Synthesis of AgNPs

A glucose solution (2 mL, 1.11 M) and NaOH (125 mg, 3.13 mmol) were added under vigorous magnetic stirring to a solution of polyvinylpyrrolidone k25 (PVP, 1.38 g, 0.055 mmol) in water (35 mL) and the mixture was heated to 90 °C; subsequently, a solution of silver nitrate (10 mL, 0.22 M) was rapidly injected into the hot mixture. The reaction was kept at the same temperature for 3 minutes, maintaining magnetic stirring, then it was allowed to cool to room temperature. The so formed AgNPs were purified by washing with water (2 x 20 mL) and concentrated using high speed centrifugation (6000 rpm, 60 min) until the final volume of 5mL.

*Synthesis of AgNPs-**1***

To a solution of ligand **1** (75 mg, 0.21 mmol) in ethanol (17 mL) a water suspension of AgNPs (5 mL) was slowly added. The mixture was allowed to react one hour in the ultrasonic bath then overnight under mechanical stirring at room temperature. After that, the so obtained AgNPs-**1** were collected and purified by centrifugation (6000 rpm, 30 min) washing with ethanol (22 mL) 3 times and re-suspended in chloroform (5 mL). Finally, the solvent was gently evaporated under nitrogen flux and the nanoparticles re-suspended again in dimethylsulfoxide (DMSO, 5 mL). The so-obtained lipophilic silver nanoparticles were immediately used in the following steps.

*Synthesis of AgNPs-**1**-PNPs*

50 mg of PLGA-*b*-PEG-COOH (7 kDa-3 kDa, 0.005 mmol) were dissolved into a 5 mL dispersion of AgNPs-**1** in DMSO. The organic phase was mixed to 50 mL of ultrapure water under vigorous stirring, maintaining water/organic ratio 10/1 with a constant removal of the resulting solution. The mixture was kept under magnetic stirring for 30 minutes then purified and concentrated using centrifugal filter devices (Amicon Ultra, Ultracell membrane with 100.000 NMWL, Millipore, USA) until the final volume of 5 mL that was filtered on syringe filter SterivexTM-GP 0.22 μm of polyether sulfone (Millipore, USA) and stored at 4 °C.

*Synthesis of AgNPs-**1**-PNPs-Cltx*

To a dispersion of AgNPs-1-PNPs (5 mL) in PBS (20 mL, 0.01 M) under magnetic stirring, *N*-hydroxysulfosuccinimide (1.3 mg, 11.0 µmol) and a solution of 1-ethyl-3-(3-dimethylaminopropyl) carbodiimide 0.28 M (7.1 mL) were added. The mixture was allowed reacting at room temperature for one hour. Subsequently, Chlorotoxin (MCMPCFTTDHQMARKCDDCCGGKGRGKCYGPQCLCR, 150 µg, 0.038 µmol) dissolved in 1 mL of water was added and reacted for 24 hours. The mixture was purified washing with PBS solution 3 times and concentrated into centrifugal filter devices (Amicon Ultra, Ultracell membrane with 100.000 NMWL, Millipore, USA), to a final volume of 5 mL. Finally, AgNPs-1-PNPs-Cltx were filtered on syringe filter SterivexTM-GP 0.22 μm of polyether sulfone (Millipore, USA) and stored at 4 °C.

Synthesis of Ali-PNPs

50 mg of PLGA-*b*-PEG-COOH (7 kDa-3 kDa, 0.005 mmol) and 9 mg of Alisertib (0.017 mmol) were dissolved into 5 mL of DMSO. The organic phase was mixed to 50 mL of ultrapure water under vigorous stirring, maintaining water/organic ratio 10/1 with a constant removal of the resulting solution. The mixture was kept under magnetic stirring for 30 minutes and subsequently purified and concentrated using centrifugal filter devices (Amicon Ultra, Ultracell membrane with 100.000 NMWL, Millipore, USA) until the final volume of 5 mL that was filtered on syringe filter SterivexTM-GP 0.22 μm of polyether sulfone (Millipore, USA) and stored at 4 °C.

Synthesis of Ali-PNPs-Cltx:

N-hydroxysulfosuccinimide (1.3 mg, 11.0 µmol) and a solution of 1-ethyl-3-(3-dimethylaminopropyl) carbodiimide 0.28 M (7.1 mL) were added under magnetic stirring to a dispersion of Ali@PNPs (5 mL) in PBS (20 mL, 0.01 M). The mixture was allowed activating at room temperature for one hour. Chlorotoxin (Cltx, 150 µg, 0.038 µmol) dissolved in 1 mL of water was added and allowed reacting for 8 hours. After that the mixture was purified washing with PBS solution 3 times and concentrated into centrifugal filter devices (Amicon Ultra, Ultracell membrane with 100.000 NMWL, Millipore, USA) to a final volume of 5 mL. Finally, Ali-PNPs-Cltx were filtered on syringe filter SterivexTM-GP 0.22 µm of polyether sulfone (Millipore, USA) and stored at 4 °C.

Synthesis of Ag/Ali-PNPs

50 mg of PLGA-*b*-PEG-COOH (7 kDa-3 kDa, 0.005 mmol) and 9 mg of Alisertib (0.017 mmol) were dissolved into 1 mL dispersion of AgNPs-**1** in DMSO. The organic phase was mixed to 50 mL of ultrapure water under vigorous stirring, maintaining water/organic ratio 10/1 with a constant removal of the resulting solution. The mixture was kept under magnetic stirring for 30 min and then purified and concentrated using centrifugal filter devices (Amicon Ultra, Ultracell membrane with 100.000 NMWL, Millipore, USA) until the final volume of 5 mL.This dispersion was then filtered on syringe filter SterivexTM-GP 0.22 μm of polyether sulfone (Millipore, USA) and stored at 4 ℃.

Synthesis of Ag/Ali-PNPs-Cltx

To a suspension of Ag/Ali-PNPs (5 mL) in PBS (20 mL, 0.01 M) under magnetic stirring, N-hydroxysulfosuccinimide (1.3 mg, 11.0 µmol) and a solution of 1-ethyl-3-(3-dimethylaminopropyl) carbodiimide 0.28 M (7.1 mL) were added. The mixture was left to react at room temperature for 30 min then Chlorotoxin (Cltx, 0.150 µg, 0.038 µmol) dissolved in 1 mL of water was added and the reaction mixture was allowed to react for additional 8h. Next, the mixture was washed with PBS solution 3 times and concentrated into centrifugal filter devices (Amicon Ultra, Ultracell membrane with 100.000 NMWL, Millipore, USA), to a final volume of 5 mL. Finally, Ag/Ali-PNPs-Cltx were filtered on syringe filter SterivexTM-GP 0.22 µm of polyether sulfone (Millipore, USA) and stored at 4 °C.

*Synthesis of GNRs-**1/2***

To a solution of ligand **1** (17.1 mg, 0.04 mmol) and of ligand **2** (25.2 mg, 0.04 mmol) in a mixture of ethanol and dimethylformamide (EtOH/DMF 1/1, 10 mL) a water suspension of GNRs-CTAB (10 mL) was slowly added. The mixture was allowed to react one hour in the ultrasonic bath, then overnight under mechanical stirring at room temperature. After that, the so obtained GNRs-**1/2** were collected and purified by centrifugation (6000 rpm, 30 min) washing with a mixture of EtOH/DMF (1/1, 20 mL) 3 times and re-suspended in DMF or THF or DMSO (5 mL). The so-obtained lipophilic GNRs-**1/2** were immediately used in the following steps.

*Synthesis of AgNPs-**1/3***

To a solution of ligand **1** (25.05 mg, 0.066 mmol) and of ligand **3** (37.28 mg, 0.056 mmol) in a mixture of ethanol and dimethylformamide (EtOH/DMF 1/1, 10 mL) a water suspension of AgNPs-PVP (10 mL) was slowly added. The mixture was allowed to react one hour in the ultrasonic bath, then overnight under mechanical stirring at room temperature. After that, the so obtained AgNPs-1/3 were collected and purified by centrifugation (6000 rpm, 30 min) washing with a mixture of EtOH/DMF (1/1, 20 mL) 3 times and re-suspended in DMF or THF or DMSO (5 mL). The so-obtained lipophilic AgNPs-**1/3** were immediately used in the following steps.

Synthesis of GNRs-click-AgNPs

- *Not catalyzed cycloaddition between GNRs-**1/3** and AgNPs-**2/3**:*

To a stirred solution of GNRs-**1/3** in DMF (5 mL), under nitrogen, was slowly added a solution of AgNPs-**2/3** in DMF. The reaction mixture was gently stirred and heated at 80 °C for 24 hours. The solution was cooled to room temperature and used for subsequent analysis without further purification.

- *Copper catalyzed cycloaddition between GNRs-**1/3** and AgNPs-**2/3***

To a stirred solution of GNRs-**1/3** in THF (5 mL), under nitrogen, was slowly added a solution of AgNPs-**2/3** in THF, a drop of triethylamine and CuI (0.76 mg, 0.004 mmol). The reaction mixture was gently stirred for 24 hours. After this period the solid was removed per decantation and the solvent evaporated under vacuum.

- *Ruthenium catalyzed cycloaddition between GNRs-**1/3** and AgNPs-**2/3***

To a stirred solution of GNRs-**1/3** in DMF (5 mL), under nitrogen, was slowly added a solution of AgNPs-**2/3** in DMF and chloro(pentamethylcyclopentadienyl)ruthenium (II) tetramer (2 mg, 0.0018 mmol). The reaction mixture was gently stirred for 24 hours. After this period the solution was purified by size exclusion cromatography to removed the catalyst (stationary phase: sephadexTM LH-20, eluent: DMF) and the solvent evaporated under vacuum.

40 mg of PLGA-b-PEG-COOH (7 kDa-3 kDa) were added to 4 mL di GNRs-click-AgNPs in DMF. The organic phase was mixed to 40 mL of ultrapure water under vigorous stirring, maintaining water/organic ratio 10/1 with a constant removal of the solution. The mixture was kept for 30 min. under vigorous stirring. After that the suspension was purified into centrifugal filter devices (Amicon Ultra, Ultracell membrane with 100.000 NMWL, Millipore, USA) washing with ultrapure water 10 times and finally concentrated obtaining a volume of 2 mL, that was filtrated by using a syringe filters phenex-PES of polyether sulfone (26mm, 0.20 μm, Phenomenex, Italy) and stored at 4 °C.

6. References

[1] B.Y.S. Kim, J.T. Rutka, W.C.W. Chan: "Nanomedicine". *N Engl J Med*, **2010,***363*, 2434-2443

[2] M. Elsabahy, K.L. Wooley. "Design of polymeric nanoparticles for biomedical delivery applications". *Chem. Soc. Rev.*, **2012**, *41*, 2545–2561.

[3] R. Siegel, D. Naishadham, A. Jemal: "Cancer statistic". *CA Cancer J* Clin, **2012**, *62*, 10-29.

[4] B. Sumer, J. Gao: "Theranostic nanomedicine for cancer". *Nanomedicine,* **2008**, 137-140.

[5] T.M. Allen, P.R. Cullis: "Drug delivery systems: entering the mainstream". *Science*, **2004**, *303*(5665), 1818-1822.

[6] F. Danhier, O. Feron, V. Préat: "To exploit the tumor microenvironment: Passive and active tumor targeting of nanocarriers for anti-cancer drug delivery". *Journal of Controlled Release*, **2010**, *148*(2), 135-146.

[7] J.D. Byrne, T. Betancourt, L. Brannon-Peppas: "Active targeting schemes for nanoparticle systems in cancer therapeutics." *Advanced drug delivery reviews,* **2008**, *60*, 1615-1626.

[8] E.D. Owens III, N.A. Peppas:"Opsonization, biodistribution, and pharmacokinetics of polymeric nanoparticles". *International Journal of Pharmaceutics,* **2006,***307*, 93-102.

[9] a) N.J. Abbott, A.A. Patabendige, D.E. Dolman, S.R. Yusof, D.J. Begley: "Structure and function of the blood–brain barrier". *Neurobiology of disease*, **2010**, *37*(1), 13-25. b) N.J. Abbott., L. Rönnbäck, E. Hansson: "Astrocyte–endothelial interactions at the blood–brain barrier." *Nature Reviews Neuroscience*, **2006**, *7*, 41-53.

[10] D.J. Begley, M.W. Bradbury, J. Kreutereds: "The blood-brain barrier and drug delivery to the CNS". New York: Dekker, **2000**.

[11] R. Siegel, D. Naishadham, A. Jemal: "Cancer statistic". *CA CANCER J CLIN*, **2013,** *63*, 11-30.

[12] D. M. Parkin, F. Bray, J. Ferlay, P. Pisani: "Global cancer statistics, 2002." *CA: CANCER J CLIN,* **2005,***55*, 74-108.

[13] B.A. Kohler, E. Ward, B.K. McCarthy, M.J. Schymura, L.A.G. Ries, C. Eheman, A. Jemal, R.N. Anderson, U.A. Ajani, B.K. Edwards; Annual Report to the Nation on the Status of Cancer, 1975–2007, Featuring Tumors of the Brain and Other Nervous System. *J. Natl. Cancer. Inst.*, **2011**, *103*, 1-23.

[14] O. Hiroko, P. Kleihues: "Genetic pathways to primary and secondary glioblastoma." *The American journal of pathology*, **2007**, 170, 1445-1453.

[15] F.B. Furnari, T. Fenton, R. M. Bachoo, A. Mukasa, J.M. Stommel, A. Stegh, W.C. Hahn, K.L. Ligon, D.N. Louis, C. Brennan, L. Chin, R.A. Depinho, W.K. Cavenee; Malignant astrocyticglioma: genetics, biology, and paths to treatment. *Genes Dev.,* **2007**, 21, 2683-2710.

[16] E.C. Halperin, P.C. Bruger: "Conventional external beam radiotherapy for central nervous system malignancies." In: Frank BD, ed. *Symposium on Neuro-Oncology*. Vol 3. 4[th]ed. New York, NY: Neurologic Clinics; **1985**, 867-882.

[17] W. Kunihiko, O. Tachibana, K. Sato, Y.Yonekawa, P.Kleihues, H.Ohgaki: "Overexpression of the EGF receptor and p53 mutations are mutually exclusive in the evolution of primary and secondary glioblastomas." *Brain pathology,* **1996** *6*, 217-223.

[18] E. C. Chu, A. S. Tarnawski: "PTEN regulatory functions in tumor suppression and cell biology". *Med. Sci. Monit.***2004**, *10*, 235-241.

[19] R. Stupp, W. P. Mason, M. J. Van Den Bent, M. Weller, B. Fisher, M. J. B. Taphoorn, K. Belanger, A. A. Brandes, C. Marosi, U. Bogdahn, J. Curschmann, R. C. Janzer, S. K. Ludwin, T. Gorlia, A. Allgeier, D. Lacombe, J. G. Cairncross, E. Eisenhauer, R. O. Mirimanoff: "Radiotherapy plus Concomitant and Adjuvant Temozolomide for Glioblastoma." *N. Eng. J. Med.*, **2005**, *352*, 987-996.

[20] M. G. Manfredi, J. A. Ecsedy, A. Chakravarty, L. Silverman, M. Zhang, K. M. Hoar, S. G. Stroud, W. Chen, V. Shinde, J. J. Huck, D. R. Wysong, D. A. Janowick, M. L. Hyer, P. J. LeRoy, R. E. Gershman, M. D. Silva, M. S. Germanos, J. B. Bolen, C. F. Claiborne, T. B. Sells: " Characterization of Alisertib (MLN8237), an investigational small-molecule inhibitor of aurora A kinase using novel in vivo pharmacodynamic assays." *Clinical cancer research*, **2011**, *17*(24), 7614-7624.

[21] U. A. Matulonis,S. Sharma, S. Ghamande, M. S. Gordon, S. A. Del Prete, I. Ray-Coquard, E. Kutarska, H. Liu, H. Fingert, X. Zhou, H. Danaee, R. J. Schilder: "Phase II study of MLN8237 (alisertib), an investigational Aurora A kinase inhibitor, in patients with platinum-resistant or-refractory epithelial ovarian, fallopian tube, or primary peritoneal carcinoma." *Gynecologic oncology*, **2012**.

[22] J. Deshane, C. C. Garner, H. Sontheimer. "Chlorotoxin inhibits glioma cell invasion via matrix metalloproteinase-2." *Journal of Biological Chemistry,* **2003**, *278*, 4135-4144.

[23] a) N. Graf, T. E. Mokhtari, I. A. Papayannopoulos, S. J. Lippard: "Platinum (IV)-chlorotoxin (CTX) conjugates for targeting cancer cells". *Journal of Inorganic Biochemistry*, **2012**, *110*, 58-63. b) C. A. Grimes: "Chlorotoxin, a small peptide derived from scorpion venom, targets cancer cells via a phosphatidylinositol phosphate"AACR Meeting Abstracts. **2005**, *1*, 1300.

[24] S. A. Lyons, J. O'Neal, H.Sontheimer: "Chlorotoxin, a scorpion-derived peptide, specifically binds to gliomas and tumors of neuroectodermal origin." *Glia,* **2002**, 39, 162-173.

[25] BS PAS 71 (2011) (English): Vocabulary. Nanoparticles

[26] A. Moores, F. Goettmann: "The plasmon band in noble metal nanoparticles: an introduction to theory and applications." *New Journal of Chemistry*, **2006**, *30*, 1121-1132.

[27] U. Kreibig, M. Vollmer eds: "Optical properties of metal clusters". Berlin, Springer, **1995**.

[28] P. Mulvaney: "Surface Plasmon Spectroscopy of Nanosized Metal Particles". *Langmuir*, **1996**, *12*, 788-800.

[29] P. K. Jain, X. Huang, I. H. El-Sayed, M. A. El-Sayed: "Review of some interesting surface plasmon resonance-enhanced properties of noble metal nanoparticles and their applications to biosystems". *Plasmonics*, **2007**, *2*(3), 107-118.

[30] M. Faraday: "Experimental relations of gold (and other metals) to light". *Philos. Trans. R. Soc. London*, **1857**, *147,* 145.

[31] J. Turkevich: "Colloidal Gold. Part II". *Gold Bulletin*, **1985**, *18*, 125-131.

[32] S. Vivek, K. Park, M. Srinivasarao: "Colloidal dispersion of gold nanorods: Historical background, optical properties, seed-mediated synthesis, shape separation and self-assembly." *Materials Science and Engineering: R: Reports* **2009**, *65*, 1-38.

[33] C. Lasagna-Reeves, D. Gonzalez-Romero, M. A. Barria, I. Olmedo, A. Clos, V.M. SadagopaRamanujam, A. Urayama, L. Vergara, M.J. Kogan, C. Soto: "Bioaccumulation and toxicity of gold nanoparticles after repeated administration in mice". *Biochemical and biophysical research communications*, **2010**, *393*(4), 649-655.

[34] C.J. Murphy, A.M. Gole, J.W. Stone, P.N. Sisco, A.M. Alkilany, E.C. Goldsmith, S.C. Baxter: "Gold Nanoparticles in Biology: Beyond Toxicity to Cellular Imaging". *Acc. Chem. Res.*, **2008**, *41*, 1721-1730.

[35] R. Weissleder: "A clearer vision for *in vivo* imaging". *Nature Biotechnol.*, **2001**, *19*, 316-317.

[36] L. Tong, Q. Wei, A. Wei, J.X. Cheng: "Gold nanorods as contrast agents for biological imaging: optical properties, surface conjugation, and photothermal effects". *PhotochemPhotobiol.*, **2009**, *85*(1), 21-46.

[37] P.K. Jain, K.S. Lee, I.H. El-Sayed, M.A. El-Sayed: "Calculated absorption and scattering properties of gold nanoparticles of different size, shape, and composition: applications in biological imaging and biomedicine". *J. Phys. Chem. B*, **2006**, *110*(14), 7238-7248.

[38] M. C. Lea: "On allotropic forms of silver". *Am. J. Sci.*, **1889**, *37*, 476–491.

[39] B. Nowack, H. F. Krug, M. Height: "120 Years of Nanosilver History: Implications for Policy Makers". E*nviron. Sci. Technol.***2011**, *45*, 1177–1183.

[40] a) H.Wang, X. Qiao, J. Chen, S. Ding: "Preparation of silver nanoparticles by chemical reduction method". *Colloids and Surfaces A: Physicochemical and Engineering Aspects*, **2005**, *256*(2), 111-115. b)H. Wang, X. Qiao, J. Chen, X. Wang, S. Ding: "Mechanisms of PVP in the preparation of silver nanoparticles." *Materials Chemistry and Physics*, **2005**, *94*(2), 449-453.

[41] E. T. Hwang, J. H. Lee, Y. J. Chae, Y. S. Kim, B. C. Kim, B. Sang, M. B. Gu: "Analysis of the Toxic Mode of Action of Silver Nanoparticles Using Stress-Specific Bioluminescent Bacteria". Small, **2008**, 4, 746-750.

[42] J. Turkevich, P. C. Stevenson, J. Hiller: "A study of the nucleation and growth processes in the synthesis of colloidal gold." *Discuss. Faraday Soc.*, **1951**, *11*, 55-75.

[43] a) M. A. Fox, F. J. Nabs, T. A. Voynick: "Chemically modified electrodes in dye-sensitized photogalvanic cells". *J. Am. Chem. Soc.* **1980**, *102*, 4036-4042. b) C. Zou, M. S. Wrighton: "Synthesis of octamethylferrocene derivatives via reaction of (octamethylferrocenyl)methyl carbocation with nucleophiles and application to functionalization of surfaces" *J. Am. Chem. Soc.* **1990**, *112*, 7578-7586. c) T. A. Heimer, S. T. D'Arcangelis, F. Farzad, J. M. Stipkala, G. J. Meyer:"An acetylacetonate-based semiconductor-sensitizer linkage." *Inorg. Chem.* **1996**, *35*, 5319-5324. d) P. G. Hoertz, R. A. Carlisle, G. J.Meyer, D. Wang, P. Piotrowiak, E. Galoppini: "Organic Rigid-Rod Linkers for Coupling Chromophores to Metal Oxide Nanoparticles". *Nano Lett.,* **2003**, *3*, 325-330. e) S. Pawsey, K. Yach, L. Reven: "Self-assembly of carboxyalkylphosphonic acids on metal oxide powders" *Langmuir,* **2002**, *18*, 5205-5212.

[44] J. C. Love, L. A. Estroff, J. K. Kriebel, R. G. Nuzzo, G. M. Whitesides: "Self-assembled monolayers of thiolates on metals as a form of nanotechnology." *Chem. Rev.*, **2005**, *105*, 1103-1169.

[45] A. Kumar, H. Joshi, P. Renu, A. B. Mandale, M. Sastry: "Phase transfer of silver nanoparticles from aqueous to organic solutions using fatty amine molecules." *Journal of Colloid and Interface Science*, **2003**, *264*, 396-401.

[46] a) J. T. Mullen, A. A. Dameron, A. M. Andrews, P. S. Weiss: "Selecting and Driving Monolayer Structures through Tailored Intermolecular Interactions". *AldrichimicaActa*, **2007**, *40*, 21-32. b) T. Sugimori, H. Masuda, N. Ohata, K. Kaiwai, A. Odani, O. Yamauchi: "Structural Dependence of Aromatic Ring Stacking and Related Weak Interactions in Ternary Amino Acid−Copper(II) Complexes and Its Biological Implication". *Inorg. Chem.*, **1997**, *36*, 576-583. c) G. B. McGaughey, M. Gagnè, A. K. Rappè: "π-Stacking Interactions. Alive and well in proteins".*J. Biol. Chem*, **1998**, *273*, 15458-15463.

[47] W. Maneeprakorn, M. A. Malik, P. O'Brien: "Developing Chemical Strategies for the Assembly of Nanoparticles into Mesoscopic Objects". *J. Am. Chem. Soc.*, **2010**, *132*, 1780-1781.

[48] H. C. Kolb, M. G. Finn, K. B. Sharpless: "You have free access to this contentClick Chemistry: Diverse Chemical Function from a Few Good Reactions". *Angewandte Chemie International Edition*, **2001**, *40*, 2004-2021.

[49] A. Padwa. J. Wiley and Sons, *1,3-Dipolar Cycloaddition Chemistry*, **1984**, New York.

[50] C. R. Becer, R. Hoogenboom, U. S. Schubert: "Click Chemistry beyond Metal-CatalyzedCycloaddition". *Angew. Chem. Int. Ed.*, **2009**, *48*, 4900–4908.

[51] L. Zhang, X. Chen, P. Xue, H. H. Y. Sun, I. D. Williams, K. B. Sharpless, V. V. Fokin, G. Jia: "Ruthenium-CatalyzedCycloaddition of Alkynes and Organic Azides". *J. Am. Chem. Soc.*, **2005**, *127*, 15998-15999.

[52] D. E. Owens III, N. A.Peppas: "Opsonization, biodistribution, and pharmacokinetics of polymeric nanoparticles."*Int J Pharm*, **2006**,*307*, 93–102.

[53] A. H.Faraji, P. Wipf: "Nanoparticles in cellular drug delivery."*Bioorg. Med. Chem*, **2009**, *17*, 2950–2962.

[54] A.Kumari, S. K.Yadav, S. C.Yadav: "Biodegradable polymeric nanoparticles based drug delivery systems."*Colloid Surf. B-Biointerfaces,***2010**, *75*, 1–18.

[55] P. A.McCarron, M. Hall: "Pharmaceutical nanotechnology."*Encycl. Nanosci. Nanotechno.,***2004**, *8,*469–487.

[56] S. V.Vinagradov, T. K.Bronich, A. V.Kabanov: "Nanosized cationic hydrogels for drug delivery: preparation, properties and interactions with cells."*Adv. Drug Deliv. Rev.***2002**, *54*, 223–233.

[57] a) K. Y.Win, S. S. Feng: "Effects of particle size and surface coating on cellular uptake of polymeric nanoparticles for oral delivery of anticancer drugs."*Biomaterials,***2005**, *26*, 2713–2722. b) D.Schmaljohann: "Thermo- and pH-responsive polymers in drug delivery."*Adv. Drug Deliv. Rev.,***2006**, *58*, 1655–1670. c) S. K.Sahoo, V.Labhasetwar: "Nanotech approaches to drug delivery and imaging."*Drug Discov. Today,***2003**, *8* (24), 1112-1120.

[58] C. J. Hawker, K. L. Wooley: "The convergence of synthetic organic and polymer chemistries."*Science*, **2005**, *309* (5738), 1200-1205.

[59] J.Panyam, V.Labhasetwar:"Biodegradable nanoparticles for drug and gene delivery to cells and tissue."*Adv. Drug Deliv. Rev.*, **2003**, *55*, 329-347.

[60] a) R. A. Jain: "The manufacturing techniques of various drug loaded biodegradable poly(lactice-co-glycolide) (PLGA) devices."*Biomaterials*, **2000**, *21*, 2475-2490. b) J. M.Lu, X. Wang, C.Marin-Muller, H.Wang, P. H.Lin, Q.Yao, C. Chen: "Current advances in research and clinical applications of PLGA-based nanotechnology."*Expert Rev. Mol. Diagn.,***2009**, *9*, 325–341.

[61] M. S.Muthu: "Nanoparticles based on PLGA and its copolymer: an overview."*Asian J. Pharm.,***2009**, *3*, 266–277.

[62] C. E.Astete, C. M.Sabliov: "Synthesis and characterization of PLGA nanoparticles."*J BiomaterSciPolym Ed*, **2006**, *17*, 247–289.

[63] S. Li, S. P. McCarthy:"Influence of crystallinity and stereochemistry on the enzymatic degradation of poly(lactide)s."*Macromolecules*, **2009**,*32*, 4454–4456.

[64] a) M. V. Cleveland, D. P.Flavin, R. A. Ruben, R. M. Epstein, G. E. Clark: " New polyethylene glycol laxative for treatment of constipation in adults: a randomized, double-blind, placebo- controlled study."*South Med J.*, **2001**, *94*, 478–481. b) US Government – Food and Drug Agency "Listing of Food Additive Status Part II". Retrieved **2011**-10-21.

[65] A.Abuchowski, T. Van Es, N. C.Palczuk, F. F. Davis: "Effect of covalent attachment of polyethylene glycol on immunogenicity and circulating life of bovine liver catalase."*J BiolChem*, **1977**, *252*, 3582–3586.

[66] R. B. Greenwald, Y. H.Choe, J. McGuire, C. D. Conover: "Effective drug delivery by PEGylated drug conjugates." *Adv Drug Deliv Rev.,* **2003**,*55,* 217–250.

[67] D.Oupicky, M.Ogris, K. A. Howard, P. R. Dash, K.Ulbrich, L. W. Seymour: "Importance of lateral and steric stabilization of polyelectrolyte gene delivery vectors for extended systemic circulation." *MolTher*, **2002**, *5,* 463–472.

[68] R.Gref, Y.Minamitake, M. T.Peracchia, V.Trubetskoy, V.Torchilin, R. Langer: "Biodegradable long-circulating polymeric nanospheres." *Science*, **1994**,*263*, 1600–1603.

[69] V. C. F.Mosqueira, P.Lengrand, J. L.Morgat, M.Vert, E.Mysiakine,R.Gref, J. L.Devissaguet, G. Barratt: "Biodistribution of long-circulating PEG-grafted nanocapsules in mice: effects of PEG chain length and density." *Pharm Res.*, **2001**,*18*, 1411–1419.

[70] a) L.Boguslavsky, S.Baruch, S.Margel: "Synthesis and characterization of polyacrylonitrile nanoparticles by dispersion/emulsion polymerization process." *J. Colloid Interface Sci.*, **2005**, *289*(1), 71-85. b) D. Quintanar-Guerrero, E. Allémann, H. Fessi, E. Doelker: "Preparation techniques and mechanisms of formation of biodegradable nanoparticles from preformed polymers. *Drug Dev. Ind. Pharm.*, **1998**, *24*(12), 1113-1128. c) J. P.Rao, K. E. Geckeler: "Polymer nanoparticles: preparation techniques and size-control parameters." *Prog.Polym.Sci.*, **2011**, *36*(7), 887-913.

[71] C. Pinto Reis, R. J. Neufeld, A. J. Ribeiro, F.Veiga: "Nanoencapsulation I. Methods for preparation of drug-loaded polymeric nanoparticles." *Nanomedicine: NBM*, **2006**, *2*(1), 8-21.

[72] a) B. C. Remziá:"Synthetic polymeric nanoparticles by nanoprecipitation. *J. Mat. Chem.,***2009**, *19*(23), 3838-3840. b) A. Minost, J. Delaveau, M. A. Bolzinger, H. Fessi, A. Elaissari: "Nanoparticles via Nanoprecipitation Process." *Recent Patents on Drug Delivery & Formulation*, **2012**, *6*(3), 250-258.

[73] J.Kreuter:"Nanoparticles as drug delivery systems."*Encycl. Nanosci. Nanotechnol.* **2004**, *7*, 161–180.

[74] F.Ganachaud, J. L. Katz: "Nanoparticles and nanocapsules created using the ouzo effect: Spontaneous emulsification as an alternative to ultrasonic and high-shear devices."*Chem. Phys. Chem.***2004**, *6*, 209- 216.

[75] J.Cheng, B. A. Teply, I. Sherifi, J. Sung, G. Luther, F. X. Gu, E. Levy-Nissenbaum, A. F. Radovic-Moreno, R. Langer, O. C.Farokhzad: "Formulation of functionalized PLGA–PEG nanoparticles for in vivo targeted drug delivery."*Biomaterials,* **2007**, *28*, 869–876.

[76] a) H.Jeffery, S. S. Davis, D. T. O'hagan: "The preparation and characterisation of poly (lactide-co-glycolide) microparticles. I: Oil-in-water emulsion solvent evaporation." *Int. J. Pharm.*, **1991**, *77*(2), 169-175. b) J.Floury, A.Desrumaux, J. Lardieres: "Effect of high-pressure homogenization on droplet size distributions and rheological properties of model oil-in-water emulsions."*Innov.Food Sci. Emerg. Technol.,* **2000**,*1*(2), 127-134.

[77] D. Gentili, G. Ori, M. Comes Franchini: "Double phase transfer of gold nanorods for surface functionalization and entrapment into PEG-based nanocarriers". *Chem. Comm.*, **2009**, 5874-5876.

[78] E. Locatelli, G. Ori, M. Fournelle, R. Lemor, M. Montorsi, M. ComesFranchini: "Click Chemistry for the Assembly of Gold Nanorods and Silver Nanoparticles". *Chem. Eur. J.*, **2011**, *17*, 9052-9056.

[79] C.J.Murphy,T.K. Sau, A.M. Gole, C.J. Orendorff, J. Gao, L. Gou, S.E. Hunyadi, T. Li: "Anisotropic Metal Nanoparticles: Synthesis, Assembly, and Optical Applications". *J PhysChem*, **2005**, *109*, 13857-13870.

[80] D.K. Smith, B.A. Korgel: "The Importance of the CTAB Surfactant on the Colloidal Seed-Mediated Synthesis of Gold Nanorods". *Langmuir*, **2008**, *24*, 644-649.

[81] L. Tong, Q. Wei, A. Wie, J. K. Cheng: "Gold nanorods as contrast agents for biological imaging: optical properties, surface conjugation and photothermal effects."*Photochem.Photobiol.*, **2009**, *85*, 21-32.

[82] J. Y. Chang, H. Wu,H. Chen, Y.C. Ling, W. Tan: "Oriented assembly of Au nanorods using biorecognition system". *Chem. Commun.*, **2005**, 1092-1094.

[83] W. Ni, Z. Yang, H. Chen, L. Li, J. Wang: "Coupling between molecular and plasmonic resonances in freestanding dye-gold nanorod hybrid nanostructures." *J. Am. Chem. Soc.*, **2008**, *130*, 6692-6693.

[84] J. C. Love, L. A. Estroff, J. K. Kriebel, R. G. Nuzzo, G. M. Whitesides: "Self-assembled monolayers of thiolates on metals as a form of nanotechnology." *Chemical reviews,* **2005**, *105*, 1103-1170.

[85] H. Chen, X. Kou, Z. Yang, W. Ni, J. Wang: " Shape- and Size-Dependent Refractive Index Sensitivity of Gold Nanoparticles". *Langmuir*, **2008**,*24*, 5233-5237.

[86] A. B. Lowe: "Thiol-ene "click" reactions and recent applications in polymer and materials synthesis". *Polym. Chem.*, **2010**, *1*(1), 17-36. A. Pucci, E. Locatelli, J. Ponti, C. Uboldi, V. Molinari, M. Comes Franchini: "Click chemistry on the surface of PLGA-b-PEG polymeric nanoparticles: a novel targetable fluorescent imaging nanocarrier". *J. Nanopart. Res.*, **2013**, *15*(8), 1-6.

[87] W. Bost, R. Lemor, M. Fournelle: "Comparison of the optoacoustic signal generation efficiency of different nanoparticular contrast agents." *Applied optics*, **2012**, *51*, 8041-8046.

[88] D. Psimadas, P. Bouziotis, P. Georgoulias, V. Valotassiou, T. Tsotakos, G. Loudos: "Radiolabeling approaches of nanoparticles with 99mTc." *Contrast media & molecular imaging*, **2013**, *8*(4), 333-339.

[89] P. Pramod, K. G. Thomas: "Plasmon Coupling in Dimers of Au Nanorods". *Adv. Mater.*, **2008**, *20*, 4300-4305. b) M. Green, D. Smyth-Boyle: "Directed growth of gold nanostructures using a nucleoside/nucleotide". *J. Mater. Chem.*, **2007**, *17*, 3588-3590.

[90] S. Kim, S. K. Kim, S. Park: "Bimetallic Gold−Silver Nanorods Produce Multiple Surface Plasmon Bands" *J. Am. Chem. Soc.*, **2009**, *131*, 8380-8381.